Experience dependent plasticity over short and long timescales

Charmaine Rebecca Lyness

Dissertation submitted for the degree of
Doctor of Philosophy
University College London

Supervisors: Martin I. Sereno & Joern Diedrichsen

Declaration

I, Charmaine Rebecca Lyness, confirm that the work presented in this thesis is my own. Where information has been derived from other sources, I confirm that this has been indicated in the thesis.

Signed Date

Abstract

The brain is constantly changing. Genetically specified developmental pathways interact with extrinsic factors including illness, injury and learning to shape the brain. This thesis presents two projects on experience dependent plasticity over different timescales.

Exerting its effect across years, deafness provides a model of long term crossmodal plasticity. In the first part of this thesis I ask how deafness affects the thalamus. Diffusion weighted imaging was used to segment the thalamus and with probabilistic tractography, thalamo-cortical connections were traced. Microstructural properties of visual and frontal thalamic segmentations, thalamo-cortical tracts throughout the brain, apart from the temporal thalamo-cortical tract were altered. The neuroanatomical sequelae of deafness are evident throughout the brain.

Deaf people have enhanced peripheral vision, facilitating a protective orienting mechanism when hearing cannot be relied upon. Widefield population receptive field (pRF) modeling with fMRI was completed to examine the functional and structural properties of primary visual cortex. Deaf participants had enlarged pRF profiles and thinner cortex in peripheral visual regions, again emphasizing plasticity across many years.

In the second part I examine plasticity over the course of days. Visuomotor transformations translate visual input to motor actions, and its neural instantiation might change with training. We used a pattern component model on fMRI data to reveal a gradient of visual to motor information from occipital to parietal to motor cortex. Strikingly, we observed motor coding in visual cortex and visual coding in motor cortex. More tentatively, our results suggest that during sensorimotor skill learning there is decreased dependence on visual cortex as motor cortex learns the novel visuomotor mapping.

In summary, I show crossmodal processing and plasticity in regions previously considered not to exhibit these properties, both in long- and short-term plasticity. This work

emphasizes the contribution that computational neuroimaging can provide to the field of experience dependent plasticity.

Acknowledgements

There are so many people to whom I am indebted for their kindness, encouragement, advice and wisdom during my time here at UCL. First of all my supervisors – Marty Sereno and Joern Diedrichsen. Marty's encyclopaedic knowledge of the brain and MRI physics has inspired me to think more broadly about my topics of interest, and meant that I have never got too badly stuck trying to interpret a weird result (there are many in this thesis). Marty has been generous, patient and a lot of fun throughout my time here at UCL. Joern's enthusiasm for statistics, programming and all things methods-related knows no bounds. I have learnt an immense amount from him and I am deeply grateful for all the time he has invested in me and my project.

I have also been fortunate with my collaborators. These include Mairead MacSweeney who has initiated me into the complexities of working with deaf people. Mairead has put an immense amount of hard work into the infrastructure of scanning of deaf people here in London; chapters 2 and 3 simply would not have happened without her commitment to working with deaf groups. Sam Schwarzkopf has been instrumental in getting the population receptive field modeling off the ground, and has worked tirelessly on the SamSrf toolbox used in this thesis, and indeed the many revisions our work has gone through. My collaboration with Velia Cardin on our review paper has been one of the most enjoyable and worthwhile parts of my time here. Velia's knowledge on so many different topics relating to plasticity in deafness meant that she had a clear line of sight through this paper, and with her sensitivity and maturity she has nudged me in the right direction. Ivan Alvarez's immense knowledge on diffusion weighted imaging was indispensable during my time working with this data set.

I would also like to thank Parob Coast for volunteering to help with recruitment and sign language interpreting during scan sessions for the studies involving deaf participants. Ewa Zotow helped to train participants and assisted the fMRI sessions during the experiments with the robot. Both Ewa and Parob showed such a high level of commitment and professionalism

during data collection, that it made this long and tiring process all the more bearable. Peter Zatka-Haas and Alexandra Reichenbach have been invaluable – they programmed the C++ to run the robot and were always there for whatever technical mishaps I ran into. Trevor and Preetha – the technicians at BUCNI - have also been brilliant. Their knowledge and patience with all the equipment used throughout the experiment with the robot was central to its success and I am really appreciative of all the effort they have put into this project.

Fortunately the PhD hasn't been all hard work – I have had some excellent office mates and colleagues to enjoy the downtime with. This includes Elif, Ewa, Alex, Christina, Naveed and George. Tessa, Tara and Heather all deserve a special mention – they have read and given comments on various parts of this thesis, and have been incredibly supportive friends throughout my time here.

My parents have provided me with support and encouragement for my academic endeavours from the beginning. I would like to thank my sisters Rachael and Rosie for their belief in me, as well as giving me perspective on many issues. Particular thanks go to Rachael and her partner Tom for their hospitality on various occasions since I moved to London.

Finally – I would like to thank Peter, who has been the person who has really shared the highs and lows of this thesis. Your contrast vectors may not always sum to zero, but your love and support have been unfaltering throughout.

Contributions

In this section I would like to clarify the contributions of my collaborators to the presented work. Throughout these experimental chapters I use the pronoun 'we' to acknowledge the effort of these collaborators.

Chapter 2

Data for chapters 2 and 3 was collected during the same scanning sessions. Mairead MacSweeney advised on ways to adapt the typical scanner set-up to be able to work with deaf participants, and with Parob Coast helped during data acquisition with deaf participants. I used the Deafness, Cognition and Language volunteer database to recruit some of my participants, which Mairead MacSweeney was heavily involved in developing. Ivan Alvarez advised on the analysis pipeline. Marty Sereno contributed to the interpretation of results. Ivan Alvarez, Marty Sereno and Mairead MacSweeney all provided comments for the manuscript 'Microstructural differences in the thalamus and thalamic radiations in the congenitally deaf', *Neuroimage* (2014), 15, 100, 347-357.

Chapter 3

Sam Schwarzkopf developed the SamSrf toolbox which completed the surface-based fitting of the difference-of-Gaussian model. Sam Schwarzkopf also developed the flickering checkerboard stimulus used during data acquisition. Sam Schwarzkopf and Marty Sereno contributed to the interpretation of results, and together with Mairead MacSweeney provided comments for the manuscript *'*Does congenital deafness affect the structural and functional architecture of primary visual cortex?*'* (under review - Neuroimage) upon which this chapter is based.

Chapter 4

Data for this project was collected in collaboration with Ewa Zotow, who presented the behavioural training data for her MSc thesis. Peter Zatka-Haas wrote the C++ code for the robot, which was adapted from code originally developed by Joern Diedrichsen and Alexandra

Reichenbach. Joern Diedrichsen developed the mathematical concept for the pattern component model, as well as the dual parameter estimation method. Joern Diedrichsen and Marty Sereno informed the interpretation of results as well as provided comments on this chapter.

For all other parts, not mentioned here, this thesis reflects my own work.

Contents

Declaration 2

Abstract 3

Acknowledgements 5

Contributions 7

List of Figures 11

List of Tables 13

List of Publications 14

Publications presented in this thesis: 14

Additional publications: 14

Chapter 1: Introduction 15

Anatomical changes in experience dependent plasticity 16

Functional changes in experience dependent plasticity 18

The use of Magnetic Resonance Imaging in studying plasticity 26

What does functional magnetic resonance imaging measure and how does this relate to neurophysiology? 27

Computational neuroimaging: a uniting framework which addresses the criticisms of fMRI? 31

Thesis Questions 34

Chapter 2: Microstructural differences in the thalamus and thalamic radiations in the congenitally deaf 38

Abstract 38

Introduction 39

Methods 43

Results 50

Discussion 58

Chapter 3: Does deafness alter the functional and structural architecture of primary visual cortex? 68

Abstract 68

Introduction 69

Methods 74

Results 82

Discussion 90

Chapter 4: How is visuomotor information and sensorimotor skill learning represented throughout the brain? 97

Abstract 97

Introduction 99

Methods 102

Results 115

Discussion 136

Chapter 5: Discussion 145

Chapter 6: Supplementary Information 155

Supplementary Information from chapter 3 155

Supplementary Information from chapter 4 158

References 162

List of Figures

Figure 2.1	FreeSurfer parcellation of the cortical lobes	47
Figure 2.2	Thalamic parcellations	50
Figure 2.3	Thalamo-cortical tracts	56
Figure 2.4	Summary of tractography results	57
Figure 3.1	Population receptive field modeling mapping stimulus, plus polar, eccentricity and Full Width at Half Maximum (FWHM) maps	82
Figure 3.2	Time series and model fit for the population receptive field modeling	83
Figure 3.3	FWHM curves by eccentricity for deaf and hearing groups	85
Figure 3.4	Average population receptive field across eccentricities	85
Figure 3.5	Population receptive field facilitatory centre curves by eccentricity for deaf and hearing groups	86
Figure 3.6	Position discrimination sensitivity in the central, middle and peripheral visual fields for deaf and hearing groups	89
Figure 4.1	Robot manipulandum training set-up	104
Figure 4.2	Schematic of the task	107
Figure 4.3	Experimental task and design	112
Figure 4.4	Functional masks - directional encoding and BOLD percentage signal change averaged over both reaching conditions and both sessions	117
Figure 4.5	Variance-covariance matrices from regions of interest	119
Figure 4.6	Visual, motor and unique encoding mapped on the cortical surface	119
Figure 4.7	Visual, motor and unique encoding from regions of interest	122
Figure 4.8	Training data from days 3-5	124
Figure 4.9	Learning effects – between session differences in BOLD activation	128
Figure 4.10	Learning effects – between session differences in directional encoding	129
Figure 4.11	BOLD activation and directional encoding for typical and mirror-reversed reaching in sessions 1 and 2 in each region of interest	130
Figure 4.12	Interaction between visual feedback condition and session for BOLD and directional encoding	132
Supplementary Figure 3.1	pRF centre size data for both groups across eccentricity when no outlier removal procedures have been applied	155
Supplementary Figure 3.2	pRF centre size data for V1, V2 and V3	156
Supplementary Figure 3.3	Beta values across eccentricity for deaf and hearing groups	157

Supplementary Figure 3.4	Cortical thickness measurements across eccentricity for deaf and hearing groups	158
Supplementary Figure 4.1	Mean unthreshold map for BOLD percentage signal change for between session differences in typical and mirror reversed conditions	159
Supplementary Figure 4.2	Mean unthreshold map for directional encoding strength change for between session differences in typical and mirror reversed conditions	160
Supplementary Figure 4.3	Mean unthreshold map for directional encoding strength change for between session differences in typical and mirror reversed conditions	161

List of Tables

Table 2.1	List of FreeSurfer labels merged to form cortical targets for connectivity based segmentation of the thalamus and tractography	49
Table 2.2	Correlations between microstructural measurements of thalamic parcellations from either hemisphere	52
Table 2.3	Post-hoc t-tests on microstructural measurements of thalamic parcellations	52
Table 2.4	Mean and standard deviation of microstructural measurements in thalamic parcellations	52
Table 2.5	Post-hoc t-tests on microstructural measurements of thalamic parcellations on group excluding participants at risk of insecure first language development	53
Table 2.6	Correlations between microstructural measurements of thalamo-cortical tracts from either hemisphere	53
Table 2.7	Post-hoc t-tests on microstructural measurements of thalamo-cortical tracts	54
Table 2.8	Mean and standard deviation of microstructural measurements in thalamo-cortical tracts	54
Table 2.9	Post-hoc t-tests on microstructural measurements of thalamo-cortical tracts on group excluding participants at risk of insecure first language development	54
Table 4.1	Training schedule	105
Table 4.2	Significant clusters of visual encoding	120
Table 4.3	Significant clusters of motor encoding	121
Table 4.4	Significant clusters of unique encoding	121
Table 4.5	Kinematic data from the scanning sessions	126
Table 4.6	Learning effects – BOLD change between session 1 and 2	128
Table 4.7	Learning effects – directional encoding strength change between session 1 and 2	129
Table 4.8	Learning effects – interaction between visual feedback condition and session for kinematic data	131
Table 4.9	Learning effects – interaction between visual feedback condition and session for BOLD activity and directional encoding strength	133
Table 4.10	Correlations between potential behavioural confounds and fMRI effects	135
Supplementary Table 4.1	Between session differences in visual, motor and unique encoding	158

List of Publications

Publications presented in this thesis:

Lyness, CR., Alvarez, I., Sereno, MI., MacSweeney, M. (2014). Microstructural differences in the thalamus and thalamic radiations in the congenitally deaf. *Neuroimage,* 15(100), 347-357.

Lyness, CR., MacSweeney, M. Sereno, MI., Schwarzkopf, DS. Does congenital auditory deprivation cause plasticity in primary visual cortex? Under review – Neuroimage.

Lyness CR., Sereno, MI., Zotow, E., Zatka-Haas, P., Diedrichsen J. The representation of visual and motor information throughout cortex. (in prep)

Additional publications:

Lyness, CR., Woll, B., Campbell, R., Cardin, V. (2013). How does visual language affect crossmodal plasticity and cochlear implant success? *Neuroscience Biobehavioural Reviews,* 37, 2621-2630.

Teki, S., Kumar, S., von Kriegstein, K., Stewart, L., **Lyness, CR.,** Moore, BC., Capleton, B., Griffiths, TD. (2012). Navigating the auditory scene: an expert role for the hippocampus. *Journal of Neuroscience,* 32(35), 12251-7.

Cardin, V., **Lyness, CR.,** Orfanidou, E., Ronnberg, J., Capek, CM., Rudner, M., Woll, B. Differential activity in Heschl's gyrus between deaf and hearing individuals is driven by auditory deprivation, and not language modality. (submitted - *Neuroimage*)

Alvarez, I., **Lyness, CR.,** Handley, S., Liasis A., Schwarzkopf, DS., Sereno, MI., Clark, CA. Characterising visual population receptive fields in human albinism. (submitted - *Brain*)

Chapter 1: Introduction

Throughout our lives, there is a dynamic interplay between genetic and environmental factors which shape our brain. Typical brain development cannot occur in a vacuum; environmental input is a prerequisite. Illness, injury or aberrations in the environmental input during development can interrupt genetically prescribed processes; the brain will adapt and continue down a modified developmental pathway. With varying degrees of success, the brain is able to compensate for atypical developmental scenarios. This appears to be dependent upon, amongst other things, the nature and extent of the injury, the age at which it was sustained, and the compensatory strategies employed. The potential for plastic reorganisation of the brain declines with age, and for many functions such as language, malleability of the underpinning circuitry is attenuated following the closure of the sensitive period. Nevertheless, we retain the ability to learn throughout our adult lives, which requires the formation and maintenance of neural circuits. Understanding the constraints and potential for plastic reorganisation will not only offer critical insight into the specification of functional and anatomical properties of the brain, but also inform therapeutic and rehabilitative interventions in instances of disease and injury. Previously, because of the role of regions such as superior temporal sulcus and parietal cortex in multisensory processing, re-weighting of these regions was thought to account for crossmodal plasticity. However, more recent research has demonstrated that multisensory processing occurs throughout the cortex and in sub-cortical structures, which suggests further investigation of plasticity in these regions may be informative.

In this thesis I will examine experience dependent plasticity which occurs over a long term time frame as a result of sensory deafferentation, as well as in the short term as a result of learning. Specifically, I will use diffusion weighted imaging to address how congenital deafness affects the thalamus and thalamo-cortical connections. In addition, I will use population receptive field modeling with functional magnetic resonance imaging (fMRI) to

assess the functional and structural architecture of primary visual cortex. Finally, I will use a pattern component model on fMRI data to examine the short term experience dependent plasticity which occurs as a result of training participants to complete a sensorimotor task over a period of eight days. Participants performed the task both with typical visual feedback, and when the feedback was mirror-reversed, allowing the dissociation of the representation of visual and motor information throughout the cortex.

In this introduction I will first review anatomical studies which suggest primary and sub-cortical structures are more densely connected with different modalities throughout the brain, suggesting a greater role for them in crossmodal processing and plasticity than has previously been acknowledged. Secondly, I will review the development of functional properties of cortex, and how the mechanisms of competition which are typically present in the developing brain contribute to the crossmodal reorganisation that is observed following sensory deafferentation. Further, I will also review the functional changes which occur in the short term with learning. Finally, I will discuss the advantages and criticisms of magnetic resonance imaging, which has been used throughout this thesis. I will briefly describe the projects in this study and how the analysis frameworks utilised aim to circumvent some of these issues.

Anatomical changes in experience dependent plasticity

To understand and make predictions about crossmodal and experience dependent plasticity we first have to understand the anatomical connections that are typically in place which facilitate the exchange of information between the different modalities. Anatomical changes can occur in at least two different ways; either entirely new connections can develop between regions, or re-weighting or reorganisation of existing anatomical connections can occur. In previous hierarchical models of multisensory processing, the dense, multimodal anatomical connectivity profiles of regions such as superior temporal sulcus and parietal cortex were thought to underpin multisensory processing (Beauchamp, 2005). However, more recent

anatomical studies have demonstrated that the anatomical connectivity profiles of primary sensory cortices are more complex and have more multimodal connections than originally thought. The anatomical connectivity profiles of primary cortices have indicated possible routes through which information from different modalities can be conveyed, and suggest that these regions are more than passive processors of information from the thalamus (Falchier et al., 2002). Anatomical tract tracing studies have provided evidence of direct connections between primary visual cortex and primary somatosensory cortex in marmosets (Cappe and Barone, 2005), between primary auditory and primary somatosensory cortex in both marmosets (Cappe and Barone, 2005) and Mongolian gerbils (Budinger et al., 2006), and between primary visual and primary auditory cortex in monkeys (Falchier et al., 2001), and cats (Hall and Lomber, 2008). In all instances it is noted that the strength of these direct connections between primary sensory cortices is vastly reduced in comparison to the strength of connections between association cortices.

Whilst there is a high degree of similarity across the anatomical connectivity profiles of mammalian brains, it has yet to be verified whether these direct connections between the primary sensory cortices are present in humans. Active transport mechanisms (which are no longer present post mortem) are required for the transport of retrograde tracers more than a few centimetres, ruling out the possibility of tracing long-range connections between cortices. The only method for *in vivo* investigations of white matter connectivity in humans is diffusion weighted imaging. This method is however, not without its flaws (for a more complete discussion of these, see chapter 2). Using diffusion tensor imaging, it has been suggested these anatomical connections between visual and auditory cortices are present in humans also (Beer et al., 2011). However, probabilistic tractography was completed between large anatomical regions, which precludes the confident assertion that primary auditory and primary visual cortices are directly connected in humans. It is instead possible that connections between association regions in visual and auditory cortex could account for these results (Beer et al., 2011). As noted above, the extent of direct connections between primary sensory cortices are

reduced in comparison to other connections. As current diffusion weighted imaging models cannot resolve white matter fibres which cross in a voxel from those which merely touch in a voxel, imaging these non-dominant tracts may be beyond the capabilities of current methods.

The thalamus has been suggested to be an important site of multimodal integration and interplay because of its anatomical connectivity profile. It receives input from each of the different sensory modalities, and is capable of rapidly affecting the flow of information throughout the cortex (Van Horn and Sherman, 2004, Sherman, 2007, Cappe et al., 2009b). In contrast, direct cortico-cortical connections are quite slow (Sherman, 2007, Cappe et al., 2009a, Cappe et al., 2009b). Overlapping thalamic territories projecting to different cortical areas has been argued to provide a putative anatomical hub for multisensory integration of different sensory stimuli, particularly sensorimotor integration, owing to the high degree of overlap with regions involved in motor control (de la Mothe et al., 2006, Cappe et al., 2009a). Because of the critical role the thalamus plays in distributing information throughout the cortex it is possible changes to this region contribute to the drastically reorganised patterns of cortical activation as seen in sensory deafferentation.

In summary, anatomical tract tracing studies with animals suggest that direct connections between primary cortices and sub-cortical structures, including the thalamus, facilitate communication between the different senses. As such, these regions could play a greater role in crossmodal processing and plasticity than previously acknowledged. Bearing this in mind, we will next turn our attention to the changes in cortical function that occur with experience dependent plasticity.

Functional changes in experience dependent plasticity

Specification is the process by which cortex develops its functional properties, and has been described as ‘a progressive restriction of fate of cortical neurons’ (Sur et al., 1990). This includes the development of cytoarchitectonics (the architecture of neuronal cell bodies), the development of connections with other areas, both cortically and subcortically, and the

connectivity within the area (Sur et al., 1990). Seminal research into cortical specification was completed using electrophysiological and histological analyses on animals which were reared in atypical environments, such as with only vertical or horizontal stripes, with no light, or with input to one eye only. Monocular deprivation (MD) rapidly affects the response properties of neurons in visual cortex (Antonini and Stryker, 1993). The representation of visual input from a single eye invades cortical territory which typically represents visual input from the other eye (Wiesel and Hubel, 1963, Hubel and Wiesel, 1970, Ramachandran and Kupperman, 1986). In contrast, dark rearing halts the functional development of the visual cortex almost entirely (Hubel and Wiesel, 1977, Fregnac and Imbert, 1978). As there is no imbalance between the eyes in this instance, the relative ability of either eye to drive cortical responses, and the cortical representation of either visual field is unchanged. These studies converge on the idea that the competitive balance between inputs is central to the process of cortical specification (Wiesel and Hubel, 1963, Hubel and Wiesel, 1970, Blakemore and Van Sluyters, 1974).

As well as within modalities, there is evidence of competitive processes occurring at a whole brain level. In the case of sensory deafferentation such as deafness or blindness, cortical territory which is typically involved in processing the lost input is commandeered by other sensory and cognitive functions. In deafness, auditory association cortex is activated for a wide range of visual stimuli, including sign language (Petitto et al., 2000, MacSweeney et al., 2002, MacSweeney et al., 2004, Sadato et al., 2004, Corina et al., 2007, Capek et al., 2008, MacSweeney et al., 2008a, MacSweeney et al., 2008b, Emmorey et al., 2011, Cardin et al., 2013), biological motion (MacSweeney et al., 2004, Corina et al., 2007), as well as simple visual stimuli such as moving dots (Finney et al., 2001, Fine et al., 2005, Sadato et al., 2005). Plastic reorganisation of somatosensory processing to auditory cortex in deafness has also been demonstrated (Auer et al., 2007), including recruitment of primary auditory cortices (Karns et al., 2012). Similarly for blind individuals, there is a wealth of data suggesting that both sensory and cognitive tasks reorganise into dormant visual cortex (Merabet and Pascual-Leone, 2010). Recruitment of visual cortices has been demonstrated for Braille reading (Sadato et al., 1996,

Buchel et al., 1998, Sadato et al., 1998, Burton et al., 2002), haptic object recognition (Pietrini et al., 2004), a variety of auditory tasks including motion perception (Poirier et al., 2006), change detection (Kujala et al., 2005), sound source discrimination (Voss et al., 2008) and sound localisation (Weeks et al., 2000, Gougoux et al., 2005). Language tasks including speech processing (Roder et al., 2002), semantic judgment tasks (Burton et al., 2003), and verb generation (Burton et al., 2002) have also been shown to recruit the visual cortex (though see Watkins et al., 2011 for an alternative explanation of these findings).

The supramodal hypothesis of crossmodal reorganisation argues that the plastic reorganisation that occurs following sensory deafferentation is not random (Meredith et al., 2011). Instead, when deafferentation causes a cortical area to lose its typical input, specialised circuits in the region become available for functional innervation by other sensory modalities (Meredith et al., 2011). That is, whilst the input to a region may change, its behaviour will remain unaltered. Blind and deaf people have strategies to compensate for the lost modality. For example, instead of using visual motion processing skills to determine whether it is safe to cross a road given how far away cars are and how fast they are moving, blind people will use auditory motion processing. Accordingly, in response to auditory (and tactile) motion stimuli, blind people will activate middle temporal (MT+) regions which are typically specialised for visual motion processing (Poirier et al., 2006, Ptito et al., 2009). Tasks which involve auditory spatial processing have been shown to recruit the middle occipital gyrus in early and congenitally blind participants, which is the typical site of visuospatial processing in sighted participants (Renier et al., 2010, Collignon et al., 2011). This phenomenon is evident in deafness also. The auditory field of the anterior ectosylvian sulcus (FAES) is typically required for acoustic orienting (Meredith and Clemo, 1989, Stein et al., 2002), and its neurons show tuning for sound location (Las et al., 2008). In early-deafened cats, this region demonstrates visual responses, and the receptive fields of these visual responses mimic those observed for auditory sound location, in that they represented the contralateral visual field (Meredith and Lomber, 2011).

Sensory substitution devices make visual information accessible to blind people, through translating this information into an alternative domain, such as the tactile or auditory domain. This allows the development and specialisation of the visual system to be observed in the absence of visual experience. Blind people trained on sensory substitution devices which translate images to soundscapes demonstrate comparable specialisation of the visual system to that observed in sighted people. The processing of body stimuli, as opposed to texture or objects, recruits the site of the extra-striate body area (EBA) (Striem-Amit and Amedi, 2014), word stimuli selectively activate the visual word form area (VWFA) (Striem-Amit et al., 2012), and shape information recruits the lateral occipital (LO) cortex, a region which is involved in visual shape processing in typically sighted people (Amedi et al., 2007). These studies suggest the brain possesses some default amodal circuitry specialised for certain functions, which process a preferred sensory input. In the case of sensory deafferentation, compensation and experience driven plasticity can cause these circuits to be driven by a different functional input.

Research into sensory substitution devices and the supramodal hypothesis of crossmodal plasticity raise important questions regarding how reorganised responses in the case of sensory deafferentation relate to typical crossmodal processing of information. There is mounting evidence that sensory deafferentation is not a necessary pre-requisite for crossmodal processing in regions which have previously been thought of as uni-sensory. Classic models of crossmodal processing proposed a hierarchical structure, in which a handful of multisensory processing hubs were responsible for multisensory integration, and the remaining cortices processed uni-sensory information only (Jones and Powell, 1970). However, reviews of electrophysiological, neuroimaging and anatomical data challenge this assumption (Ghazanfar and Schroeder, 2006, Driver and Noesselt, 2008), instead arguing that there is evidence for crossmodal processing of stimuli at the earliest stages of cortical processing, and indeed sub-cortical processing.

Through learning, circuitry specialised for one modality can begin to exhibit crossmodal responses. Shape is not a natural concept in the auditory domain for humans. However, when participants are trained to discriminate auditory shape stimuli, activation occurs in lateral occipital cortex (LOC), which is typically associated with visual shape recognition (Kim and Zatorre, 2011). Without training, the LOC is involved in somatosensory sensory processing of shapes, though the magnitude of activation is reduced in comparison to visual shape processing (Amedi et al., 2001).

Therefore there is evidence that certain cortical areas possess circuitry optimised for a specific computation, which typically favour processing information in one modality, but can come to process information in another modality following sensory deafferentation. Weaker representations of other modalities are present in these regions even in the absence of sensory deafferentation. These examples relate to a handful of higher visual processing regions which are known to be densely anatomically connected with other modalities. As such, it is perhaps not so surprising these regions are capable of representing information from more than one modality. However, there is also mounting evidence that primary cortices are crucial to crossmodal processing.

Activation in response to visual stimuli has been demonstrated in primary auditory cortex (A1). When completing speech-reading tasks, hearing participants will activate auditory cortex, including auditory core (Calvert et al., 1997, Calvert et al., 2000, Calvert and Campbell, 2003, Reale et al., 2007, Capek et al., 2008). This activation is likely to be functionally relevant as the extent of activation in these regions correlated with performance on speech reading tasks (Pekkola et al., 2005, Capek et al., 2010). It is plausible that the function of A1 activation in speech-reading is auditory imagery, which facilitates speech comprehension. Patterns of neural activation in primary auditory cortex in response to silent video clips which imply sound (for example, of a rooster crowing) can be reliably distinguished from one another (Meyer et

al., 2010). These findings are also interpreted in terms of visual stimuli resulting in auditory imagery in A1 (Meyer et al., 2010).

Comparable findings have also been reported in early visual cortex. The neural activity patterns in early visual cortex of blindfolded participants in response to different exemplars from the categories of bird song, traffic noise and talking crowds can be reliably distinguished from one another (Vetter et al., 2014). This study extends previous findings by demonstrating that it is not merely stimulus-specific information, but rather that abstract categorical information is represented in these regions (Vetter et al., 2014). The activity patterns in early visual cortex in response to real stimuli could be used to classify the imagined stimuli (and vice versa), demonstrating there is shared categorical information between these real and imagined stimuli (Vetter et al., 2014). These stimuli could still be distinguished when the category was the same though the exemplars were pictorially different, demonstrating that the analyses is sensitive to shared categorical information rather than the pictorial features of the stimuli being re-instated in early visual cortex (Vetter et al., 2014). By highlighting the categorical information in mental imagery, this study begins to suggest that the function of crossmodal responses in primary sensory cortices may include prediction of upcoming sensory information.

The presence of visual responses in pre-motor cortex is well established (Graziano et al., 1994). Visual responses have also been demonstrated in primary motor cortex (M1) in monkeys (Alexander and Crutcher, 1990, Shen and Alexander, 1997, Graziano and Gandhi, 2000, Zach et al., 2008). More recently, visual directionally selective responses have been demonstrated in primary motor cortex of humans using functional magnetic resonance imaging (fMRI) (Eisenberg et al., 2011). Unfortunately this study used only M1 as a region of interest (ROI). Therefore until now, the representation of visual and motor information underpinning visually guided reaching movements has not been properly examined throughout the cortex.

Motor information, specifically the speed of locomotion is represented in primary visual cortex (V1) in mice (Saleem et al., 2013). In this study, mice with implanted electrodes were able to run freely in a virtual reality environment, allowing the dissociation of the speed of locomotion and visual feedback (Saleem et al., 2013). The authors found evidence for a population code for self-motion in V1, as neurons encoded positively weighted averages of speed from both visual and locomotion inputs (Saleem et al., 2013). It should be noted, however, that the visual cortex of mice has a truncated hierarchy (Wang and Burkhalter, 2007), and as such, V1 in a mouse is not equivalent to V1 in humans.

These findings challenge previous assumptions that the integration of multimodal information is restricted to a few multisensory hubs, suggesting instead that we need to examine the possibility that multimodal information is present throughout the cortex, albeit some forms of information are less strongly represented in certain parts of cortex. The presence of crossmodal processing and plasticity in primary cortices raises the issue of how this relates to within modality plasticity that occurs with learning.

Visual perceptual learning (VPL) has been used as a model to explore short term experience dependent plasticity in the adult brain. V1 plasticity has been implicated in VPL (Karni and Sagi, 1993, Schoups et al., 2001, Furmanski et al., 2004, Yotsumoto et al., 2008, Hua et al., 2010, Shibata et al., 2011). In a study using neurofeedback, participants were given feedback on their neural activity patterns in early visual cortex, which was designed to sculpt these patterns to look more like the activity patterns which had been previously elicited in these participants in response to one of three orientated grating stimuli (Shibata et al., 2011). Therefore the authors were able to alter the functional activation patterns in V1/V2 in the absence of a stimulus, and also the participants' knowledge of what they were meant to be learning (Shibata et al., 2011). This is strong causal evidence for V1/V2 underpinning experience dependent plasticity.

Primary motor cortex (M1) has also been proposed to be an important site for experience dependent plasticity. M1 has been argued to encode motor memories, as its modulation with transcranial direct current stimulation (tDCS) has been shown to improve performance on finger sequencing tasks (Reis et al., 2009). Transcranial magnetic stimulation (TMS) paradigms have also been linked to long-term potentiation (LTP) like mechanisms in motor cortex (Stefan et al., 2000, Ziemann, 2004). Whilst brain stimulation methods are argued to permit causal inferences regarding a regions role in a task, these methods suffer from poor spatial localisation and as such it is problematic to conclude M1 exclusively contains circuitry underpinning experience dependent plasticity, as adjacent regions may have been stimulated and contributed to the observed effects.

The plasticity underpinning complex tasks which require the co-ordination of the visual and motor system is less well characterised. Electrophysiological recordings were made from middle temporal (MT+) as well as lateral intraparietal (LIP) area whilst monkeys were trained to complete a visual motion discrimination task (Law and Gold, 2008). Behavioural improvements were associated with modulation of the firing rates of LIP, but not MT+. The authors interpreted the results as demonstrating that learning is reflected in regions relating to the interpretation and decision making regarding a sensory stimulus (LIP), rather than those associated with sensory processing (MT+) (Law and Gold, 2008). Recording from these two sites does cannot exclude the possibility of contributions from other regions. It is possible that with a more complex visuomotor task which includes a visuomotor transformation, changes could be observed both in the primary cortices which represent the visual and motor aspects of the movement itself, as well as regions in parietal and pre-motor cortex which have a greater role in planning the movement and applying the visuomotor transformation. It is clear a whole brain approach is required to assess the contribution of different regions to the experience dependent plasticity associated with complex visuomotor tasks.

The use of Magnetic Resonance Imaging in studying plasticity

Magnetic resonance imaging (MRI) enables *in vivo* study of human brain structure and function. Almost simultaneous acquisition of whole brain data with resolution in the millimetre range can be achieved. Specifically for the field of plasticity, neuroimaging allows the study of awake, behaving participants who have been deafferented of a sense or have sustained an injury. Experience dependent plasticity which occurs over the course of days, weeks or months can also be examined in training studies. For several reasons, research with humans is a necessary adjunct to animal models when studying neuroplasticity. Firstly, certain cognitive capabilities are unique to humans. Language is perhaps the most important and obvious of these. Secondly, it is often the case with sensory deafferentation in humans, the environment is enriched in other ways to compensate for the loss of this sense, which in itself becomes a driver for plastic change. Blind people often learn to read Braille, deaf people are more reliant upon visual language, and those who have suffered a limb amputation may differ in how they use their remaining limbs to compensate for this loss. Animal studies do not typically provide this sort of environmental enrichment, which may influence plastic change in the brain. Finally, work with humans is necessary to address translational and clinical questions.

MRI has been used throughout this thesis. In the following sections, I explain the rationale behind using this methodology, and the drawbacks which require consideration. Functional magnetic resonance imaging is a technique in its infancy. Since the endogenous blood oxygen level dependent (BOLD) signal was first discovered in 1992 there has been an explosion in the use of this method and the resulting publications. Despite this, functional magnetic resonance imaging (fMRI) has come under intense criticism, which can be considered to fall under two main arguments.

The first argument relates to the extent to which fMRI is able to interrogate cognitive theories and inform our understanding of the brain. Proponents of this viewpoint often argue that fMRI is a modern day phrenology. A one-to-one mapping does not exist between different

tasks and brain areas: most brain areas are involved in a multitude of different tasks, and most complex realistic tasks will activate a distributed network of regions. Successful localisation of a task to a given region does not help us understand how the brain completes this task, or how we can fix it when it breaks down either through illness or injury. These criticisms are in part encouraged by the mass-univariate framework approach to fMRI, which is the predominant method used for functional localisation.

The second major criticism of fMRI concerns the BOLD signal and the paucity of our understanding of its relationship with the underlying neural processes. At each voxel, the conglomerate BOLD signal reflects the metabolic demands of the activity of approximately one million neurons. There are an infinite number of combinations of processes which could occur at each voxel, each of which could contribute to the changes in BOLD signal measured during fMRI. Both of these criticisms will be addressed in greater depth in the next section, as well as analysis frameworks which attempt to ameliorate these issues.

What does functional magnetic resonance imaging measure and how does this relate to neurophysiology?

Typically during functional magnetic resonance imaging (fMRI) we measure the blood-oxygen-level-dependent (BOLD) signal. Oxygenated and deoxygenated blood have different magnetic properties and when a brain region becomes more metabolically active, the increased conversion of oxygenated to deoxygenated blood will cause measureable distortions in the magnetic field (Ogawa and Lee, 1990). This has been exploited as an endogenous contrast for the measurement of brain function (Bandettini et al., 1992, Kwong et al., 1992, Ogawa et al., 1992). In addition to blood oxygenation levels as the name suggests, the BOLD signal additionally reflects blood flow and volume. Pericytes control these parameters which influence the BOLD signal (Hall et al., 2014). However, how this relates to neural activity is still a matter of intense controversy, and as such, constitutes one of the main criticisms of fMRI.

That is, if we do not know what we are measuring, how can we meaningfully interpret changes to this signal?

Prior to neuroimaging, single unit neurophysiology was the dominant methodology used in neuroscience to explore functional properties of the brain. This involves inserting a microelectrode near to the soma or axon of a neuron to record the signal of the electrical activity associated with spike traffic through that neuron. fMRI is clearly very different to single unit neurophysiology. Each method has associated advantages and disadvantages making it appropriate for answering different questions and therefore useful for complementary approaches for hypothesis evaluation. The first and perhaps most obvious difference between the two methodologies is scale. In single unit neurophysiology, the activity of one neuron is measured, which enables precise characterisation of its response properties to a given stimulus or task. Although multi-unit electrode recordings are available, the number of neurons recorded from is still of the magnitude of tens to hundreds, which is negligible in proportion to the total number of neurons in the brain. These will typically be focused in a single anatomical region, as multiple surgeries or surgical sites for implanting a range of electrodes has deleterious effects on the animal. Multiple recording sessions can be used to gain a more complete picture of the response properties of neurons in the region to a wide range of stimuli. However, as well as response biases in terms of the neurons which are recorded from, as may occur in single cell studies, practice and learning effects will become apparent over time. In contrast, with fMRI simultaneous recording of activity from the whole brain can be achieved, which enables the study of the brain as a network. This comes at the not inconsiderable cost of losing all specificity with regards to the activity of the neural population under study. Apart from in V1, there are 100,000-150,000 cells (neurons plus glia) under each square millimetre of cortex (Carlo and Stevens, 2013). Including pre-processing steps such as spatial smoothing, it has been estimated that in a single voxel in a typical fMRI study, the response properties of up to 5.5 million neurons are collated (Logothetis, 2008). In the 7 years since this figure was published, advances in high resolution imaging and the

increased popularity of analysis techniques which do not require spatial smoothing mean that this figure has dropped considerably, though it is still likely to be approximately a million neurons in most instances.

Neurophysiological recordings are based on the electrical activity of neural spike trains, whereas the BOLD signal is a surrogate signal of the metabolism underpinning this activity. Neurophysiological recordings reflect the output of a computation in a given area, whereas the BOLD signal reflects pre and post synaptic activity in the different inputs which come together for the computation to take place (Viswanathan and Freeman, 2007). Despite early optimism that the BOLD signal correlated with spiking activity (Rees et al., 2000), it is by definition an equivocal signal as it indexes the metabolic demands of all neuronal processes in a region. The BOLD signal has been posited to reflect the mass action of excitatory-inhibition networks (EIN), with its closest electrophysiological correlate found in the local field potential (LFP) (Logothetis, 2008). LFPs reflect integrated synaptic activity (synaptic potentials, afterpotentials of somatodendritic spikes and voltage-gated membrane oscillations) of excitatory and inhibitory neurons in a given region (Logothetis, 2003). Unsurprisingly, the LFP signal is also ambiguous. Further, more recent evidence has also suggested the relationship between LFP and the BOLD signal is not as straightforward as previously thought, and can break down in certain regions of the brain (Bartolo et al., 2011).

Every anatomical region has a distinct pattern of feedback and feedforward connections from throughout the brain, as well as local intra-areal and horizontal connections within a region (see Clavagnier et al., 2004 for a description of V1). All these connections contribute to the firing rate of a neuron although they will differ in terms of whether they drive or modulate its response (Logothetis, 2008). Despite this, these connections are not considered in the classical receptive field model of a single neuron. There are numerous combinations of changes in the EIN, which could occur as a result of a particular stimulus or task manipulation which would result changes in the metabolic requirements of a given area,

without this necessarily being driven by an increase in the firing rates of neurons in a given region (Logothetis, 2008). For example, a particular stimulus or task could cause both tonic excitation and inhibition in the region to change, but in a balanced manner. This would cause the BOLD signal in a region to change, without affecting firing rates, demonstrating how these two signals could diverge. Analogously, there are scenarios in which several processes may be occurring in a region, each of which have an antagonistic effect on the BOLD signal, thus despite extensive computations occurring in the region, there will be no mean change in the BOLD signal.

As fMRI reflects mass action, this can be interpreted as a disadvantage associated with this methodology: it is problematic to disambiguate top-down from bottom-up processing and function-specific from modulatory processing (Logothetis, 2008). On the other hand, the measurement of neuromodulatory effects is of great potential interest for studying neural function. Broadly, neuromodulation refers to the mechanisms by which feedback projections influence how information is processed. This reflects 'higher cognitive processes' such as attention, arousal, prediction and learning. The poor temporal resolution of fMRI means activity is typically averaged over a period of seconds, in comparison to neurophysiological studies which typically concentrate on the first few hundred milliseconds following stimulus onset or during task performance. Feedback projections from other brain regions by definition succeed the feedforward responses to stimuli, and therefore will appear over longer timescales which fMRI measures and neurophysiology typically overlooks. Thus BOLD to a large extent reflects cortical feedback, which traditional neurophysiology is totally blind to (Muckli, 2010). Modulatory effects can be studied using intra-cellular recordings. However, there are disadvantages associated with this method. Slice preparations are typically required to achieve stable recordings, which prevents study of the brain as a network. Furthermore, the complexity of this method means there is a limitation on the number of cells which can realistically be recorded from, and cells die after a short period of recording.

The pervasiveness of neuromodulation was not clear prior to neuroimaging studies. Despite V1 being the most extensively studied area of cortex, only approximately 40% of the response variance in V1 can be accounted for (Carandini et al., 2005). There are many reasons for why this is the case (see Carandini et al., 2005), which include the bias in neurophysiology in which models are created based on data measuring the spiking output of neurons only. Neurophysiology had assumed that receptive fields in V1 are static and could be entirely classified with their complex receptive field properties, however with neuroimaging, several previously unknown and unanticipated properties of V1 have been discovered. V1 is involved in visual attention (Ress et al., 2000, Silver et al., 2007), encodes the expected rather than the actual properties of stimuli as demonstrated by work with visual illusions (Muckli et al., 2005, Larsen et al., 2006, Murray et al., 2006, Sterzer et al., 2006), and also encodes memory traces of stimuli (Harrison and Tong, 2009). Thus V1 has many properties and performs many computations which were not readily apparent when studying this region with neurophysiological methods.

Computational neuroimaging: a uniting framework which addresses the criticisms of fMRI?

Traditionally, fMRI has been used for functional localisation, which is the process of circumscribing the activity associated with a given task to a particular anatomical region. For this, data is analysed in a mass-univariate framework which involves determining the regions with BOLD modulation when the aspect of interest in the task or stimulus is isolated by the experimental design. Data is spatially smoothed, and in order for an effect to be detected, signal change has to be uniform (that is, either increases or decreases) and spatially contiguous. Functional localisation has the implicit assumption of a perception-cognition-action cognitive framework. However, despite the high degree of modularity in the brain, even regions such as V1 the extent of feedback projections is immense (Clavagnier et al., 2004). Therefore developing an analysis framework designed to circumscribe tasks to a particular region based on a signal which is mainly sensitive to neuromodulatory effects may be

susceptible to misascribing the computational role of a region. This use of a neuromodulatory signal for functional localisation relates to the criticism that fMRI is unsuitable for testing cognitive theories. That is, it is debatable the extent to which knowledge that task A is performed in area B informs our understanding of the brain. There is a many-to-many mapping between stimuli/tasks and brains regions, and therefore there is no sensible end in sight for the functional localisation approach.

Due to the ambiguous nature of the BOLD signal, there are scenarios in which this functional localisation approach can be open to interpretation. An example pertinent to the field of plasticity and addressed in chapter 4 in this thesis is the changes in BOLD signal which occur over time with learning. Increased activation for expert compared to novice task performance has been interpreted as demonstrating a more enhanced representation of this skill, with more neural resources devoted to it (Karni et al., 1995). However, the converse finding has also been reported in which the expert group has a decreased amount of activation. This has been interpreted as demonstrative of 'neural efficiency' in which an expert representation has been pruned and refined over time (Jenkins et al., 1994, Ungerleider et al., 2002, Poldrack et al., 2005). These discrepant findings and interpretations of global signal changes within the mass-univariate framework highlight the fact that this analysis framework alone is insufficient to characterise many of the processes we would be interested in studying with fMRI.

These problems associated with the mass-univariate framework and the inherent ambiguity of the BOLD signal means it is critical to have knowledge of the underpinning electrophysiology of an area, and constrain interpretations of BOLD data with data from other methodologies (Logothetis, 2008). If we seek triangulation of our findings from studies using fMRI with the neurophysiology literature, we must utilise analyses frameworks in which this can occur. In the next section I will discuss in greater depth more recent approaches to analysing neuroimaging data, which go some way in terms of bridging the gap between the

neuroimaging and neurophysiology, and how they can be applied to elucidate the mechanisms of plasticity.

During the course of this thesis I have used multivariate analysis and population receptive field modeling, which are alternatives to the mass-univariate framework for analysing fMRI data. Multivariate pattern analysis (MVPA) including methods such as representational similarity analysis (RSA) and pattern component modeling (PCM) are becoming the dominant methods for analysing neuroimaging data, replacing the mass-univariate framework. The aim of these methods is to study neural representations rather than functional localisation. A neural representation is the activity pattern of a population of neurons associated with a specific stimulus or task. MVPA can be used to determine whether a region is coding information about a variable of interest. For example, a region may be metabolically active in response to Gabor patches, and we can determine whether this region is also responsive to colour by varying the colour of these stimuli. If by using a pattern classification method such as linear discriminant analysis, Gabor patches of varying colours can be reliably distinguished from one another, this region can be said to be encoding information regarding colours. With RSA we can take this one step further by asking questions about the structure of how information is encoded. Returning to the colour example, a distance metric can be computed between the neural activity patterns elicited by stimuli of different colours and from this we can discern whether the neural representations of green and red are more dissimilar to those of red and orange. Thus we can test theoretically driven models, or models derived from other types of data, against our findings regarding how information is represented with PCM.

Using MVPA to analyse representations in fMRI data also has the advantage of making results more comparable to the analyses performed in the neurophysiology literature, as single cell recording studies also have the aim of studying representation. For example, to study directional selectivity for arm movements, many directions need to be sampled to determine

directionally selective preference or a tuning curve for the neuron, and this needs to be completed over many neurons to build up a picture of directional selectivity for the region. Population receptive field modeling and PCM can therefore act as a conduit between the fMRI and electrophysiology literatures, as data from either of these experimental methodologies can be used to evaluate the veracity of these computational models.

Thesis Questions

In light of this review of crossmodal experience dependent plasticity and the advantages and limitations associated with magnetic resonance imaging, I will detail the projects undertaken as part of the thesis.

This thesis answers three main questions;

1) **Does congenital auditory deprivation affect the microstructural properties of the thalamus, and thalamic radiations?**

As well as dystrophic effects, auditory deprivation creates a compensatory drive to use the senses in a different way. As stated previously, the thalamus is an important structure for conveying information from different modalities throughout the brain. Prior to this thesis, whether plasticity occurred in the thalamus or thalamo-cortical radiations in deafness had not yet been examined. Establishing whether there are thalamic alterations in deafness is critical to explaining the wider pattern of plasticity that is observed in deafness. Diffusion weighted magnetic resonance imaging of the thalamus was used to address this question. Specifically, probabilistic tractography was used to trace the thalamo-cortical connections, and complete an anatomically informed segementation of the thalamus. Microstructural measurements of tissue properties in these regions were contrasted between deaf and hearing groups.

2) **Does congenital auditory deprivation affect the structure and function of early visual cortex?**

Deaf people cannot rely on audition to alert them to new and salient information in the environment, and so through experience dependent plasticity, develop enhanced peripheral vision to compensate for this. Auditory cortex has been shown to be involved in this process. However, the visual processing stream is hierarchically organised: we would expect changes in auditory and higher visual areas to be preceded by changes lower down in the visual processing stream. Studies of perceptual learning have highlighted V1 is critical to this process, suggesting experience dependent plasticity in these regions may underpin the visual enhancements in the deaf group. Using fMRI with population receptive field modeling we can examine the functional properties of the earliest stages of the visual processing stream.

Population receptive field modeling is an example of a voxel-based encoding model. Like other computational imaging methodologies, pRF modeling attempts to bridge the gap between spiking properties of a neuron measured at the micron scale and voxel-based neural signal which are measured at the millimetre scale. The concept of a receptive field – the stimulus (or combination of stimuli) which optimally drive a neurons response is fundamental to how we think about sensory neuroscience. A receptive field of a neuron corresponds to the region of stimulus space which will excite a neuron. This can be an auditory stimulus such as a certain pitch, or as we have used it here, in terms of a location in visual space. During population receptive field modeling, a summary statistic for properties of each voxel is generated.

In contrast to mass-univariate style approaches, pRF modeling allows a more fine-grained examination of functional properties in the cortex. Despite the issues discussed above regarding how the BOLD signal at each voxel does not map onto the summed activity of all neurons in the voxel under study, concordance has been found between receptive field sizes estimated using pRF modeling with fMRI and invasive electrophysiological recordings (Gattass et al., 1981, Van Essen et al., 1984, Burkhalter and Van Essen, 1986, Felleman and Van Essen, 1987, Gattass et al., 1987, Rosa et al., 1988). From the neurophysiology literature, there have

been many studies which demonstrate the remapping of receptive field properties following injury or abnormal developmental conditions. A classic example of this is following the denervation of the upper limb in macaque, electrophysiological recordings from somatosensory cortex have demonstrated that receptive fields representing the face becomes expanded, and eventually takes over the dormant hand representation (Jones and Pons, 1998). Therefore using neuroimaging methodology which allows us to begin to approximate the receptive field properties of humans will help reconcile these two literatures.

3) **How is visual and motor information represented throughout the brain? How do neural representations of sensorimotor tasks change with learning?**

I have highlighted that the extent of multisensory information throughout the cortex is only just coming to light. Previous underestimations are in part a result of the focus in electrophysiology in measuring the spiking output of neurons, which overlooks the sub-threshold modulation by other modalities. One advantage of functional magnetic resonance imaging (fMRI) is that we can acquire (almost) simultaneous data from throughout the brain, which is not a possibility in electrophysiology experiments. Despite this, until now no fMRI studies have investigated the representation of visual and motor information throughout cortex. In this thesis, I have used fMRI to explore the gradient of visual and motor information throughout the cortex. Participants were trained on a complex task in which they had to reach to targets in both typical and mirror-reversed environments, which allowed the dissociation of visual and motor information. Scanning participants both when they were expert and novice at the task allows us to assess how experience dependent plasticity (learning) affects how these two types of information are represented throughout the cortex. As previously discussed, interpreting absolute BOLD signal changes in the context of learning is fraught with confounds. I have used a pattern component model which allows the direct assessment of the neural activity patterns associated with each of the movements, and therefore I can assess the structure of how these movements are represented in each region, which enable inferences

regarding whether these regions are representing information in a visual or motor coordinate framework, or whether both coordinates frameworks are evident.

Chapter 2: Microstructural differences in the thalamus and thalamic radiations in the congenitally deaf

Abstract

The loss of the auditory modality and the consequent compensatory strategies used by deaf people create strong drivers for neuroplasticity. There is evidence for reorganisation of both visual and somatosensory function into auditory cortex in the deaf brain. However, the consequences for communication throughout the brain of this plasticity are unclear. In this chapter, we investigated whether there was evidence for plasticity in the thalamus and in thalamo-cortical afferents. The thalamus is of particular interest due to its critical role in controlling the flow of information throughout the cortex. We contrasted microstructural measurements of tissue properties derived from diffusion weighted magnetic resonance imaging data from 13 congenitally deaf and 13 hearing participants, all of whom had learnt British Sign Language after 10 years of age. Findings from two main analyses are presented. Firstly, we completed a connectivity based segmentation of the thalamus and contrasted the microstructural properties within each of these thalamic regions. This revealed changes to mean and radial diffusivity in the occipital and frontal thalamic regions. These differences may be linked to enhanced peripheral visual acuity, and differences in how visual attention is deployed in the deaf group. Following this, probabilistic tractography was used to trace tracts between the thalamus and its cortical targets, and microstructural measurements were extracted from these tracts. Group differences were found in microstructural measurements of occipital, frontal, somatosensory, motor and parietal thalamo-cortical tracts. These findings of thalamic plasticity and widespread alterations to the thalamo-cortical tracts suggest that the neuroanatomical consequences of congenital deafness are neither restricted to, nor focussed in auditory cortex. Instead, there is evidence that communication throughout the brain is affected.

Introduction

There is evidence of a number of different plastic processes in the deaf brain, which occur in response to, and to compensate for the atypical sensory environment. These include crossmodal (Nishimura et al., 1999, Petitto et al., 2000, Finney et al., 2001, MacSweeney et al., 2004, Fine et al., 2005), and intermodal plasticity (Buckley et al., 2010, Bottari et al., 2011, Codina et al., 2011), in addition to the dystrophic changes which occur in auditory cortex (Emmorey et al., 2003, Li et al., 2012). The thalamus is an important structure for regulating both the flow of information into the cortex and between cortical areas. Whether this structure is altered in congenitally deaf humans has not yet been investigated.

Crossmodal plasticity is evident in the congenitally deaf brain. Activation in secondary auditory cortices has been robustly demonstrated in fMRI studies in response to a wide range of visual stimuli, including sign language (Petitto et al., 2000, MacSweeney et al., 2002), biological motion (MacSweeney et al., 2004), as well as more simple visual stimuli such as dot motion (Finney et al., 2001). Controversy remains as to whether there is visual colonisation of Heschl's gyrus, the typical site of primary auditory cortex (A1). In deaf people, activation in response to visual stimuli has been reported in studies using spatial normalisation procedures (Finney et al., 2001), and in studies which do not contrast visual stimuli to a resting baseline (Karns et al., 2012, Scott et al., 2014). However, Cardin (2013) did not find activation in a cytoarchitectonically based definition of A1 when visual stimuli was contrasted to a resting baseline in deaf participants.

Somatosensory processing has been shown to be enhanced (Levanen and Hamdorf, 2001), and reorganised into auditory cortex in deaf people (Levanen et al., 1998, Auer et al., 2007, Karns et al., 2012). The use of spatial normalisation to a common template for MRI data (Auer et al., 2007), and MEG data (Levanen et al., 1998) preclude confident anatomical localisation of this activation to primary auditory cortex. However, when anatomical definitions of the regions are used, there is strong evidence of somatosensory takeover of

primary auditory cortex (Karns et al., 2012). Findings from the animal literature also concur with this (Allman et al., 2009, Meredith et al., 2012). Single unit recordings from the auditory cortex of early deafened ferrets (oto-toxic lesions) have demonstrated somatosensory afferents in auditory cortex (Meredith and Allman, 2012). Tracer injections to the auditory core of these deafened animals revealed the same auditory thalamo-cortical projection sources as the hearing ferrets, which the authors interpreted as indicating that rather than new or unmasked latent projections, reorganisation occurred at the level of the brainstem (Meredith and Allman, 2012).

In addition, there is evidence of intermodal plasticity in deafness. Deafness enhances detection of both static and motion targets in the visual periphery (Neville and Lawson, 1987, Loke and Song, 1991). This behavioural advantage is thought to facilitate orienting to targets in the absence of sound (Merabet and Pascual-Leone, 2010). These changes have been linked to increases in the area of neural rim within the optic nerve head, and thicker retinal nerve fibre layer in temporal (peripheral) retina (Codina et al., 2011). Differences in visual event-related potentials (ERPs) have also been observed in early visual cortex in deaf groups, which in turn were correlated with improved performance in a visual target detection task (Bottari et al., 2011).

That the function of a brain region is tightly coupled with its extrinsic anatomical connections is a widely held assumption in neuroscience. It follows that the inputs to a region affect what information is available to a region, and where the outputs of a region terminate determines the influence a region will have. Empirical tests of this hypothesis have supported this assumption (Passingham et al., 2002, Saygin et al., 2011), and indeed, anatomical connectivity data can be used to define functionally distinct regions (Behrens et al., 2003, Johansen-Berg et al., 2004, Behrens et al., 2006, Rushworth et al., 2006). Thus we argue that functional imaging studies concerning plasticity as a result of deafness should be considered in the context of changes to anatomical connectivity patterns. This complementary approach

may elucidate why certain patterns of reorganisation are seen in one brain region or modality, but not others.

Plastic change in the deaf brain may occur via a number of different mechanisms, none of which are mutually exclusive, and are likely to have a different impact depending on the brain region (Bavelier and Neville, 2002). For example, visual activation in secondary auditory cortices may occur through synaptic re-weighting of these regions, which typically act as a site for audiovisual integration (Calvert et al., 2000, Lee and Noppeney, 2011, McGettigan et al., 2012). Alternatively, the 'brainstem theory of crossmodal reorganisation' proposes that neither new nor latent projections are responsible for reorganisation, but instead, somatosensory inputs are able to takeover dormant auditory inputs found in the typically developing auditory brainstem at several nodes (Meredith and Allman, 2012). Subcortical connectivity changes have been suggested to contribute to crossmodal reorganisation as a result of congenital deafness, however, research into this possibility has as yet been limited to animal studies (Proksch and Bavelier, 2002).

In this chapter, we investigated how congenital deafness affects the thalamus, and thalamo-cortical projections. The thalamus has a critical role in regulating the flow of information into the cortex, as a substantial amount of information coming into the cortex does so through the thalamus (Sherman, 2007). In addition, and perhaps more importantly, the thalamus mediates cortico-thalamo-cortical connections, which make it ideally positioned functionally and anatomically to modulate a variety of different cognitive functions, which include emotion, motivation and multimodal perception (Sherman, 2007, Jones, 2009). Based on the overlapping nature of projections from different sensory modalities, the thalamus has additionally been suggested as a site of multimodal interplay (Cappe et al., 2009a, Cappe et al., 2009b). This has led to recent interest in the functional consequences of thalamic stroke (Carrera and Bogousslavsky, 2006), and the role of the thalamus in neurodevelopmental disorders such as autism spectrum disorder (Nair et al., 2013). Therefore, it is possible that

looking at changes to the anatomy of the thalamus and thalamo-cortical tracts may illuminate the functional consequences of auditory deprivation.

Diffusion weighted magnetic resonance imaging (DW-MRI) is currently the only method for characterising neural tissue microstructure and reconstructing white matter tracts *in vivo*. Magnetic field gradients are used to sensitise the MRI signal acquisition to the displacement of water molecules due to Brownian motion. The application of diffusion gradients along multiple geometric directions allows the estimation of directional molecule displacement in the tissue sampled (Johansen-Berg and Rushworth, 2009). These data can be summarized by a diffusion tensor model, which describes the magnitude of the three principal axes of molecule displacement at each voxel sampled. Diffusion of water molecules is hindered by tissue properties, and in the case of white matter these include (but are not specific to) axonal ordering, axonal density and the degree of myelination (Johansen-Berg and Behrens, 2006). These underlying tissue properties can be approximated using tensor-derived microstructural metrics. These include fractional anisotropy (degree to which the first eigenvector dominates the second two), mean diffusivity (overall water diffusion in the specific voxel), and radial diffusivity (diffusion perpendicular to the principal eigenvector of the diffusion tensor).

Tractography with DW-MRI involves reconstructing continuous long range trajectories from voxel-wise estimates of the fibre orientation (Jones et al., 2013). From a seed region, streamlines can be traced in a probabilistic iterative fashion to determine the most likely path of the white matter tract of interest (Behrens et al., 2003). Tractography can be used to determine whether tracts exist between regions, and also to compare tracts in terms of their microstructural properties between groups (Johansen-Berg and Rushworth, 2009). Additionally, connectivity based segmentations of anatomical structures can be completed, in which structures are segmented on the basis of the highest probability of connection with different anatomical targets (Behrens et al., 2003). Behrens et al., first demonstrated this by

generating a connectivity based segmentation of the thalamus, which closely resembled those derived from both animal anatomical tract tracing studies (Jones, 1985), and histological analyses (Morel et al., 1997).

DW-MRI data only detects the axis of diffusion (Johansen-Berg and Rushworth, 2009), and so we cannot differentiate between anatomical connections carrying information from the thalamus to its cortical targets (thalamo-cortical feedforward connections) from those carrying information from cortical targets to the thalamus (cortico-thalamic feedback connections). For simplicity, and to indicate that we have traced from thalamus to cortex, throughout this chapter these tracts are referred to as thalamo-cortical connections with the understanding that they are likely to incorporate both feedforward and feedback connections.

To investigate the possible influence of congenital deafness on the anatomy of the thalamus, we first parcellated the thalamus based on connectivity profiles with its primary cortical targets. We contrasted the scalar microstructural measures of fractional anisotropy (FA), mean diffusivity (MD), and radial diffusivity (RD) in each parcellation between deaf and hearing groups. Second, to investigate the possibility of altered thalamo-cortical connectivity in congenital deafness, we reconstructed the tracts between the thalamus and its primary cortical targets, extracted microstructural measures from each of these tracts, and then contrasted these between deaf and hearing groups.

Methods

Participants

Thirty right-handed participants were scanned. Fifteen were congenitally deaf and 15 were hearing. Deaf participants were either severely or profoundly deaf in both ears. All participants were screened to ensure they had no previous neurological or psychiatric history, current health problems, and were not taking psychoactive medication. One male deaf participant was excluded due to excessive motion artefacts, and a further deaf and a hearing male were excluded due to poor image quality. One hearing female participant was found to

have an arteriovenous malformation, and was excluded from further analysis. This left 13 hearing (10 female) and 13 deaf (7 female) participants. For the 13 deaf participants, 5 were deaf through maternal rubella, 3 reported genetics as their cause of deafness, and 5 had an unknown cause of deafness. As vascular lesions causing intellectual disability can also occur as a result of maternal rubella, all images were screened by an experienced neuroanatomist (MIS). No other neuroanatomical anomalies were detected. Furthermore, all deaf participants were either in skilled employment or higher education at the time of testing. The groups (following exclusion) did not differ in terms of age (*t(24)=-0.11, p=0.921*, hearing mean 38.7(sd=8.1), deaf mean 39.08 (sd=11.08)).

Here, we study deaf people who did not learn British Sign Language (BSL) until 10 years of age, as previous studies of the neural bases of visual motion processing have reported an interaction between the influence of deafness and native acquisition of sign language (Bavelier et al., 2001, Brozinsky and Bavelier, 2001). All deaf participants were born to hearing parents. To control for the effect of having learnt a visual manual language, we recruited hearing participants who had also learnt BSL after the age of 10. The deaf group were younger than the hearing group when they began to learn (*t(24)=3.263, p=0.003,* hearing mean 25.6 (sd=7.63), deaf mean 17.29 (sd=4.68)). Many of the hearing group used BSL in a professional context as interpreters, teachers of the deaf or researchers in the field. With regard to language use before exposure to BSL, of the 13 deaf participants, 11 reported that they could fluently converse with hearing people in everyday situations through the use of lip-reading. This suggests that for these deaf participants, spoken English was used as a robust and secure first language. The remaining 2 reported they were unable to make use of speech-reading in everyday situations, which indicates they may have insecure first language development. We additionally completed analyses excluding these participants, to test whether they were driving any observed effects. None of the participants were educated in BSL. Eleven deaf participants reported they were educated via spoken language only, whereas 2 reported their school made use of sign supported English (using manual signs to support spoken English).

The study was approved by UCL Ethics Committee and participants provided informed consent.

Imaging Protocol

Data acquisition was carried out at the Birkbeck UCL Centre for Neuroimaging using a 1.5T Siemens Avanto MRI scanner (Erlangen, Germany). Diffusion weighted images were acquired using a diffusion weighted EPI sequence (TR=7500ms TE=104ms) with a 32 channel head coil. Whole brain volumes were acquired with 46 contiguous axial slices. Voxel size was 2.3mm^3. Diffusion-sensitizing encoding gradients were applied in 64 directions (b=1000s/mm^2) and 1 volume was acquired without diffusion weighting (b=0s/mm^2).

Two diffusion weighted scans were acquired from participants in all instances, apart from one female hearing participant who had her second scan aborted due to reporting shoulder pain.

An MPRAGE structural sequence with voxel size of 1mm^3, flip angle of 7°, T1=1000ms, TR=8.4ms, TE=3.57ms and BW=190 Hz/pix was acquired, also using the 32 channel head coil.

Image Analysis

Cortical reconstruction was completed using FreeSurfer 5.0.0 (http://surfer.nmr.mgh.harvard.edu/). Comprehensive details of these procedures are provided in previous publications (Dale et al., 1999, Fischl, 1999, Fischl et al., 1999, Fischl and Dale, 2000, Fischl et al., 2001, Fischl et al., 2002, Fischl et al., 2004, Segonne et al., 2004, Han et al., 2006, Jovicich et al., 2006). Briefly, brightness and contrast normalization are performed on the images, and then all non-brain tissue are removed with a hybrid watershed/surface deformation procedure (Segonne et al., 2004). Images then undergo Talairach transformation, subcortical white matter and deep grey matter structures are segmented (Fischl et al., 2004), the grey white matter boundary is tessellated, topology automatically corrected (Fischl et al., 2001, Segonne et al., 2007), and surface deformation is performed using intensity gradients to

optimally place the grey/white and grey/CSF borders where the greatest change in intensity signifies transition to the other tissue class (Dale et al., 1999).

DW MRI Pre-processing

All processing and analysis of DW-MRI data was completed in FSL 5.0 (http://fsl.fmrib.ox.ac.uk/fsl/fslwiki/). Eddy current and movement correction were completed with the FMRIB Diffusion Toolbox (FDT). Following this, the two DW-MRI scans taken of each participant were averaged by taking the arithmetic mean of each voxel across scans. Each individual's structural T1 image was registered with their diffusion data using the FMRIB Linear Image Registration Tool (FLIRT). DTIFIT was then used to fit a diffusion tensor model and generate FA, MD and RD maps, and the BEDPOSTX toolbox was used subsequent to this to fit a ball-and-stick model to the data. The complexity of underlying tissue structure can be estimated, and this information incorporated in a Bayesian manner into a crossing fibres model to account for situations in which two fibre bundles cross within a voxel (Behrens et al., 2007). This algorithm runs Markov Chain Monte Carlo sampling to build up distributions of diffusion parameters at each voxel, enabling the modeling of crossing fibres within a voxel, and the number of crossing fibres present in each voxel (Behrens et al., 2007).

Regions of Interest

The FreeSurfer cortical and subcortical segmentation were used to generate regions of interest (ROI). Specifically, the thalamus label generated in either hemisphere was used for the seed mask. A total of 6 target masks were used, which included occipital, temporal, parietal and frontal lobes, in addition to somatosensory cortex in the postcentral gyrus, and motor cortex in the precentral gyrus, which were analogous to cortical targets for thalamic parcellation in Behrens et al., (2003). Labels generated from the FreeSurfer cortical reconstructions were merged to form these regions, as demonstrated in figure 2.1. Specific labels from the Destrieux atlas in FreeSurfer in each parcellation are detailed in table 2.1

(Destrieux et al., 2010). These masks were additionally registered to the diffusion data using FLIRT, and subsequently binarised to carry out the tractography procedures.

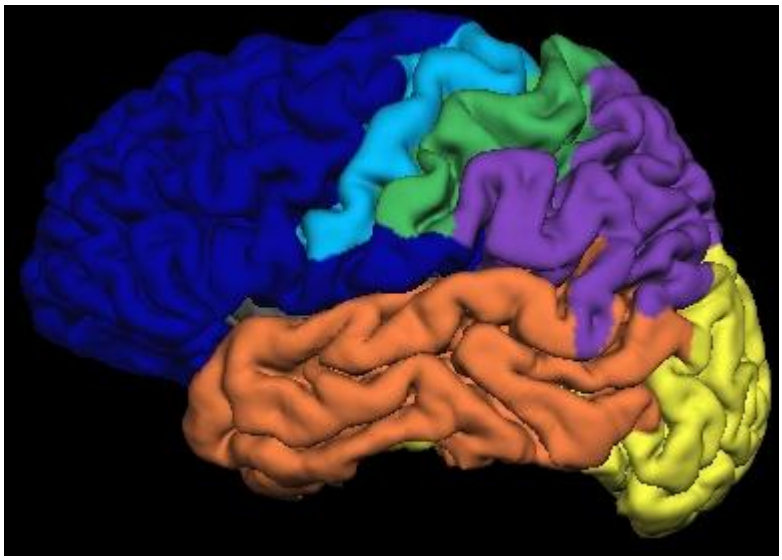

Figure 2.1: *Cortical target masks are demonstrated in a representative participant. The cortex has been divided into frontal (dark blue), motor (light blue), somatosensory (green), parietal (purple), temporal (orange) and occipital (yellow) regions.*

Connectivity Based Segmentation of Thalamus

The probtrackx software in FDT was used to generate probabilistic tracts from the seed ROI (thalamus) to the cortical target masks (occipital / parietal / temporal / motor / somatosensory / frontal). For every seed and target pair, 5000 streamlines were initiated, and a curvature threshold of 0.2 was set in order to prevent the generation of anatomically unlikely tracts. Step size was set to 0.5mm, and the number of steps to 2000. To reduce the complexity (and resulting ambiguity) of the tractography, and as the thalamus is predominantly unilaterally organised, only ipsilateral thalamo-cortical connections were considered. An exclusion mask along the midline of the contralateral hemisphere was generated to prevent the crossing of tracts into this region.

Following this, segmentation was performed with a 'winner takes all' approach, whereby each voxel in the thalamus is classified based upon the cortical target with which it has the highest probability of being connected to. The parcellations generated from this were thresholded so

all tracts which did not have at least 3000 of the 5000 streamlines (60%) reaching the target were discarded, in order to remove all connections with a low associated probability. The resulting images were then used as ROIs to extract FA, MD and RD values.

Thalamo-cortical Tracts

In addition to the thalamic parcellations, we examined tracts between the thalamus and individual cortical targets. Grey matter is more isotropic than white matter, and as such, the signal to noise ratio is lower, making diffusion indices in regions such as the thalamus relatively insensitive in comparison to those measured in white matter. To keep the analysis of tracts independent from the analysis of the thalamic parcellations, we used the entire thalamus as the seed region (as opposed to the parcellation derived from the connectivity based segmentation). The same cortical target masks were used as before. Again, 5000 streamlines were initiated, a curvature threshold was set to 0.2, step size was constrained to 0.5mm and number of steps to 2000. To ensure anatomical specificity of the tracts, we completed a 'winner takes all' segmentation of cortical white matter voxels. When a voxel appeared in more than one thalamo-cortical tract, it was removed from all thalamo-cortical tracts, apart from the tract with the greatest probability of connection (highest number of streamlines). The output of the tractography was thresholded at 60% in order to reduce the contribution to the microstructural analysis of voxels with a low connection probability.

Cortical Target	Labels	
Occipital	• *h.S_oc_middle_and_Lunatus • *h.G_and_S_occipital_inf • *h.G_occipital_middle • *h.G_occipital_sup • *h. h.G_oc-temp_lat-fusifor • *h.Pole_occipital • *h.G_cuneus • *h.G_oc-temp_med-Lingual	• *h.S_calcarine • *h.S_collat_transv_post • *h.S_oc_middle_and_Lunatus • *h.S_oc_sup_and_transversal • *h.S_occipital_ant • *h.S_oc-temp_lat • *h.S_oc-temp_med_and_Lingual
Parietal	• *h.S_subparietal • *h.G_parietal_sup • *h.G_pariet_inf-Supramar • *h.G_precuneus • *h.S_parieto_occipital • *h.G_pariet_inf-Angular • *h.S_intrapariet_and_P_trans	
Temporal	• *h.G_temp_sup-G_T_transv • *h.G_temp_sup-Lateral • *h.G_temp_sup-Plan_polar • *h.G_temp_sup-Plan_tempo • *h.G_temporal_inf • *h.G_temporal_middle • *h.S_temporal_inf • *h.S_collat_transv_ant	• *h.S_temporal_sup • *h.S_temporal_transverse • *h.Pole_temporal • *h.S_interm_prim-Jensen • *h.Lat_Fis-post
Frontal	• *h.G_front_inf-Opercular • *h.G_front_inf-Orbital • *h.G_front_inf-Triangul • *h.G_front_middle • *h.G_and_S_frontomargin • *h.G_and_S_transv_frontopol • *h.G_rectus • *h.S_front_inf • *h.S_orbital_lateral • *h.S_orbital_med-olfact	• *h.S_orbital-H_Shaped • *h.Lat_Fis-ant-Horizont • *h.Lat_Fis-ant-Vertical • *h.S_front_middle • *h.G_front_sup • *h.G_orbital • *h.S_suborbital • *h.S_front_sup • *h.G_and_S_subcentral
Motor	• *h.G_precentral • *h.S_precentral-inf-part • *h.S_precentral-sup-part	
Somato-sensory	• *h.S_central • *h.S_postcentral • *h.G_postcentral • *h.G_and_S_paracentral	

Table 2.1*:FreeSurfer labels from the Destrieux atlas which were merged from each hemisphere in order to form the cortical target.*

Results

Connectivity Based Segmentation of Thalamus

We first completed a connectivity based segmentation of the thalamus, using 6 cortical targets including occipital, parietal, temporal, frontal, motor and somatosensory cortex. An example of the thalamic parcellation is provided in figure 2.2. The thalamic parcellations generated here are comparable to those generated by other researchers using this method (Behrens et al., 2003).

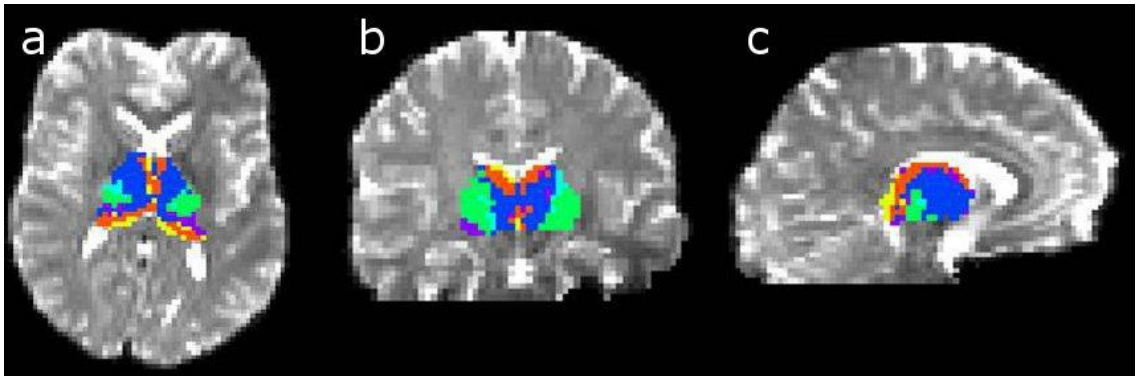

Figure 2.2: *The connectivity based thalamic parcellation is demonstrated in a representative hearing participant in; a)axial, b)coronal and c)sagittal views. The thalamus has been divided into frontal (dark blue), motor (light blue), somatosensory (green), parietal (purple), temporal (orange) and occipital (yellow) regions.*

To determine whether microstructural measures recorded from the same thalamic parcellation in either hemisphere were independent, and so should be treated as such in statistical analyses, we first correlated microstructural measurements from each parcellation measured in the right and left hemisphere. Table 2.2 shows the results of this analysis, which demonstrates that MD and RD measures are highly correlated. FA measures are correlated in the frontal parcellation, and there was also a trend towards correlation in the somatosensory tract. As such, we accounted for the non-independence of the hemispheres in the analyses.

For FA, MD and RD data, we used a mixed model repeated measures ANOVA with a between-subjects factor of group (deaf/hearing), 6 within-subjects factors of thalamic parcellation (occipital / temporal / parietal / motor / somatosensory / frontal), and modelled participants as random effects to account for correlated random errors between the hemispheres for each participant. For FA, there were main effects of group (*F(1,300)=4.71, p=0.031*), parcellation (*F(5,300)=105.65, p<0.001*), but no interaction between group and parcellation (F(5,300)=1.59, p=0.162). For MD, there were main effects of group (*F(1, 300)=13.61, p<0.001*), parcellation (*F(5, 300)=81.68, p<0.001*), and an interaction between group and parcellation (*F(5,300)=5.41, p<0.001*). Analysis of the RD measurements revealed there were main effects of group (*F(1,300)=12.05, p=0.001*), parcellation (*F(5, 300)=92.08, p<0.001*), and an interaction between group and parcellation (*F(5,300)=5.95, p<0.001*). Thus microstructural measurements in thalamic parcellations differed between groups.

We further investigated these findings with post-hoc t-tests, the results of which are displayed in table 2.3. The p values presented have had a false discovery rate correction (FDR) applied to control for multiple comparisons. This demonstrates that results were driven by the deaf group having increased MD and RD in both frontal and occipital thalamic parcellations. Table 2.4 shows mean values and standard deviations for microstructural measures for the groups in each thalamic parcellation.

	Frontal		Motor		Somatosensory		Temporal		Parietal		Occipital	
	R^2	p	R^2	p	R^2	p	R^2	p	R^2	p	R^2	p
FA	0.4814	0.0128	0.1744	0.3942	0.3615	0.0696	0.1866	0.3614	0.1737	0.369	0.3187	0.1125
MD	0.8714	<0.001	0.8829	<0.001	0.9004	<0.001	0.4067	0.0392	0.8589	<0.001	0.5307	0.1125
RD	0.8775	<0.001	0.8636	<0.001	0.8369	<0.001	0.4073	<0.039	0.8526	<0.001	0.5101	0.0078

Table 2.2: *Correlation coefficient (R^2) and p values are displayed for the correlation of microstructural measurements from parcellations in either hemisphere.*

	Frontal		Motor		Somatosensory		Temporal		Parietal		Occipital	
	t	p	t	p	T	p	t	p	t	p	t	p
FA	1.4432	0.3791	1.7911	0.2380	1.8654	0.2380	1.3974	0.3791	0.8806	0.4985	0.1803	0.8577
MD	7.8439	**<0.001**	0.6783	0.5647	0.8713	0.4985	0.5734	0.6024	0.9473	0.4985	3.5274	**0.0055**
RD	8.1209	**<0.001**	1.0848	0.4985	1.1505	0.4985	0.6764	0.5647	1.0010	0.4985	3.4298	**0.0055**

Table 2.3: *Microstructural measurements for each thalamic parcellation. T statistics and p values (with a FDR correction applied, α=0.05) are provided, the degrees of freedom is 50 in all instances. Significant results are denoted in bold typeface.*

	Frontal		Motor Zone		Somatosensory		Temporal		Parietal		Occipital	
	H	D	H	D	H	D	H	D	H	D	H	D
FA	0.3458 (0.0202)	0.3371 (0.0252)	0.3954 (0.0666)	0.4251 (0.0521)	0.4135 (0.0479)	0.4338 (0.0278)	0.2966 (0.0249)	0.3093 (0.0393)	0.3468 (0.0283)	0.3556 (0.0420)	0.2767 (0.0501)	0.2744 (0.0379)
MD	0.0009 (0.0001)	0.0011 (0.0001)	0.0008 (0.0002)	0.0008 (0.0001)	0.0008 (0.0001)	0.0007 (0.000)	0.0012 (0.0002)	0.0012 (0.0002)	0.0008 (0.0001)	0.0009 (0.0002)	0.0011 (0.0002)	0.0013 (0.0002)
RD	0.0007 (0.0001)	0.0009 (0.0001)	0.0006 (0.0002)	0.0006 (0.0001)	0.0006 (0.0001)	0.0006 (0.000)	0.0010 (0.0002)	0.0010 (0.0002)	0.0007 (0.0001)	0.0007 (0.0002)	0.0010 (0.0002)	0.0012 (0.0002)

Table 2.4: *Mean (standard deviation) for hearing and deaf groups in microstructural measurements in thalamic parcellations.*

	Frontal		Motor Zone		Somatosensory		Temporal		Parietal		Occipital	
	t	p	t	p	t	p	t	p	t	p	t	p
FA	1.1016	0.3827	2.2856	0.0970	1.8629	0.2066	1.2477	0.3827	0.8886	0.4546	0.2255	0.8226
MD	7.8008	**<0.001**	1.329	0.3827	0.9257	0.4546	0.5932	0.5887	1.1617	0.3827	3.3680	**0.0078**
RD	8.0257	**<0.001**	1.7213	0.2364	1.1487	0.3827	0.7257	0.5307	1.232	0.3827	3.3283	**0.0078**

Table 2.5: *Microstructural measurements for each thalamic parcellation when participants from the deaf group with insecure first language acquisition are excluded. T statistics and p values (with a FDR correction applied, α=0.05) are provided, the degrees of freedom in 46 in all instances.*

	Frontal		Motor		Somatosensory		Temporal		Parietal		Occipital	
	R^2	p	R^2	p	R^2	p	R^2	p	R^2	p	R^2	p
FA	0.824	<0.001	0.933	<0.001	0.891	<0.001	0.655	<0.001	0.818	<0.001	0.867	<0.001
MD	0.751	<0.001	0.776	<0.001	0.675	<0.001	0.623	<0.001	0.695	<0.001	0.397	<0.001
RD	0.752	<0.001	0.826	<0.001	0.749	<0.001	0.644	<0.001	0.673	<0.001	0.394	0.046

Table 2.6: *Correlation coefficient (R^2) and p values for the correlation between microstructural measurements in left and right hemisphere in all cortico-thalamic tracts.*

	Frontal		Motor Zone		Somatosensory		Temporal		Parietal		Occipital	
	t	p	t	p	t	p	t	p	t	p	t	p
FA	3.3446	**0.0071**	3.4278	**0.0071**	4.4131	**0.0010**	0.1368	0.8918	3.1912	**0.0088**	4.1722	**0.0011**
MD	1.5819	0.2073	2.4871	**0.0418**	1.5533	0.2073	1.0803	0.4278	0.8570	0.5086	0.3689	0.7558
RD	2.2424	0.0588	2.6846	**0.0295**	2.3787	0.0478	0.9410	0.4863	0.443	0.7420	0.5225	0.7244

Table 2.7: *T statistics and p values are shown for post hoc t tests on thalamo-cortical tracts. A FDR correction has been applied (α=0.05), and the degrees of freedom is 50 in all instances.*

	Frontal		Motor Zone		Somatosensory		Temporal		Parietal		Occipital	
	H	D	H	D	H	D	H	D	H	D	H	D
FA	0.3593 (0.0326)	0.3345 (0.0193)	0.3747 (0.0731)	0.3237 (0.0200)	0.4014 (0.0672)	0.3390 (0.0262)	0.3007 (0.0294)	0.2996 (0.0286)	0.3890 (0.0495)	0.3554 (0.0211)	0.3820 (0.0462)	0.3408 (0.0199)
MD	0.0008 (0.00004)	0.0009 (0.00004)	0.0008 (0.0001)	0.0009 (0.00004)	0.0008 (0.0001)	0.0009 (0.00005)	0.0010 (0.00008)	0.0010 (0.00009)	0.0008 (0.00006)	0.0008 (0.00003)	0.0010 (0.0001)	0.0010 (0.00009)
RD	0.0007 (0.00004)	0.0007 (0.00004)	0.0007 (0.0001)	0.0007 (0.00004)	0.0006 (0.0001)	0.0007 (0.00005)	0.0008 (0.00008)	0.0008 (0.00009)	0.0007 (0.00007)	0.0007 (0.00003)	0.0008 (0.0001)	0.0008 (0.00009)

Table 2.8: *Mean and standard deviation are presented for each of the microstructural measurements in each tract for hearing and deaf groups.*

	Frontal		Motor		Somatosensory		Temporal		Parietal		Occipital	
	t	p	t	p	T	p	t	p	t	p	t	p
FA	3.4282	**0.0077**	2.9832	**0.0155**	3.8106	**0.0037**	0.4246	0.7219	3.1046	**0.0147**	3.9812	**0.0037**
MD	2.3777	**0.0484**	2.3306	**0.0484**	1.4557	0.2492	0.5413	0.7219	0.4909	0.7219	0.2065	0.8373
RD	2.9366	**0.0155**	2.4683	**0.0446**	2.1122	0.0722	0.4127	0.7219	0.6403	0.7219	0.6138	0.7219

Table 2.9: *T statistics and p values for microstructural measurements in each of the thalamo-cortical tracts, once the 2 participants who may not have secure first language development have been excluded. A FDR correction has been applied (α=0.05), and degrees of freedom is 46 in all instances.*

To discern whether results were influenced by two of the deaf participants potentially having insecure first language development, we repeated the analyses excluding these two participants. For FA, there were main effects of group ($F(1,276)=5.99, p=0.015$), parcellation ($F(5,276)=101.05, p<0.001$), and a trend towards a significant interaction between group and parcellation ($F(5,276)=2.07, p=0.069$). For MD, there were main effects of group ($F(1,276)=11.8, p=0.001$), parcellation ($F(5,276)=76.81, p<0.001$), and an interaction between group and parcellation ($F(5,276)=5.98, p<0.001$). For RD, there were main effects of group ($F(1,276)=10.76, p=0.001$), parcellation ($F(5,276)=87.02, p<0.001$), and an interaction between group and parcellation ($F(5,276)=6.64, p<0.001$). Again, we followed up these results with post-hoc t-tests (table 2.5), which revealed elevated MD and RD values in the deaf group in both frontal and occipital thalamic parcellations. This replicates the group results when these participants were included.

Thalamo-cortical Tracts

As a second analysis, we calculated microstructural measures in the tracts between the thalamus and each of the cortical targets. Figure 2.3 demonstrates these reconstructed tracts in a representative participant.

Table 2.6 demonstrates that in the majority of tracts, microstructural properties measured in either hemisphere were highly correlated. As such, we used a mixed model repeated measures ANOVA with between-subjects effects of group (deaf/hearing) and within-subjects thalamo-cortical tract (occipital / temporal / parietal / motor / somatosensory / frontal), and modelled participants as random effects to account for correlated random errors between each participant's hemispheres.

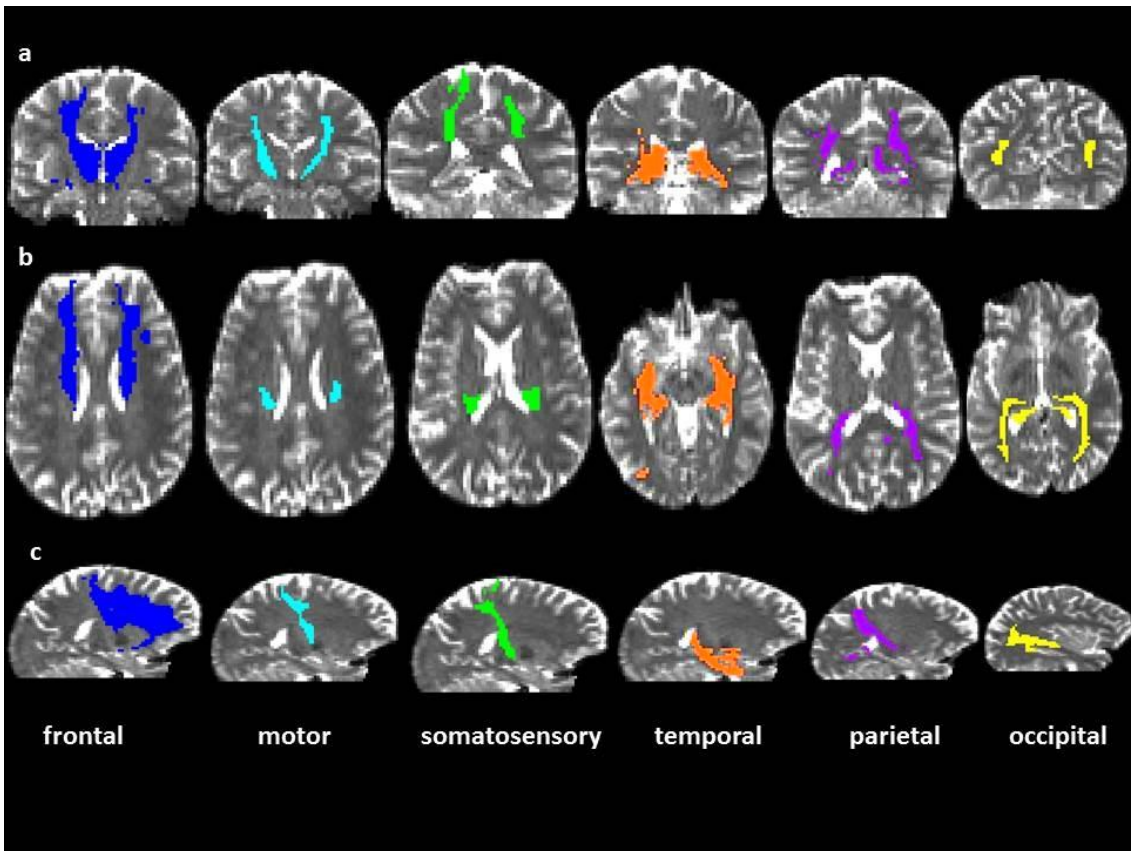

Figure 2.3: *In a representative hearing participant each of the thalamo-cortical tracts are demonstrated in axial, coronal and sagittal slices; a)frontal, b)motor, c)somatosensory, d)temporal, e)parietal and f)occipital.*

For FA, there were main effects of group (*F(1, 300)=61.19, p<0.001*), tract (*F(5, 300)=22.53, p<0.001*), and an interaction between group and tract (*F(5, 300)=3.68, p=0.003*). Analysis of the MD data revealed no main effect of group (*F(1, 300)=1.24, p=0.297*), but a main effect of tract (*F(5, 300)=61.338*), and no interaction between tract and group (*F(5, 300)=2.16, p=0.059*). Finally, for the RD measures there were main effects of group (*F(1, 300)=7.77, p=0.006*), tract (*F(5, 300)=54.72, p<0.001*) and an interaction between group and tract (*F(5, 300)=2.35, p=0.041*).

Following this, we performed post hoc t-tests to determine the source of the differences between groups; these results are presented in table 2.7, and the mean and standard deviation of these tracts for each of the groups are presented in table 2.8.

Again, the p values presented have had a false discovery rate correction (FDR) applied to control for multiple comparisons. FA is reduced in the frontal thalamo-cortical tract in the deaf group. The motor thalamo-cortical tract is profoundly affected by deafness, with the deaf group demonstrating lower FA, increased MD and increased RD in this tract. The somatosensory thalamo-cortical tract is similarly affected, with decreased FA and increased RD in the deaf group. In both the parietal and occipital thalamo-cortical tracts, FA is reduced in the deaf group. These results are summarised in figure 2.4.

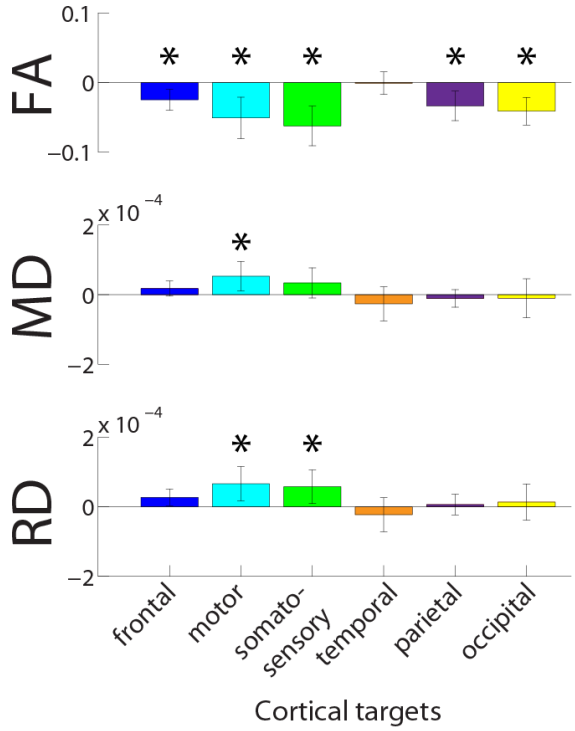

Figure 2.4: *For microstructural measures in each of the thalamo-cortical tracts, the difference of the deaf group relative to the hearing group is displayed. Error bars denote confidence interval of the t-test statistic. Colour scheme is the same as figures 2.1-2.3.*

Again, we completed the analysis excluding the two subjects with insecure first language acquisition, and found for the FA values main effects of group (*F(1, 276)=53.07, p<0.001*), tract (*F(5,276)=20.71, p<0.001*), and an interaction between tract and group (*F(5,276)=2.52, p=0.03*). For the MD values, there was no main effect of group (*F(1,276)=2.6, p=0.108*), but a main effect of tract (*F(5,276)=55.5, p<0.001*). There was no interaction between group and tract (*F(5,276)=1.53, p=0.18*). For the RD values, there were main effects

of group (*F(1,276)=9.39, p=0.002*), tract (*F(5,276)=49.99, p<0.001*), but no interaction between group and tract (*F(5,276)=1.55, p=0.175*).

Post-hoc t-tests which are presented in table 2.9 demonstrate that the frontal thalamo-cortical tract has decreased FA, and increased MD and RD in the deaf group. The motor thalamo-cortical tract has reduced FA, and increased MD and RD in the deaf group. FA is also decreased in the deaf group in the somatosensory, parietal and occipital thalamo-cortical tracts. The findings were comparable to when the entire group was analysed.

Discussion

From previous studies there is evidence of plasticity throughout the deaf brain. This includes crossmodal plasticity, in which visual and somatosensory stimuli come to be processed in auditory cortex (Levanen et al., 1998, Nishimura et al., 1999, Finney et al., 2001, MacSweeney et al., 2004, Fine et al., 2005, Auer et al., 2007, Karns et al., 2012), and intermodal plasticity (Buckley et al., 2010, Bottari et al., 2011, Codina et al., 2011), whereby the visual system is altered to compensate for hearing loss. In addition to this, there are dystrophic changes in auditory cortex (Kim et al., 2009, Li et al., 2012). In this study, we show that following connectivity based segmentation of the thalamus, the microstructural measurements of mean diffusivity (MD), and radial diffusivity (RD), were increased in the deaf group in the frontal and occipital thalamic parcellations. The thalamus supports many functions including relaying information to the cortex, modulating the communication between different cortical areas, and is suggested to be a site of multimodal interplay. Microstructural measurements were affected in the thalamo-cortical tracts to frontal, somatosensory, motor, parietal and occipital cortical targets, and the frontal and occipital thalamic parcellations. Changes in these microstructural measurements of thalamic parcellations and thalamo-cortical tracts suggest congenital deafness affects communication throughout the brain.

The mapping between DW-MRI diffusion tensor data and brain microstructure is a complex non-linear problem, which requires certain assumptions and provides no unique solution (Jones et al., 2013). Voxel-wise diffusion measures generated during the course of fitting the tensor model do not correspond directly to the anatomical features of potential interest, such as membrane integrity, axon diameter, axon count, myelin thickness and packing density of cells (Johansen-Berg and Rushworth, 2009). Therefore the biological significance of these metrics can be unclear. Nevertheless, we can interpret differences between groups in these microstructural measurements in light of findings from both the anatomical literature in animals and functional imaging studies with deaf participants. This enables us to draw tentative inferences about what underlying differences in grey and white matter tissue may be responsible for the differences in diffusion we have found.

Recently, the increased ability of deaf people to be able to detect motion and static targets in the visual periphery has been linked to plasticity in the visual processing stream. Increased neuroretinal rim area (which is thought to be linked to increased retinal ganglion cell number) has been demonstrated in deaf participants, as well as thicker retinal nerve fibre layer in peripapillary regions which correspond to temporal retina (Codina et al., 2011). These changes are linked to changes in visual field size as measured by Goldmann Perimetry (Codina et al., 2011). The optic nerve projects to the lateral geniculate nucleus of the thalamus, which projects to visual cortex. Previous studies have shown alterations in FA in the forceps major and splenium of the corpus callosum at the site of inter-hemispheric connections between visual cortices (Kim et al., 2009, Li et al., 2012), suggesting deafness affects connectivity in the visual system. In this chapter, in the occipital thalamic parcellation, both MD and RD were increased in the deaf group. An increase in MD corresponds to an increase overall in the amount of diffusion which occurs in each voxel, and the concomitant increase in RD indicates that this is a result of increased diffusion in the axis parallel to the principal direction of diffusion. The visual thalamo-cortical tract additionally exhibited reduced FA. These changes

may suggest increased tissue complexity in these regions. It is possible that these changes are linked to the enhanced peripheral acuity and visual field size reported in deaf people.

The fronto-parietal attention network is implicated in the top down modulatory signals to both the thalamus and early sensory areas (Gilbert and Sigman, 2007). Information in each of these regions then competes for representation in working memory in pre-frontal cortex (Knudsen, 2004), which is implicated in attentional selection signals (Buschman and Miller, 2007). A role for the lateral intraparietal area in generating a spatial priority map through behavioural prioritisation of stimuli in a modality independent manner has also been posited (Bisley and Goldberg, 2010). Thus the increased MD and RD in the frontal thalamic parcellation and decreased FA in the frontal and parietal thalamo-cortical tracts in the deaf group may reflect the instantiation of altered attentional control and multimodal perception in the deaf brain.

The brainstem theory of crossmodal reorganisation proposes that in deafness, somatosensory afferents commandeer inert auditory afferents in auditory brainstem (Meredith and Allman, 2012). This results in crossmodal reorganisation, without the generation of new projections. We find no evidence of changes to somatosensory or auditory thalamus, which is consistent with this theory. Whilst it is problematic to interpret a null result, findings of significant alterations to frontal and occipital thalamus indicate that the methods can be sensitive to microstructural differences in grey matter in the populations studied. The somatosensory thalamo-cortical tract has decreased FA and increased RD in the deaf group. These findings may be the anatomical correlate of there being an enhanced and more spatially distributed somatosensory representation in the deaf brain.

Somewhat counter-intuitively, we do not find differences between the deaf and hearing groups in the temporal thalamic parcellation, or thalamo-cortical tract. Decreased FA has been reported in deaf people in superior temporal regions, as well as white matter volume reductions in superior temporal gyrus, and temporal sub-gyral areas (Kim et al., 2009). Li et al

(2012) contrasted congenitally deaf participants and acquired deaf participants to hearing controls. In auditory cortex, they report reduced FA values bilaterally in superior temporal cortex (Li et al., 2012). These findings are correlated with the age of onset of deafness, as opposed to the duration of deafness, which the authors interpret as being indicative of an early sensitive period for typical development of auditory cortex (Li et al., 2012). Using manual delineations of Heschl's gyrus, decreased white matter volume (normalised for the overall volume) has been reported in pre-lingually deaf signing participants in comparison to hearing control participants (Hribar et al., 2014). In the same group of participants, tract based spatial statistics (TBSS – a spatially normalised group method) revealed bilateral differences in auditory areas, including the superior temporal gyrus, Heschl's gyrus, planum temporale and planum polare, which were more pronounced in the right hemisphere (Hribar et al., 2014). Using the same methodology with a group of pre-lingually deaf adolescents, white matter microstructural alterations have been reported bilaterally in the superior temporal gyrus, Heschl's gyrus, planum polare, and also in the splenium in the corpus callosum (Miao et al., 2013).

There are reasons why our findings and these previous reports might diverge. First and foremost, in all of the above studies, as well as differing in hearing status, participants differed in terms of their language modality and perhaps also the security of first language acquisition (particularly for deaf participants born to hearing parents). No information is provided on language background by Kim et al., (2009), whereas in Li et al., (2012) Miao et al., (2013) and Hribar et al., (2014), all deaf participants used a sign language as their primary language whereas none of the hearing control participants had any knowledge of sign language. Bilingualism and language deprivation have both been shown to affect neuroanatomy (Mechelli et al., 2004, Penicaud et al., 2012). Without further knowledge about participants it is possible that these factors may have caused previous studies to overestimate the impact of deafness on the auditory cortex. To redress this issue, and because the majority of studies on deafness in humans use deaf native signing participants despite the fact that this group is far

out-numbered by deaf non-native signers, Olulade et al., (2014) used voxel based morphometry (VBM) to contrast deaf and hearing native signers, deaf non-native signers and hearing control participants. Voxel based morphometry measures the macroscopic properties of brain tissue (volume) whereas diffusion weighted imaging measures the microstructural properties of the tissue within each volume, and as such, these methods are not directly comparable. Nevertheless, this study demonstrated effects in regions which were altered in deaf native signers relative to hearing native signers, which were not replicated when deaf non-native signers were contrasted to hearing controls (Olulade et al., 2014). The authors found a main effect of hearing status on white matter in superior temporal gyrus (Olulade et al., 2014). Whilst this effect is considerably less widespread in comparison to reports of Heschl's gyrus, planum temporale and planum polare being affected (Miao et al., 2013, Hribar et al., 2014), we have not managed to replicate these findings of white matter abnormalities in the auditory cortex.

Remaining reasons which may account for this discrepancy (aside from the above mentioned difference in the macroscopic and microscopic measurements compared) include that the regions of interest between these studies are different. Using a group approach (TBSS) we did not find differences in these regions which may be due to a lack of statistical power. However, it remains a possibility that using a region of interest approach we would be able to detect differences in auditory cortices. It is worth mentioning that language differences still persist between groups; the hearing group Olulade et al., (2014) used to contrast to the deaf non-native signers had no knowledge of sign language. As their non-native signers learnt sign language at a later age, it could be argued that this is an inappropriate control group, as the deaf group are bimodal bilinguals whereas, to the best of our knowledge, the hearing groups are monolingual. Differences in hearing aid assistive technology may also differ between participants in either study. This is a limitation, given that hearing aid usage has been linked to functional plasticity (Philibert et al., 2002), although its effect on neuroanatomy remains (to the best of my knowledge) uninvestigated.

Owing to the complexities of matching deaf and hearing participants in factors relating to language use, and eliminating the potential impact of hearing aid use, it is useful to look to animal models to determine the neuroanatomical consequences of auditory deprivation. To investigate anatomical changes associated with the dorsal zone (DZ) of auditory cortex supporting enhanced motion detection thresholds in deaf cats (Lomber et al., 2010), Kok et al., (2014) injected retrograde tracers into this region in early and late deafened cats. They found a pattern of enhanced connectivity with areas typically responsible for visual motion processing (PLLS/PLMS –posterolateral lateral sulcus/posterolateral medial sulcus) and reduced connectivity with visual areas responsible for complex visual processing (ALLS – anterolateral lateral suprasylvian area), which was more pronounced in the early rather than the late deafened cats (Kok et al., 2014). Changes were consistent with amplified existing connections, rather than the development of new connections (Kok et al., 2014). Importantly, no differences in connectivity were reported in auditory cortex itself (Kok et al., 2014). Analogously, Barone et al., (2013) report the extent of reorganisation in auditory cortex in congenitally deaf cats is small, and that re-weighting of crossmodal connections from either modality is likely to be responsible for the majority of crossmodal plasticity in the area. There is a lack of consensus regarding the size of A1 following neonatal deafening in cats; evidence for increases in size have been reported (Raggio and Schreiner, 1999), as well as decreases (Lomber et al., 2010, Wong et al., 2013), and no change (Kral et al., 2002). Anatomical tracers were used to study the projections between the medial geniculate body of the thalamus and A1 in deaf cats, which were unaltered by neonatal deafening despite the disorganised cochleotopy in A1 (Stanton and Harrison, 2000). These inconsistent and null results do not concord with the human findings of dystrophic change in primary and secondary auditory regions, which is more pronounced in the right hemisphere. This suggests that the results in humans could be compounded by language differences between studied groups.

Patterned firing in response to auditory input is necessary for the development of dense reciprocal connections between different regions in auditory cortex, which are a

prerequisite for its typical function (Kral, 2007). Absence of auditory input during the early critical period for auditory development has been argued to result in functional decoupling of auditory core from the rest of auditory cortex (Kral and Sharma, 2012). The central auditory evoked potential (CAEP) has been used to index the functional integrity of auditory cortex (Sharma et al., 2005). This has been used to determine suitability for cochlear implantation, and it has been shown that if children experience more than 7 years of auditory deprivation they will never have a normal CAEP (Sharma and Dorman, 2006, Dorman et al., 2007, Sharma and Campbell, 2011) (although all variance in cochlear implant outcome cannot be explained by this measure and the child's pre-existing language skills additionally require consideration (Lyness et al., 2013)). Therefore all participants studied in this chapter would have functional decoupling of their auditory cortex. We may not have observed differences between the groups because the use of the entire auditory cortex masked reduced anatomical connectivity with some regions, and potentiated connections from other modalities to other regions, including potentially auditory association areas. Considering smaller target ROIs may clarify the pattern of anatomical differences present.

Finally, there is evidence the FA is decreased, and MD and RD are increased in the deaf group in the motor thalamo-cortical tract. It is not clear why this would be the case, as the effects of congenital deafness on motor skills are not fully understood. Whilst all participants learnt sign language after the age of 10, the deaf group began to learn significantly earlier than the hearing. It is also possible that the groups differ in the extent of their usage, both of which may affect the motor thalamo-cortical tract. Allen et al., (2013) contrasted cortical volume in motor cortex in deaf signers, hearing signers and hearing control participants. They reported a trend towards leftward volume asymmetries in the deaf group, whereas in the hearing non-signing group the pattern was towards a rightward volume asymmetry in motor cortex, and in the hearing signing group a symmetrical pattern (Allen et al., 2013). They attribute this to activity dependent changes as a result of greater reliance on sign language in the deaf group (Allen et al., 2013). Finally, the motor thalamo-cortical tract includes contributions from axons

involved in sensorimotor control of the mouth, which are necessary for speech production. Differences may exist between the deaf and hearing groups in speech usage. Additionally, the deaf group do not integrate auditory feedback when they perceive speech. These reasons may contribute to the alterations observed in the motor thalamo-cortical tract.

There are several important caveats to bear in mind when interpreting DW-MRI data. Firstly, strong anatomical connections between regions do not necessarily correspond to equally important functional connections (Johansen-Berg and Rushworth, 2009). We have endeavoured to link our results to findings from the behavioural and neuroimaging literature on deaf participants. There are many factors which can affect tractography results, including data quality, the distance between connected anatomical centres, as well as the complexity and geometry of the underlying fibres (Behrens et al., 2003, Behrens et al., 2007, Johansen-Berg and Rushworth, 2009, Jones et al., 2013). We addressed the issue of poor data quality through visual inspection of the data, which resulted in excluding three participants from further analysis. Poor quality data will tend to result in failure of paths to reach their cortical targets, rather than introducing any systematic error (Behrens et al., 2003). We thresholded data (60% of streamlines in each tract had to reach their cortical target) to try to reduce the impact of false positive connections between the seed region and cortical targets. Furthermore, the 'winner takes all' segmentation of cortical voxels into the cortico-thalamic tracts means that the contribution of voxels surrounding the thalamic area to microstructural measures is reduced. The limits of DW-MRI resolution mean that voxels in this region may contain genuine white matter connections to more than one cortical target, but the less strongly connected tracts are ignored for the purposes of extracting microstructural values. While this may be considered a bias in data selection towards the more peripheral parts of the thalamo-cortical tracts, it ensures the independent sampling of tracts, necessary for investigating tract-specific group differences. Additionally, the physical proximity of the cortical target to the seed region will affect the ease with which a track is traced; tracts with a closer cortical target will necessarily have a greater probability associated with them.

However, as we were contrasting tracts and thalamic parcellations derived from these between groups (rather than different tracts within the same brain), differences in tract connection probability related to cortical target proximity are unlikely to have systematically distorted results.

There are also caveats to be considered regarding the participants tested in the current study. Although animal models can be used to examine the influence of auditory deprivation, when considering humans, there is no perfect group contrast that allows the influence of auditory deprivation to be isolated from language experience. Previously, the majority of research into the effect of congenital deafness on brain anatomy or function in humans has contrasted deaf native signers with hearing native signers. This approach has the benefit of restricting aetiology of deafness to genetic causes and controlling for native exposure to a signed language. However, language experience inevitably differs between these groups as hearing native signers are more balanced sign/ speech bilinguals than their deaf siblings. Furthermore, there is some evidence that hearing status interacts with native acquisition of sign language to influence the neural bases of visual motion processing (Bavelier et al., 2001, Brozinsky and Bavelier, 2001). Sign language is a complex, dynamic visual stimulus, and it is possible that this form of 'visual environmental enrichment' will have a differential impact on deaf and hearing brains during early development.

We argue that a worthwhile contribution to this field is to contrast deaf and hearing individuals who have learnt a signed language later in life. However, this approach is also not without its drawbacks. Two of our deaf participants indicated they could not converse fluently with hearing people through speechreading alone. However, our findings were unchanged following analyses excluding these participants, demonstrating our results were not due to insecure first language acquisition in the deaf group. Another drawback in research with individuals who are born deaf to hearing parents is the difficulty in controlling for aetiology of deafness, which is often unknown. A common cause of deafness in those with hearing parents

is maternal rubella (Morzaria et al., 2004): five of the thirteen participants in the current study report this as the aetiology of their deafness. Intellectual disability caused by white matter lesions can also be a consequence of maternal rubella (Sugita et al., 1991, Lane et al., 1996). To reduce the chances of neurological problems or intellectual disability confounding our results, we sought deaf participants who were broadly matched in terms of education and occupational success to the hearing participants. In addition, all images were thoroughly screened for abnormalities. Whilst it is impossible to entirely rule out the possibility of undiagnosed neurological problems in this group, these steps minimize the risk that our group differences were driven by changes specific to those deaf through rubella. Concordance between results from studies which contrast deaf and hearing individuals with a range of different language backgrounds and different aetiologies will, in time, provide greater clarity regarding the true influence of auditory deprivation on brain anatomy and function.

Our findings demonstrate congenital deafness causes plasticity in the thalamus and thalamo-cortical projections, which ultimately have an effect on the control of information flow into and throughout the cortex. Microstructural measurements in the visual and frontal thalamic parcellations are altered in deafness, possibly suggesting more complex tissue in these regions, which may correspond to how visual information and visual attention is deployed differently by deaf people. Thalamo-cortical tracts to each cortical target, excluding temporal cortex, were altered. Differences in motor thalamo-cortical tracts may be linked to differences in speech, speech usage, age of sign language acquisition or sign language usage between the groups. Altered diffusivity of the somatosensory and occipital thalamo-cortical somatosensory tract may be the result of the enhanced somatosensory representation, and visual peripheral representation in deaf participants. Finally, changes to frontal and parietal connections may be the anatomical correlate of altered multimodal perception and attentional control in the absence of sound. Thus the neural sequelae of congenital auditory deprivation can be observed throughout the brain and are not restricted to auditory cortex.

Chapter 3: Does deafness alter the functional and structural architecture of primary visual cortex?

Abstract

Deafness results in greater reliance on peripheral vision to orient to novel environmental information when the auditory modality cannot be used for this purpose. It is unknown whether the cortical architecture of the visual system is optimized to carry out this compensatory function. In this chapter we performed widefield population receptive field (pRF) mapping of visual cortex during fMRI in the same participants that were studied in chapter 2. We found larger pRFs overall, as well as larger facilitatory centre zones of the pRF profile concentrated in the near and far periphery in the deaf group. pRF density was comparable between groups, indicating pRFs overlapped more in the deaf group. This suggests a coarse coding strategy underlies enhanced peripheral visual skills in deaf people. Cortical thickness was also decreased in V1 in the deaf group. The findings presented in this chapter suggest deafness causes structural and functional plasticity at the earliest stages of visual cortex.

Introduction

Classic experiments by Hubel and Wiesel demonstrated the role of environmental input in shaping the development of primary visual cortex (V1), through manipulating animals' visual environments, and using electrophysiological and histological methods to discern the neural consequences. Dark rearing has a profound effect on visual development, severely disrupting development of the visual system (Hubel and Wiesel, 1977, Fregnac and Imbert, 1978), whereas depriving one eye causes the remaining eye to have an increased cortical representation (Wiesel and Hubel, 1963, Hubel and Wiesel, 1970, Ramachandran and Kupperman, 1986). This demonstrates specification of cortex is a competitive balance between inputs, in this instance, the two eyes (Blakemore and Van Sluyters, 1974). Subsequent visual development and plasticity research in humans using methodologies such as functional magnetic resonance imaging (fMRI), has borne out the principles discovered by Hubel and Wiesel (Levin et al., 2010, Baseler et al., 2011, Raemaekers et al., 2011). However, the impact of deprivation of one sense on the cortical architecture of remaining intact senses is less well understood. In this chapter, we begin to address this question by studying the visual changes which occur in congenitally deaf people.

Deaf people demonstrate superior detection of targets (Loke and Song, 1991), and motion discrimination in the peripheral visual field (PVF)(Neville and Lawson, 1987). These enhancements are specific; contrast sensitivity (Finney et al., 2001), brightness sensitivity (Bross, 1979), colour discrimination (Mitchell et al., 1997), and temporal resolution (Bross and Sauerwein, 1980, Mills, 1985, Tallal and Poizner, 1985) remain unaltered. Using electroencephalograms (EEG), deaf native signers, hearing native signers and hearing non-signers were studied in a task in which they were required to identify apparent motion of dot stimuli in either the central or peripheral visual field (C/PVF)(Neville and Lawson, 1987). In the CVF, both performance and event related potentials (ERPs) were comparable across groups. However, in the PVF, deaf native signers were better able to detect changes in motion, and demonstrated significantly larger and more distributed N1 amplitudes (Neville and Lawson,

1987). These changes are thought to be evidence of compensatory plasticity as deaf people rely on peripheral vision to orient to new information in the periphery as the typical division of labour with audition is not possible (Merabet and Pascual-Leone, 2010). Importantly, changes were not observed in hearing native signers, demonstrating that deafness, rather than native use of a sign language, causes changes to peripheral vision.

Enhanced peripheral acuity in deaf people has been explored with the attentional load paradigm (Lavie, 1995), and explained in terms of differences in the 'gradient of visual attention' from the centre of the visual field to the periphery(Proksch and Bavelier, 2002). People have a fixed amount of attentional resource; completing a simple task in the CVF means resources are 'left over' to process information in the PVF. Increasing the complexity of this task will increase the attentional resource allocated to the CVF, reducing surplus resources available to the PVF (Lavie, 1995). Proksch and Bavelier (2002) have argued that deaf participants dedicate greater attentional resources to the periphery in contrast to hearing non-signers and hearing native signers, at the cost of reduced attention to the central visual field. The authors do not preclude that changes in sensory processing may contribute to their findings, but argue differences in visuo-spatial attention are sufficient to explain differences between the groups (Proksch & Bavelier, 2002).

Explanations for the visual peripheral advantage in deaf people have also been sought in visual cortex. In a study by Bavelier et al., (2001) deaf native signers, hearing native signers, and hearing non-signers viewed flow fields of moving dot stimuli during fMRI scanning to explore differences in motion processing across the visual field. Participants were required to attend to either the CVF or PVF. Greater activation in medial temporal and medial superior temporal (MT/MST) visual motion processing regions occurred in hearing participants when they attended to the CVF, whereas deaf participants activated these regions to a greater extent when they attended to the PVF (Bavelier et al., 2001). While there was an equal amount of activation in lower visual areas (V1/V2), deaf participants recruited posterior parietal cortex

(PPC) and posterior superior temporal sulcus (p-STS) to a greater extent in the peripheral motion condition. The authors concluded enhanced peripheral vision in deaf people was mediated by increased involvement of attentional regions such as PPC (Bavelier et al., 2001).

Crossmodal plasticity, specifically functional takeover of auditory cortex by visual processing, has also been studied as a candidate neural mechanism to explain differences in deaf peoples' peripheral vision. This has been tested against explanations based on 'compensatory hypertrophy' of the visual system. Evidence for compensatory hypertrophy was sought through measuring the amount of activation and surface area of the regions V1/V2/V3/V4 and MT+ during standard retinotopic procedures in groups of deaf native signers, hearing native signers and hearing non-signers (Fine et al., 2005). There were no differences between groups in these measures, which the authors interpreted as demonstrating there is a lack of evidence of compensatory hypertrophy of the visual system (Fine et al., 2005). Crossmodal plasticity was characterised through measuring responses in auditory cortex to a peripheral visual motion stimulus which was either attended to or ignored. Deaf native signers activated auditory areas to a greater extent, in comparison to hearing native and non-signers group. Activation was modulated by attention. Changes in visual processing due to deafness were argued to be restricted to higher visual areas (including middle temporal visual areas) as the developmental trajectory of these areas is more prolonged and malleable in comparison to early visual areas (Fine et al., 2005).

The neural locus of enhanced visual processing skills as a result of deafness has been examined in congenitally deaf cats (Lomber et al., 2011). The contribution of the dorsal zone (DZ) and the primary auditory field (PAF) of auditory cortex makes to enhanced localisation and motion detection in the visual periphery was examined by cooling these areas (Lomber et al., 2011). Cooling of DZ eliminated deaf cat's superior motion detection thresholds, whereas cooling of the PAF eliminated cat's superior visual localisation in the contra-lateral visual field. Critically, these performance deficits were not observed in hearing cats when these areas were

cooled, demonstrated that the absence of auditory input during development is a critical condition for the visual functional innervation underpinning these enhanced abilities to occur (Lomber et al., 2011).

In summary, these behavioural, neuroimaging and animal studies support an account of enhanced peripheral vision in deaf people which is supported by reallocation of visuospatial attention, changes in higher visual areas, and crossmodal responses in auditory cortex rather than plasticity in early visual cortex. However, these studies provide no explanation of how changes in higher visual areas occur, or how visual information comes to be processed in auditory cortex. The visual system is hierarchical. Retinotopic structure in MT+ has been discerned, which strongly suggests regularities in information processing throughout the visual system (Huk et al., 2002, Amano et al., 2009, Sereno et al., 2013). As such, changes in higher visual areas are likely to be preceded by changes lower down this hierarchy. Subsequently, optic coherence tomography (OCT) has been used to demonstrate larger neuroretinal rim areas in deaf participants, which is thought to reflect retinal ganglion cell number (Codina et al., 2011). Additionally, the retinal nerve fiber layer in peripapillary regions corresponding to the temporal retina was significantly thicker in deaf participants; the extent of changes was correlated with sensitivity in the PVF as measured by Goldmann Perimetry (Codina et al., 2011). In chapter 2 of this this thesis, we have shown alterations in microstructural properties of the visual thalamus and visual thalamo-cortical projection in congenitally deaf participants. In concert with findings from Codina et al., (2011), the findings presented in chapter 2 strongly imply that changes are present throughout the visual processing stream deaf people.

Recent advances in neuroimaging methods enable examination of cortical functional architecture in greater depth. Traditional retinotopic mapping procedures use phase encoded stimuli to map polar angle and eccentricity in visual areas (Sereno et al., 1995). Population receptive field (pRF) modeling adds a statistical summary of the receptive field properties of neuronal populations in each voxel to the measurements derived from retinotopic mapping

(Dumoulin and Wandell, 2008). Naturally, these pRF parameters do not simply reflect the average of receptive field sizes of individual neurons in the voxel as measured in electrophysiological experiments. Measurements could be influenced by factors such as scatter of the individual receptive fields, as well as contextual interactions between the neurons both within the population measured and those outside of it. Despite these caveats, pRF modeling is a non-invasive method enabling closer approximation of receptive field properties, which constitute the cortical architecture.

In this chapter we used visual psychophysics, MR imaging with population receptive field modeling to measure the structural and functional properties of primary visual cortex (V1), in order to contrast hearing and congenitally deaf participants and determine whether plasticity in these regions could account for enhanced peripheral vision noted in deaf people. We employed visual stimulation of a wide field of view up to an eccentricity of 37.5° to particularly assess differences in the peripheral visual field, as we predicted differences would be concentrated in these regions. Based on previous findings that increased cortical magnification factor (Duncan and Boynton, 2003) (and so decreased population receptive field size (Harvey and Dumoulin, 2011)) is associated with increased acuity, we predicted that the deaf group would have decreased population receptive field sizes in V1 representations of the visual periphery. Chapter 2 demonstrates anatomical changes to the visual thalamus and visual thalomo-cortical afferent, which suggests that in addition to the functional properties of V1, there may be anatomical changes in this region also. Increased cortical thickness in visual areas has been reported in blind participants (Jiang et al., 2009, Park et al., 2009), as well as linked to reduced visual acuity during development (Bridge et al., 2012). As such we predicted thinner visual cortex in the deaf group.

Methods

Participants

Participants were the same as detailed in Chapter 2. However, different participants were excluded from this scanning session. One male deaf participant was excluded from MRI analysis due to excessive motion in the scanner. Psychophysics data were not collected from another deaf male participant due to time restrictions during the experimental session. Following these exclusion criteria, participants did not differ in age ($t(27)=0.2$, $p=0.843$, hearing mean 38.32(+/- 7.9 SD), deaf mean 39(+/- 10.2 SD)).

As discussed in the introduction, animal models have been developed in which deaf animals have enhanced peripheral visual processing skills (Lomber et al., 2010, 2011, Meredith et al., 2011). This unambiguously demonstrates that peripheral advantages observed in deaf people are a result of deafness rather than the use of a sign language. However, depending on whether a person is hearing or deaf, native acquisition of a sign language has been shown to have a different effect on the neural representation of visual motion processing (Bavelier et al., 2001; Neville & Lawson, 1987), and lateralisation of face processing (Emmorey and McCullough, 2009). Therefore, contrasting deaf to hearing native signers may not be the most appropriate contrast with which to isolate the effect of deafness on the visual system. Plasticity is greatest in during development, and as such any influence sign language is likely to have on the development of the visual system will be greater earlier in development in comparison with later in development. To attenuate the effect sign language will have on the development of visual cortex, we tested only people who had learnt sign language after the age of 10 years. To attempt to control for any residual effect of sign language on visual processing we tested hearing participants who had also learn to sign after the age of 10 as a control group. Details of the groups' language characteristics are provided in chapter 2. In chapter 2, we reported 2 analyses including and excluding deaf participants who were at risk of insecure language development. However, as we use primary visual cortex as a region of

interest in this chapter, we report data from all included participants, as there is no literature to suggest variation in language characteristics affects primary visual cortex.

During testing, all participants' vision was corrected to normal. Research was approved by UCL Research Ethics Committee.

Psychophysics Task

Stimuli for the psychophysical experiment were generated and displayed using the Psychophysics toolbox in Matlab 2012a, and presented on a Toshiba Satellite Pro laptop (resolution: 1280*800). Owing to technical failure, 3 participants were tested using a Macbook Pro (1440*900). Viewing position was stabilized at 34 cm from the participants eyes to the fixation cross with a chin rest. The eccentricities at which stimuli were presented were comparable across laptops.

In separate runs, we measured position discrimination at central, middle and peripheral visual field locations (C/M/P VF). Two vertically arranged pairs of white Gaussian dots were presented for 300ms at either side of the fixation dot at 1.3°, 10.2° or 20.3° eccentricity (corresponding to the CVF, MVF, and PVF conditions). The standard deviation of each Gaussian dot in the CVF was 0.13°, and the vertically arranged pair was 0.64° apart. In the MVF condition standard deviation was 0.21° and dots were 1.06° apart, and in the PVF condition standard deviation was 0.47° and dots were 2.33° apart. Of these two pairs, one pair was misaligned. To discourage participants from saccading to one dot pair, they were informed that both pairs were misaligned, and therefore a strategy based on only looking at one pair of dots would fail. Participants were required to identify which pair was more misaligned, and indicate their response via a right or left arrow key press. The brief stimulus duration of 300ms prevented saccades to both locations within a trial. Participants were allowed unlimited time to make their responses, previous findings suggest deaf peoples speed accuracy trade-off is different to that of hearing people (Bosworth and Dobkins, 2002). Thresholds were estimated using a simple 2-down, 1-up staircase procedure which converged on a performance of ~70.7%

correct. The threshold was calculated by excluding those reversals with ±2 mean absolute deviations from the mean, and then calculating the mean across the latter half of these reversals. There were 5 short blocks within each staircase. This position discrimination task was favored over other visual acuity tasks owing to the speed and ease with which it can be completed, which was of particular importance when working with this special population who are unfamiliar with visual psychophysics.

Imaging Parameters

The same scanner was used to collect the data as presented in chapter 2. In addition to the MPRAGE structural sequence (used for data analysis in this chapter as well as chapter 2), echo planar images were acquired (TR=2000ms, TE=39ms, voxel resolution 3mm isotropic, flip angle 90°, BW=1474 Hz/pix) with 24 axial slices, acquired in an interleaved order, centered on and tilted to be parallel with the calcarine sulcus. The front of the head coil was removed to avoid obscuring participants' view, leaving 20 remaining channels for data collection.

fMRI Stimuli and Task

For the pRF modeling, a dynamic, high-contrast 'ripple' pattern was used as this maximizes the visual response, which is displayed in figure 3.1a. The pattern was defined as follows;

$$I(x,y) = \sqrt{x^2 + y^2}\cos\left\{\frac{2\pi(\sin\frac{\delta\pi x}{180} + \cos\frac{\delta\pi y}{180})}{4} + \theta\right\} \quad (3.1)$$

In which *I* is pixel intensity at a pixel in Cartesian coordinates (*x, y*), defined relative to the centre of the screen. The parameters θ and δ, correspond to the phase and spatial frequency of the pattern. Parameter θ varies with time from 0 to 4π in 72 equal steps of 32ms, completing each cycle approximately every 1.15 s. Parameter, δ, was a function of θ,

$$\delta = \frac{\sin\theta}{4} + \frac{1}{2} \quad (3.2)$$

Positive pixel intensity values were set to white, whereas negative or zero values were set to black. The background was uniform grey.

For the mapping, this stimulus was viewed through an aperture consisting of a rotating ring and expanding/contracting wedge in two runs each lasting 6 min 30 s. The wedge subtended a polar angle of 36° and subtended eccentricities from 1-37.5°. It rotated through the visual field in 20 discrete steps of 18°, one per fMRI volume acquired. To drive sufficient responses in the periphery, the ring width was logarithmically scaled with increasing eccentricity up to a maximal eccentricity of 37.5°. It changed in 16 discrete steps. The wedge rotated clockwise in the first run, followed by a counter-clockwise rotation in the second run, while the ring expanded in the first run and contracted in the second run. The wedge rotated for 8 cycles, while there were 10 expansions/contractions of the ring. The runs ended with 60 seconds of mean luminance to estimate the baseline response.

We modeled the haemodynamic response function (HRF) based on a run lasting 5 min 10 s, using a full screen version of stimulus with a radius of 37.5° visual angle from fixation. In both mapping and HRF runs at the central and outer edge of the stimulus, the contrast of the ripple pattern was ramped linearly down to zero over a range of 1.2° visual angle. The stimulus was bounded by a mean luminance screen. The stimulus appeared for 2 seconds followed by 28 seconds of mean luminance, which was repeated 10 times.

Throughout scanning participants were instructed to monitor the colour of the fixation dot subtending 1°, and count how many times this changed from blue to red. Every 200ms the fixation dot could change colour from blue to red for 200ms with a probability of 0.05, though

these colour changes never occurred in succession. Participants were then asked to report how many times the colour change happened at the end of each run. This task was designed to ensure participants maintained fixation. The ease of the task ensured all participants could perform it, therefore avoiding introducing group differences. To facilitate fixation stability, a low-contrast 'radar screen' pattern covered the screen (Tyler et al., 2005). This pattern consisted of 12 evenly spaced radial lines extending from outside of the fixation dot to the horizontal edge of the screen, and 11 equally spaced concentric rings centered on fixation, extending to the vertical edges of the screen. All stimuli were generated in MATLAB R2012a (MathWorks, Inc.) and displayed using the Psychtoolbox package (http://psychtoolbox.org).

Stimuli were projected onto a large screen in the scanner bore, approximately 13cm from the participants' eyes. Participants viewed this directly without the use of a mirror. The head coil was elevated, so the participants' gaze was perpendicular to the screen. This position precluded the use of eye tracking equipment. Having the large screen in the scanner bore placed body size restrictions on participants. A smaller screen was therefore used for 3 people (2 deaf, 1 hearing) allowing participants a field of view up to 16° eccentricity.

MRI Data Analysis

FreeSurfer (http://surfer.nmr.mgh.harvard.edu/) was used for surface reconstructions. Pre-processing of functional images was completed in SPM8 (http://www.fil.ion.ucl.ac.uk/spm/). Software built in-house was used to complete the pRF mapping analysis. A 1.5mm^3 smoothing kernel was applied to the structural images before they underwent cortical reconstruction and volumetric segmentation in FreeSurfer 5.0.0. More details of this procedure are provided in the methods section in chapter 2. In pre-processing functional images, the first 7 volumes were discarded from each run, ensuring magnetization transfer stabilization. Images were unwarped (Andersson et al., 2001), realigned and co-registered to the structural scan with SPM8.

Primary visual cortex and areas V2 and V3 were manually delineated in FreeSurfer. Anatomically V1 is situated in the calcarine sulcus, and contains a complete representation of the contralateral half of the visual field (Sereno et al., 1995). Vertices within the regions were labeled to extract data for further analyses.

For population receptive field (pRF) modeling, data were projected on the surface generated in the FreeSurfer cortical reconstruction by finding the voxel in the functional image that fell midway between each pair of vertices in the pial and white matter surface mesh. For each run, the observed time series were z-score normalized and linear detrending was applied. Participants' HRF models were calculated by averaging the 10 instances of the HRF stimulus using only visually responsive vertices (those for which the mean response minus the standard error across trials and between the second and tenth volume of the HRF was above zero). We further fitted a two-gamma function with four free parameters (delay for peak, delay for undershoot, amplitude ratio of peak/undershoot, overall amplitude) to these average HRF data.

During model fitting, a predicted time series was calculated from the overlap between the pRF model and binary stimulus aperture for each point in time, and then convolving it with the specific participant's HRF model (Dumoulin and Wandell, 2008). We fitted a Difference of Gaussian (DoG) receptive field model, which is comprised of a subtraction of 2 Gaussian functions, whereby the Gaussian with the larger standard deviation is subtracted from the Gaussian with the smaller standard deviation. Thus there are six parameters: visual field position (x and y in Cartesian coordinates), the spatial spreads of the facilitatory centre of the pRF (σ_1), the spread of the surrounding suppressive region (σ_2), the amplitude ratio of the 2 Gaussians relative to each other (δ), which corresponds to a suppression index, and finally the overall signal amplitude (β). The full width at half maximum (FWHM) of the entire pRF structure was calculated from these parameters. The DoG model has been argued to provide a more physiologically plausible model of the data as it is capable of modeling contributions

from centre surround receptive field structures (Zuiderbaan et al., 2012), which are well characterized from the electrophysiology literature (Cavanaugh et al., 2002). This model accounts for negative BOLD responses (defined as when the fMRI signal deviates below levels observed when viewing a mean luminance screen), which are observed in spatial proximity to active regions (Zuiderbaan et al., 2012).

A coarse-to-fine approach was used in which the parameters are disambiguated and then refined further. Data were initially smoothed on the spherical cortical surface with a large kernel (FWHM= 8.3 mm). The coarse fit generated thousands of permutations of the pRF parameters and calculated the predicted time series for each. The prediction showing the maximal Pearson correlation with the observed (smoothed) data was then selected. During the fine fit, the parameters from this fit were then used to optimize the pRF parameters of the DoG model at each vertex, were the squared residuals between the model and the data were minimized using a Nelder-Mead simplex search optimization procedure (Lagarias, 1998). The fine fit then used unsmoothed data and included a beta parameter to estimate the amplitude of the signal. Only vertices for which a reasonable coarse fit (R^2>0.05) was found were used. Finally, parameter maps were smoothed again (FWHM=5 mm) to create smooth maps. This is important for analysis of particular portions of the visual field (e.g. specific eccentricity bands) and because high frequency fluctuations at the scale of single vertices/voxels are likely due to measurement noise rather than a reflection of true scatter in pRF properties. The coarse fit stage involved only the three parameters of a standard Gaussian (i.e. x, y, and σ_1).

We then calculated mean pRF sizes (both for facilitatory centre and suppressive surround) in specific eccentricity bands within each hemisphere and visual area. Eccentricity and pRF size are positively correlated (Harvey and Dumoulin, 2011); hemispheres which did not display a significant positive correlation in V1 were excluded from further analysis (2 hearing, 5 deaf), as these were considered to be biologically implausible due to measurement noise. This higher than normal rate of data exclusion is likely to be a result of the brief

scanning time and awkward scanning position with this special population with whom communication in the scanner is a challenge, as well as lack of eye position data on which we could have based our exclusion criteria. For each parameter, data points which did not fall within three standard deviations of the mean were additionally excluded. Preliminary data analysis demonstrated evidence of an 'edge effect', whereby pRF size plateaued around 7-8° at 30° eccentricity. It is possible that pRF sizes continued to increase beyond this range; however, because the stimulus did not extend beyond 37.5° eccentricity, there may be an artefactual deflation of pRF size for pRFs outside this range. Generally, the reliability of model fits at these locations is poor. Thus we restricted our analysis to an eccentricity range of 3 to 30°. However, even in spite of this we observed a gradual saturation of the relationship between pRF size and eccentricity, which may have resulted in an underestimation of increasing pRF size with eccentricity and consequently an underestimation in the difference between groups. The central visual field was truncated for the same reason (the fixation dot extended up to 1° eccentricity and beyond that the stimulus was gradually ramped up in contrast up to an eccentricity of 2.2°). These issues with edge effects additionally meant that participants who were scanned using the smaller screen were excluded from the MRI analysis, although their data from the visual psychophysics tasks was still analysed. All of these data exclusion steps were taken to eliminate artefacts and help reduce noise in the data, however, the pattern of results without any of these steps is qualitatively the same (see supplementary information figure 3.1).

To assess the differences between the two groups we used a curve fitting approach, in which we fitted either cumulative Gaussian or exponential functions to averaged pRF data within each group. The cumulative Gaussian curve of MRI measured parameter *z* as a function of eccentricity (*p*) was defined as follows;

$$fz(\rho) = a\left(1 + \frac{erf^{\rho - b}}{\sqrt{2}c}\right) \quad (3.3)$$

were *a* corresponds to amplitude, *b* horizontal shift, and *c* the slope of the function. The exponential curve of MRI measured parameter *z* as a function of eccentricity (*ρ*) was defined as follows;

$$fz(\rho) = me^{k\rho} + l \quad (3.4)$$

were *m* corresponds to the amplitude of the curve, *k* the decay factor, and *l* the asymptote.

Additional curve fits employed polynomials of second (quadratic), third (cubic) or fourth order to describe the relationship between group-average pRF data and eccentricity.

A bootstrapping approach was then used to test for significant differences between the groups. We resampled the data within each group with replacement (separately in each eccentricity band) and refitted the function curves 1000 times. For each pair of resampled curve fits we calculated the difference between the individual parameters as well as the area under the curves. We then calculated the p-statistic for each parameter difference by quantifying what proportion of these 1000 differences had the opposite sign as the observed difference.

Results

To discern whether deafness resulted in changes to the functional architecture of early visual cortex, we collected retinotopic mapping data using fMRI on groups of deaf and hearing participants, matched in terms of having learnt sign language after 10 years of age. Figure 3.1b-d shows typical polar, eccentricity and FWHM maps.

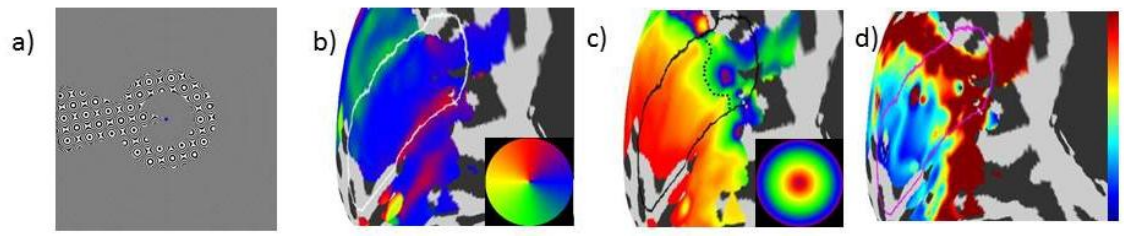

Figure 3.1: *Mapping stimulus and retinotopic maps. (a) In the scanner participants viewed rotating wedge and expanding ring stimuli containing a high contrast flickering checkerboard*

pattern whilst maintaining fixation on a small blue dot in the centre of the screen. (b-d) Maps of population receptive field (pRF) parameters for one participant. Data are projected onto an inflated model of the left cortical hemisphere. Polar angle (b), eccentricity (c) and Full Width at Half Maximum (FWHM) of the pRF profile (d) are shown. Primary visual cortex is outlined in each map. The dashed black line on the eccentricity map denotes the maximum eccentricity analysed (30°). All maps are thresholded at R^2=0.1, corresponding to the model fit required for the inclusion of the data point for analysis.

We were able to detect retinotopic map structure in all participants, confirming there are no macroscopic differences between deaf and hearing groups (Fine et al., 2005). Figure 3.2 demonstrates BOLD time series and model fits from the DoG Model, and shows the detrending of these time series data did not produce artefacts during the mean luminance periods in which the stimulus was not displayed.

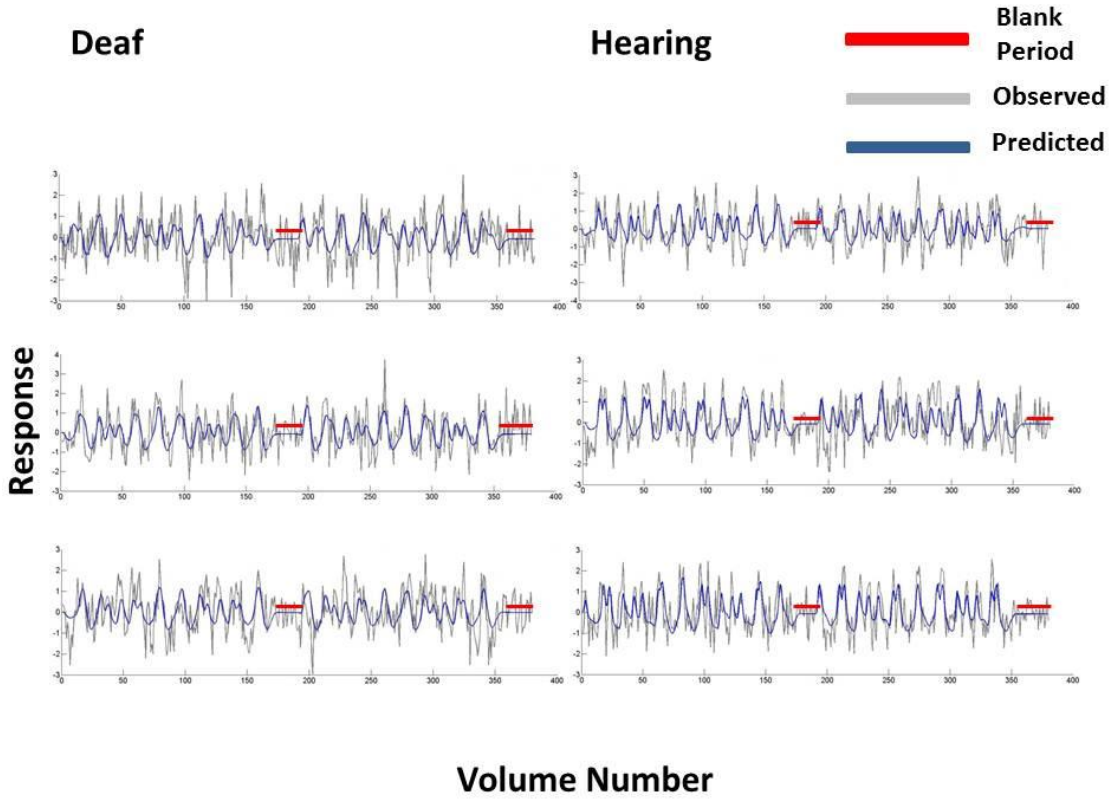

Figure 3.2: *For 3 participants in the deaf and hearing groups we have plotted the Difference-of-Gaussian model predictions and BOLD time series data at vertices in primary visual cortex, which were at the 80th percentile of all model fits. The model predictions are plotted in blue and*

the observed BOLD response at that vertex is plotted in grey. Blank periods in which a blank grey screen was presented rather than a mapping stimulus are highlighted in red.

Difference of Gaussian Model

We used a difference of Gaussian model which can characterise contributions from the inhibitory surround of the population receptive field by modeling negative BOLD responses to stimulation near the receptive field centre (Zuiderbaan et al., 2012). We contrasted parameters derived in each participant's native space from the population receptive field model (σ_1, σ_2, δ and β) between groups. For each participant, analysis was performed on the mean of these parameters from either hemisphere or, or a single hemisphere should the other hemisphere have been excluded owing to poor data quality.

We calculated the FWHM of the Difference-of-Gaussian pRF profile (figure 3.3). This measurement corresponds to the width of the facilitatory part of the DoG profile. The relationship between eccentricity and FWHM was well described with a cumulative Gaussian curve (*hearing R^2=0.96, deaf R^2=0.98*), and bootstrapping analysis revealed a significant difference between the two groups in that the slope with eccentricity was greater in the deaf group as compared to the hearing group (*p=0.0031*). Eccentricity based bin-wise independent samples t-tests demonstrated the differences were concentrated in the near and far periphery. Figure 3.4 demonstrates the average pRF profile for deaf and hearing groups every 4° which again demonstrates the differences between groups are concentrated in the near and far periphery.

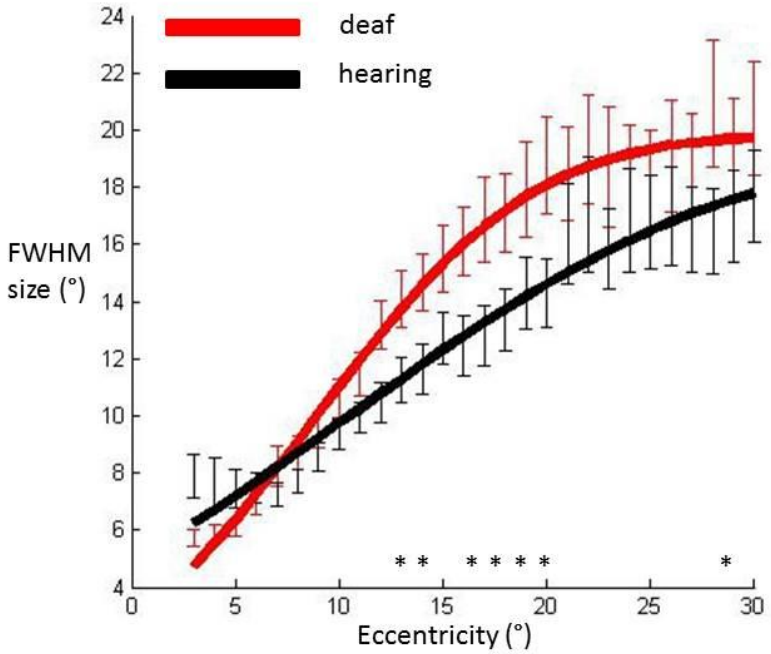

Figure 3.3: *Full width at half maximum (FWHM) sizes of the pRF are averaged across participants' hemispheres in each group and plotted against eccentricity in primary visual cortex. Data have been fitted with a cumulative Gaussian curve. Independent samples t-tests were used to assess whether there were differences between groups for each eccentricity bin. Significantly different bins are denoted with an asterisk. Red: Deaf participants, Black: Control group. Error bars denote +/- standard error of the mean.*

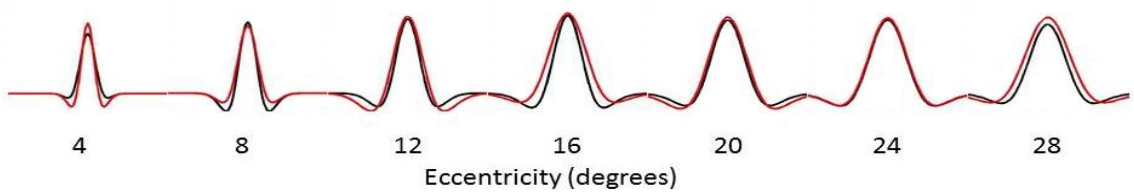

Figure 3.4: *Average pRF profile illustrating differences between the deaf (red) and hearing (black) groups in steps of 4° eccentricity.*

Figure 3.5 shows that the cumulative Gaussian curve also provided a good fit for the relationship between the facilitatory centre parameter (σ_1) and eccentricity (hearing R^2=*0.98*, deaf R^2=*0.98*). There was a steeper increase in facilitatory pRF size with eccentricity in the deaf group (*p=0.027*). Amplitude and horizontal shift parameters did not differ between groups

(*p=0.501*, *p=0.254* respectively). We investigated the spatial specificity of these results using eccentricity based bin-wise independent samples t-tests. This demonstrates differences in pRF centre size were concentrated in the near periphery. The relationship of the inhibitory surround parameter (σ^2) with eccentricity was also well described by a cumulative Gaussian curve (hearing $R^2=0.97$, deaf $R^2=0.96$). None of the curve parameters differed significantly between groups (all *p's>0.076*).

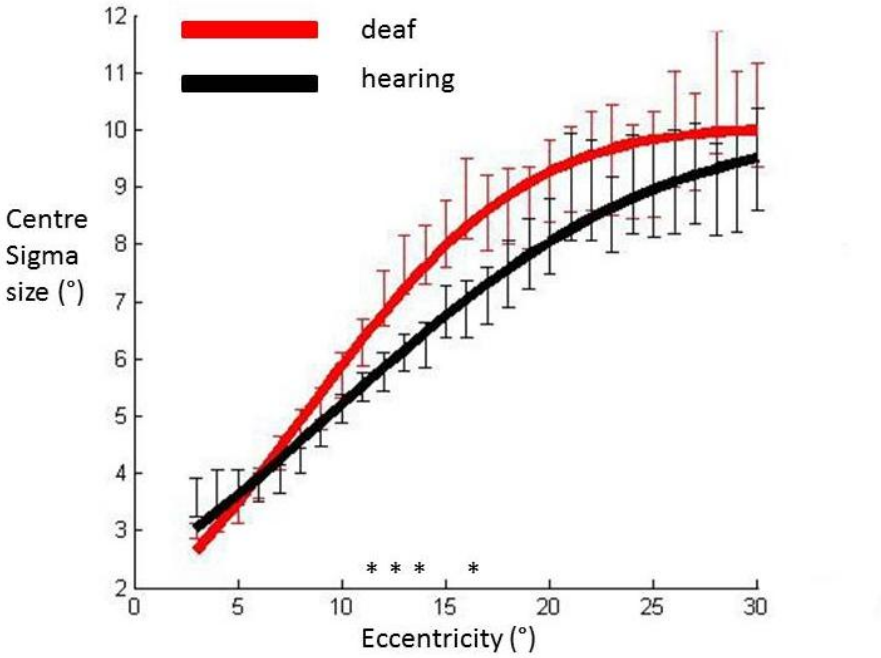

Figure 3.5: *pRF centre sizes were averaged across participants' hemispheres in each group and plotted against eccentricity in primary visual cortex. Data have been fitted with a cumulative Gaussian curve. Independent samples t-tests were used to assess whether there were differences between groups for each eccentricity bin. Significantly different bins are denoted with an asterisk. Red: Deaf participants, Black: Control group. Error bars denote +/- standard error of the mean.*

Following this, we contrasted the overall signal amplitude (β) between the groups (see Supplementary Information figure 3.3). The data was fit with a third order polynomial (hearing $R^2=0.87$, deaf $R^2=0.73$). There was a trend suggesting a main effect of group, in which the deaf

group displayed greater signal amplitude in comparison with the hearing group (p=0.053). None of the other curve parameters were significantly different (all *p's>0.229*). We investigated this trend further by completing eccentricity based bin-wise independent samples t-tests between the groups, none of which were significantly different between groups. This suggests that there were no reliable differences between groups at any eccentricity.

Critically, we also analysed the amplitude ratio between centre and surround components (δ). With lower order polynomials, there were large discrepancies between the fit achieved for each group, which may have led to misleading results. Accordingly, we fitted the curves with a fourth order polynomial (hearing $R^2=0.79$, deaf $R^2=0.72$). We examined only the main effect of group (corresponding to area under the curve), which was not significant ($p=0.168$).

We also contrasted the pRF density between groups. This is defined as the amount of visual space between any given pRF position and its neighbours, and thus is informative regarding how pRFs are arranged spatially. The relationship between this measure and eccentricity was well described with a cumulative Gaussian fit (hearing $R^2=0.97$, deaf $R^2=0.98$). There were no differences in pRF density in V1 between groups (all *p's>0.19*). Finding no differences between groups in terms of pRF density, while the pRF size increased, necessarily translates to an increase in the overlap of pRFs.

Following this, additional analyses were used to test whether the effects reported could be explained by haemodynamic or model fit differences between the groups. In contrast to the above analyses, we did not average across hemispheres for each participant. Typically deaf people will differ in the extent of hearing loss in either ear which could have consequences for either the model fit or haemodynamic response; averaging across hemispheres would remove this variance which may be important in elucidating a difference between groups. Further, this approach has greater statistical power than averaging across hemispheres, making it a more stringent test regarding whether these haemodynamic or

model fit differences could have contributed to differences between groups. The hearing group was exposed to considerable scanner noise, in contrast to the deaf group who would be subject to minimal, if any, scanner noise. Thus, it is plausible that intermodal stimulus competition in the hearing group, in which auditory cortex activation reduced the amount of blood available for visual processing (Laurienti et al., 2002, Johnson and Zatorre, 2005), contributed to the differences between groups. We explored this possibility by contrasting the peak amplitudes from the HRF measurement. The sparse stimulus presentation during HRF modeling enabled more effective estimation of baseline. An exponential function was used to model the fit between eccentricity and peak amplitude (hearing $R^2=0.96$, deaf $R^2=0.95$). There were no significant differences between groups for any of the parameters of this curve (all $p's>0.067$). A quadratic function was used to model the fit between eccentricity and model fit (hearing $R^2= 0.78$, deaf $R^2=0.80$). There were no significant differences between the groups (all $p's>0.13$). Therefore it is unlikely differences in either haemodynamics or model fit could have caused the observed differences between groups.

Visual Psychophysics

To test whether the groups differed in position discrimination at different visual field locations (figure 3.6), we completed a repeated measures ANOVA with a between subjects factors of group (deaf/hearing) and a within subjects factor of visual field location (C/M/PVF). Data deviated from the assumption of sphericity ($W(2)=0.47, p<0.001$), and as such a Greenhouse-Geisser correction was applied. There was an interaction between group and visual field location ($F(1.3,35.3)=5.138, p=0.022$). Post-hoc t-tests revealed no group differences in the CVF ($t(27)=0.31, p=0.757$), nor the MVF ($t(27)=1.58, p=0.127$), but the deaf group had significantly more sensitive position discrimination than the hearing group in the PVF ($t(27)=2.66, p=0.013$).

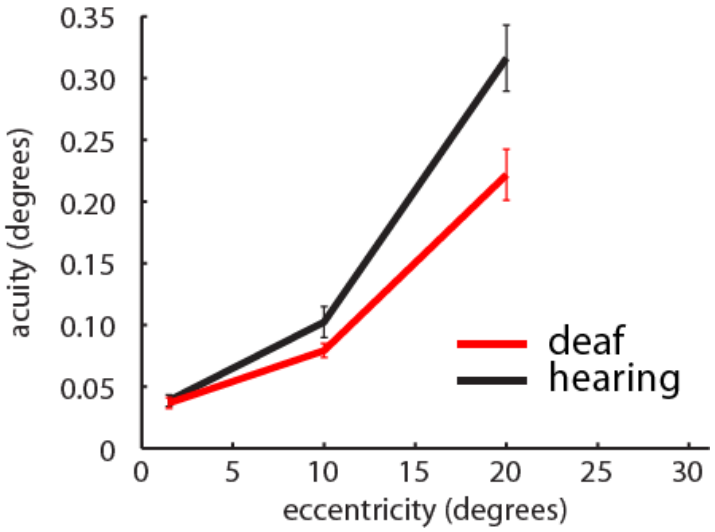

Figure 3.6: *Visual positional discrimination measurements in the central (1.5°), middle (10°) and peripheral visual field (20°). Red: Deaf participants, Black: Control group. Error bars denote +/- standard error of the mean. Analysis is based on 13 deaf participants and 15 hearing participants.*

Structural Data

We additionally contrasted cortical thickness measurements from functionally defined V1 between the groups. Convincing curve fits were not found between cortical thickness and eccentricity with any function; there appeared to be no systematic relationship between eccentricity and cortical thickness (this is shown in Supplementary Information figure 3.4). As such, we binned data across eccentricity and contrasted groups using a linear mixed model. We modelled a fixed effect of group, and a random effect of participant to account for the correlated sources of random error from either hemispheres of each participant. This revealed the deaf group had thinner cortex in V1 (*F(1,1247)=4.485 p=0.034*). We repeated this analysis with all the data before the outlier removal procedures based on the functional data. This demonstrated a main effect of group (*F(1,1913)=5.47 p=0.019*), in which the deaf group had thinner cortex in comparison to the hearing group. Thus, effects were not dependent upon the outlier removal procedures.

MRI – visual psychophysics correlations

We used correlations to determine whether there was a linear relationship between MRI derived cortical architecture variables; specifically the centre and surround size parameters from the DoG model, cortical thickness, and position discrimination ability. As we did not map within the central 2°, for the central visual field we correlated position discrimination ability with MRI derived cortical architecture variables at 3°. There was a significant negative correlation between cortical thickness and position discrimination at 10° (MVF) (*R=-0.56, p=0.003*). Aside from this, none of the MRI derived cortical architecture metrics correlated with position discrimination ability.

Discussion

Specification of cortex has been shown to result from a competitive balance of inputs. However, whether auditory deafferentation affects the functional and structural architecture of primary visual cortex had not been examined prior to this thesis. In this chapter we examined population receptive field properties in V1 in congenitally deaf and hearing participants. Using a difference-of-Gaussians pRF model it was demonstrated that the deaf group had larger pRFs as estimated by the full width at half maximum of the pRF profile. The facilitatory centre component of the pRFs was larger in the deaf group. These effects were specific to the visual periphery. Cortical thickness was decreased in the deaf group. These functional and anatomical changes may contribute to the observed increased peripheral position discrimination ability in the deaf group.

Finding increased pRF sizes in the deaf group who also demonstrated enhanced peripheral acuity is perhaps counter-intuitive, since small (population) receptive field sizes are thought to underpin high resolution vision in the fovea. However, enhancing visual resolution throughout visual cortex by employing a strategy of decreasing receptive field sizes would require cortical expansion to maintain visual coverage. Given the physical size constraints on the brain, this is unrealistic. Alternatively, increasing receptive field size and thus receptive

field overlap could improve localisation and spatial discrimination through pooling signal across several noisy units. The density of pRFs remains unaltered between groups. By definition, if the density of pRFs remains the same while the size of the pRFs increases, overlap between pRFs will increase. This 'coarse coding' provides a means of increasing acuity without the need for cortical expansion (Eurich and Schwegler, 1997).

Owing to the coarse spatial resolution of fMRI relative to individual neurons, it is inevitable pRF size estimates will include extra-classical effects (regions in visual space where stimuli do not elicit a spiking response but instead modulate the response to stimuli in the classic receptive field). We used a Difference-of-Gaussians model to account for some of the effects of these extra-classical properties of neurons (Zuiderbaan et al., 2012). This demonstrated a larger overall pRF profile (FWHM), which was driven by the differences in the facilitatory centre, rather than the inhibitory surround parameter. The suppression estimated by this pRF model may reflect extra-classical receptive field effects, and other factors may also contribute to this parameter, including extra-classical receptive field interactions and the positional scatter of neuronal receptive fields. Future research into neuronal parameters giving rise to pRF size will be important to understand the mechanism behind our results, as well as the relationship of these components with measure of visual function.

Thickness measurements were negatively correlated with visual acuity thresholds in the middle visual field only, that is, better visual acuity was associated with thicker cortex. This correlational relationship is the opposite of what we would predict from the ANOVA and means testing, in which the deaf group who have improved acuity (decreased value) have decreased cortical thickness. The deaf group have improved acuity (decreased value) and decreased cortical thickness, however, the group effect shows a relationship whereby those with worse acuity (increased value) tend to have decreased cortical thickness. This suggests this relationship requires further examination, with an increased amount of psychophysics data collected, including different measures of visual function. Additionally, no correlations

were observed between centre and surround parameters of the DoG model, and visual acuity. Many reasons could potentially account for why we do not see these correlations. Firstly, the relationship between the population receptive field parameters and acuity may not be linear in the periphery, as it is at more foveal eccentricities (Duncan and Boynton, 2003). An interaction between different parameters may account for increased acuity. Secondly, if the deaf group employ a 'coarse coding' mechanism in the periphery whereas the hearing group do not, the relationship between pRF size and acuity may differ between the groups. Finally, as we were motivated to reduce the demands associated with completing an extensive visual psychophysics battery at different visual field locations, our visual acuity task was a combined measure of acuity in both visual hemifields. We also averaged pRF parameters across participants' hemispheres. This may have removed fine-grained information required to detect correlational relationships. Previously, correlational relationships between visual acuity measures and measures of cortical architecture have only been shown when considerably more data has been collected, including estimates of acuity for each visual quadrant, and with participants familiar with visual psychophysics testing, as opposed to the special populations tested here (Duncan and Boynton, 2003). Thus, possible relationships between these variables in our data may have been obscured by these potential sources of noise.

One of the ways attention exerts its effects is through the manipulation of receptive field properties (Moran and Desimone, 1985, Anton-Erxleben et al., 2009, Anton-Erxleben and Carrasco, 2013). In electrophysiology experiments, receptive fields have been shown to shrink and move towards the foci of attention (Moran & Desimone, 1985). Conversely, receptive fields which do not cover areas at the centre of attention increase in size and 'zoom out' (Moran & Desimone, 1985). Recently, it has been shown that pRF modeling is capable of measuring changes due to attentional load (de Haas et al., 2014), and visuospatial attention (Klein et al., 2014). Our fixation task, which required participants to monitor the number of times the fixation dot flashed from blue to red, was performed with a high degree of accuracy (greater than 95%) by all participants. This easy task avoided introducing group performance

differences, which may have confused the interpretation of fMRI data. However, this also meant that attention was not completely controlled during scanning. As such, attentional differences between the groups may have contributed to the findings; the mapping stimulus was irrelevant to the task of counting the dot flashes and the deaf group may have excelled at ignoring the mapping stimulus, causing them to have enlarged receptive field sizes. However, we find this explanation unlikely. Undoubtedly, attentional effects can be observed at early stages of the visual processing stream, including subcortical structures (Shipp, 2004, Hulme et al., 2010). Nevertheless, direct comparison of the extent of these effects reveals they are more pronounced further up the visual hierarchy (Saygin and Sereno, 2008, de Haas et al., 2014). This is the opposite of what we have found here, as effects are concentrated in V1 (see supplementary figure 3.2).

Eye movements could be a potential source of variance which contributed to the differences observed between groups. Unfortunately the tilted head position as a result of the elevated head coil precluded the use of eye tracking equipment. However, as previously noted, participants performed the fixation task accurately during fMRI scanning. This prevents large or extended periods of eye movements, which in any case are more likely to result in the inability to reconstruct visual maps rather than a systematic increase in the estimate of population receptive field size. Eye movements would have to have been excessive to produce even subtle pRF size increases, and would have caused increases across the entire range of eccentricities rather than just in the periphery (Levin et al., 2010). Furthermore, there is evidence deaf people are better at sustaining fixation (Buckley et al., 2010), and therefore our results are the opposite of what would be anticipated should eye movements account for the differences between groups. Finally, we find it implausible that differences in age of sign language acquisition or sign language usage account for our effects, as differences between the groups emerge beyond the eccentricity at which sign language is received (~7°) (Bosworth, 2000).

Population receptive field size measurements were larger than those generated in previously published studies (Dumoulin and Wandell, 2008, Levin et al., 2010, Harvey and Dumoulin, 2011, Binda et al., 2013). However, the aforementioned studies used 3T scanners, whereas here we used a 1.5T scanner. This affects the functional resolution of the blood-oxygen dependent signal, which may lead to differences in the estimation of pRF size. Moreover, pRF sizes are likely to depend on the mapping stimulus, as that determines which neuronal populations are driven to respond. We used a dynamic stimulus containing strong motion energy which may have increased estimates of pRF size. Finally, using a much wider field of view than any previous study mapping pRFs in humans may have changed within-area interactions. Nevertheless, the group comparison remains valid even if the absolute pRF sizes are different than they might have been under another experimental setup.

Deafness and age of sign language acquisition have been linked to anatomical changes in visual cortex. Penicaud et al., (2012) have demonstrated grey matter volume in early (V1/V2) and dorsal association visual cortex is negatively correlated with age of sign language acquisition in deaf participants. They rule out the effect of auditory deprivation by contrasting deaf participants with different ages of sign language acquisition to hearing non-signers. However, this is not a stringent test for the effect of auditory deprivation; neuroanatomical variance due to language within the deaf group may be greater than neuroanatomical variance between groups due to auditory deprivation. We replicate this finding of decreased cortical thickness in V1 of deaf late learners of sign language. Our groups differed in age of sign language acquisition and thus we cannot entirely exclude the possibility of contributions from this factor. However, Allen et al., (2013) used hand delineated ROIs of the calcarine sulcus to demonstrate that deaf native signing participants had increased volume in these regions relative to hearing non-signing participants, but not hearing native signing participants, implying an interaction between sign language age of acquisition and auditory deprivation (Allen et al., 2013). Hand delineated ROIs are more anatomically specific in comparison to spatial normalization to a common template (as in Penicaud et al., 2012). There are

discrepancies between the ROI delineated by Allen et al (2013), regions specified by Penicaud et al., (2012) and functionally defined V1 reported here, meaning our results are not directly comparable. Nevertheless, we concur with Allen et al., (2013) that auditory deprivation contributes to anatomical alterations of early visual cortex. However, we show decreases in deaf late learners of sign language rather than increases in deaf native signers, either of which could contribute to the correlation observed by Penicaud et al., 2012.

Penicaud et al., 2012 interpret their findings as demonstrating native signers have greater computational power in early visual cortex. However, it is not evident that increased grey matter volume in early visual cortex translates to increased computational power. Increased occipital cortical thickness has been reported in congenitally (Park et al., 2009), and early blind participants (Jiang et al., 2009). High resolution vision has been argued to be required for typical pruning mechanisms to occur during development, the absence of which leaves thicker, immature cortex (Jiang et al., 2009, Bridge et al., 2012). From the same participants studied by Penicaud et al (2012), fMRI data acquired while they completed a grammatical judgment task demonstrated late signers preferentially recruited visual cortex, in contrast to native signers who engaged classic perisylvian language networks (Mayberry et al., 2011). Thus, instead of native signers increased thickness in occipital cortex being due to increased computational power (Penicaud et al., 2012), we propose an alternative interpretation, that the lack of plasticity of perisylvian cortex for late learners forces visual cortex to adapt to processing the complex and dynamic sign language signal. This may require adaptations including the thinning of cortex, which will have the effect of facilitating communication by reducing the length of connections between neurons. Explanations based on deafness and sign language use are not mutually exclusive, but raise the intriguing possibility that there is an additive effect of sensory deafferentation and environmental enrichment (specifically visual environment in terms of the sign language signal).

In conclusion, we have shown enhanced peripheral acuity in congenitally deaf adults is accompanied by increased cortical pRF size, in the absence of any change in the density of pRFs. This may suggest a 'coarse coding' strategy, in which overlapping neurons are better able to localise and discriminate peripheral stimuli. The lack of increased surround representation of the population receptive field suggests these effects are not mediated by suppression effects, but are a result of an enlargement of the whole pRF, and in particular the facilitatory centre region. These results demonstrate auditory deprivation is capable of causing both structural and functional plasticity of the cortical architecture in primary visual cortex.

Chapter 4: How is visuomotor information and sensorimotor skill learning represented throughout the brain?

Abstract

Visuomotor transformations translate visual information in retinotopic coordinates into muscle space firing patterns for movement. We trained participants over a period of 8 days to make reaching movements with a robot manipulandum controlling an on-screen cursor towards 6 visually presented targets. Participants completed this task with typical visual feedback, and when the visual feedback was mirror-reversed, allowing the dissociation of visual and motor task components. We completed functional magnetic resonance imaging on participants both when they were novice and expert at completing this task. These data were analysed using a pattern component model. This allowed us to address two related questions.

Firstly, how is visual and motor information represented throughout the cortex? We found evidence of visual encoding in visual cortex, parietal regions including intraparietal sulcus (IPS) and occipito-parietal junction (OPJ), as well as throughout sensorimotor cortex, including primary motor cortex (M1). Motor encoding was present throughout sensorimotor cortex, and overlapped with visual encoding in the superior parietal occipital cortex (SPOC). Strikingly, there was also evidence of motor encoding in primary visual cortex (V1), which we interpret as indicating V1 is predicting the visual consequences of actions. Visual and motor encoding was the most equally balanced in superior parietal cortex, which suggests an important role for these regions in visuomotor coordinate transformations. These findings suggest the amount of multimodal information throughout the brain has previously been underestimated.

We then wanted to determine whether we could identify changes in the neural representations of sensorimotor skill which occurred with short term experience dependent plasticity. Increases in directional encoding strength were found in the isthmus cingulate for typical reaching between sessions, whereas decreases in directional encoding strength were

found in inferior parietal and postcentral regions with learning of mirror-reversed reaching movements. An interaction was found between the visual feedback conditions (typical and mirror-reversed) and session (1 and 2) for directional encoding strength in lateral occipital regions, and also in superior temporal sulcus (STS), supramarginal gyrus (SMG) and in lingual gyrus. The decrease in directional encoding strength was more pronounced in the mirror-reversed condition. This pattern of results tentatively suggests that learning a mirror-reversal results in decreased reliance on visual and parietal cortices to perform remappings, and that motor cortex has learnt this model instead.

Introduction

Underpinning every visually guided movement is a visuomotor transformation; visual target information is received in retinotopic coordinates, and this must be translated to a muscle space coordinate frame for the firing patterns of motoneurons to execute the correct action. We can also learn and perform additional visuomotor transformations in scenarios were either visual feedback or the motor action is distorted, for example when visual feedback is mirror-reversed or when using a tool. Here we trained participants on a sensorimotor skill learning task over a period of eight days. Participants were required to make reaching movements with a robot manipulandum towards six visually presented targets, both when the visual feedback was typical and when it was mirror-reversed. Therefore visual and motor information were dissociated. There were 2 main questions we wanted to address.

There is a gradient of information from primary visual cortex, which has a retinotopic coordinate system, to the muscular coordinate system of motoneurons in primary motor cortex. Visuomotor transformations translate between these coordinate frames, and have been repeatedly shown to recruit parietal and premotor cortices (Kalaska and Crammond, 1992, Graziano et al., 1994, Graziano and Gross, 1998, Snyder, 2000, Andersen and Buneo, 2002, Buneo et al., 2002, Merriam et al., 2003, Buneo and Andersen, 2006, Graziano, 2006). However, the representation and coordinate transformation of information for visually guided reaching movements is not confined to these regions. There is evidence that information can be represented in extrinsic coordinate frames in primary motor cortex (M1). Direction selectivity for preferred movement direction has been shown in electrophysiological recordings of macaque monkey M1 (Georgopoulos et al., 1986, Georgopoulos et al., 2007). Kakei et al., (1999) developed a task to dissociate extrinsic (direction of movement in space), muscle (activity of individual or groups of muscles) and joint (related to the angle of the wrist joint) based coordinate frames. They acquired single unit neuronal recordings from hand area neurons in both M1 and the ventral region of premotor cortex (vPMV) (Kakei et al., 2003). Just over half of the M1 neurons identified as active during the execution of arm movements

exhibited directionally selectivity (Kakei et al., 2003). These neurons exhibited muscle, visual and combined properties in approximately equal proportions. The vast majority of PMv neurons (81%) were responsive to the extrinsic visual properties of the stimulus (Kakei et al., 1999).

Functional magnetic resonance imaging (fMRI) with multivariate pattern analysis can be used to study directional tuning for movement throughout the cortex. To investigate how reach direction and grip are represented in the brain, Fabbri et al., (2014) had participants make reaching movements which differed in terms of movement direction and grip type (touch, pincer or whole hand). Dorsal premotor cortex (PMD), superior parietal lobule (SPL), M1, primary sensory cortex (S1), supplementary motor area (SMA), and intraparietal sulcus (IPS) all exhibit directional tuning, with a subset of these regions additionally representing grip information (Fabbri et al., 2014). Directional encoding can be decomposed further into its visual and motor components. Eisenberg et al., (2011) instructed participants to make reaching movements with a joystick with typical and rotated visual feedback. With M1 as a region of interest, correlations were found between BOLD activity patterns not only when movement directions were matched, but also when the visual feedback (on-screen cursor) matched between conditions in which movement directions were different. This provides evidence M1 is coding goals in both motor and visual coordinate frames. However, such decomposition of visual and motor information has not been performed throughout the cortex. Therefore the first aim of this chapter was to map the distribution of visual and motor directional coding across the cortical sheet.

Participants were scanned both when they were novice and expert at completing this reaching task, allowing us to examine how neural representations change throughout sensorimotor skill learning. Motor skill learning has been extensively studied using fMRI, consistently implicating the cortico-cerebellar and the cortico-striatal parallel loops for learning (Doyon et al., 2009, Penhune and Steele, 2012). However, there is a lack of consensus

regarding the functional role of each region which is caused, in part, by inconsistent findings from BOLD activation studies. For example, some researchers report increased brain activity in M1 when participants learn a motor behaviour (Grafton et al., 1995, Hazeltine et al., 1997, Karni et al., 1998, Penhune and Doyon, 2002, Debaere et al., 2004a, Floyer-Lea and Matthews, 2005, Penhune and Doyon, 2005). This has been interpreted as a greater number of cortical units being recruited into the representation, which consequently increases the metabolic demands in the region of performing the task. Other researchers find the converse; learning is associated with decreased neural activity in M1 (Toni et al., 1998, Ungerleider et al., 2002), which has been interpreted as learning resulting in 'neural efficiency' (Poldrack, 2000, Poldrack et al., 2005, Ma et al., 2010). However, the usefulness of the concept of efficiency in explaining learning-related changes has recently been questioned (Poldrack, 2014). The typical definition of efficiency, as applied to neural data, states the same neural computation is performed under reduced metabolic demands. However, in fMRI this cannot be distinguished from a different neural computation taking place (Poldrack, 2014). Similarly, with learning the computation might occur at a reduced intensity or for a shorter time period, which can be conflated with the computation having reduced metabolic demands (Poldrack, 2014).

Further discrepancies may arise in BOLD activation studies because learning is a non-linear process. Hardwick et al., (2013) completed a meta-analysis on tasks which were broadly sequence learning (action selection) or sensorimotor learning (novel movements dynamics and kinematics, eg. visuomotor adaptation) tasks. This identified left PMD in a conjunction analysis and as being modulated for both these types of motor skill learning, suggesting a learning critical role for this region (Hardwick et al., 2013). Activity in PMD both increased and decreased during the course of motor skill learning, highlighting that the role and recruitment of different regions likely changes over the learning process (Hardwick et al., 2013; for a meta-analysis of motor skill learning over different timescales see Lohse et al., 2014). Due to the ambiguity in the BOLD signal we cannot confidently conclude what attributes of the learning processes are reflected in the signal. Moreover, the BOLD signal is very sensitive to higher

cognitive functions such as attention, which are likely to fluctuate over the course of learning. This further compounds the problem of relating learning to fMRI activations.

How then can we use fMRI to study the plasticity associated with motor skill learning? Wiestler et al. (2013) used representational similarity analysis (RSA) to examine the neural populations underpinning skilled movements. With training, the neural activity patterns associated with different finger sequences can be more easily distinguished from one another with multivariate pattern classification (Wiestler and Diedrichsen, 2013). Initially each finger movement within a sequence is thought to be controlled by a separate neural activity pattern, but with learning, representations develop which encode the sequential transitions between several finger presses (Matsuzaka et al., 2007), which over time will reduce the overlap between different neuronal populations. Sensorimotor tasks are dependent on distributed neural circuitry for the integration of visual and proprioceptive information for accurate motor execution, rather than combining chunks of motor programs as is the case in sequence learning. It is not yet known whether the development of specialised neuronal populations underpinning sensorimotor skill learning can be measured with fMRI.

Methods

Participants

A total of 16 participants completed the entire experiment (11 females). Data from 2 of these participants (1 male 1 female) were discarded prior to analysis owing to one participant sleeping during a scanning session, and one participant moving out of the field of view following the localisation scan. An additional 5 participants were excluded from the experiment on the initial 'pre-screening', which was designed to assess their motivation to learn the task. Participants were right handed (as measured by the Edinburgh handedness inventory), had no history of neurological illnesses, no injuries or diseases affecting the upper limbs, and were not taking any psychoactive medication. Participants were additionally asked to not take any recreational drugs or drink more than 2 units of alcohol per night during the

training sessions. Participants were recruited through online advertising on a subject database. Participants were remunerated at the conclusion of the study. The UCL Ethics Committee approved the study, and we obtained informed written consent before commencing testing with each participant.

Apparatus and visual display

Participants completed out of the scanner behavioural testing sessions in addition to scanning testing sessions. They completed the training component of the task on a mock scanner bed where participants were required to lie in the supine position with their head elevated slightly, viewing a screen tilted by approximately 30° degrees from the vertical position, positioned approximately 30cm from their eyes (figure 4.1).

Figure 4.1: *Participants were required to lie in the supine position whilst holding a robot manipulandum which controlled an on-screen cursor. Eye position and fixation was monitored in this position and participants were given feedback regarding their performance at the end of each run.*

Participants moved a robotic arm device which controlled an on-screen cursor (2mm diameter) from a central fixation cross to targets 8cm from the central fixation point which appeared in one of six visual field locations, and back into the central fixation point. The robotic arm device was obscured from the participants' field of view. The robotic device allowed for unrestrained movement in the horizontal plane, and measured position of the hand at 200Hz. Reaching for the targets required movements involving the shoulder, elbow and wrist, moving over the participants torso. Visual feedback was displayed on a monitor

(60Hz refresh rate, 65ms delay). Participants fixated centrally throughout the experiments. Their eye movements were monitored with a ViewPoint eye tracker, and they were given verbal feedback at the end of each block of trials regarding their fixation stability.

Scanning and training were performed with the same fMRI-compatible device. Participants viewed their visual feedback via a mirror to a back projection set up (60Hz refresh rate, 100ms delay). We provided a bite bar to stabilise head position, though 6 participants refused this due to finding it uncomfortable. An iViewX eye tracker was used to monitor participant's eye movements. However, owing to the bite bar fixing participants head in the central location and the shadow from the head coil, recordings were unreliable and were not analysed further.

General Procedure

We trained participants over a period of 8 days (with a 2 day 'weekend' between days 5 and 6) to perform accurate reaching movements (see Table 4.1). Functional magnetic resonance imaging (fMRI) took place on both day 2 and day 8 of the training regime.

Day 1	Day 2	Day 3	Day 4	Day 5	Day 6	Day 7	Day 8
DRP TYP	DRP MR	Speeded MR	Speeded MR	Speeded MR	DRP Switch	DRP Switch	**fMRI Switch**
	fMRI Switch						

Table 4.1: *All participants underwent the following training regime with 'weekend' between days 5 and 6. Day 2 was the only day with 2 experimental sessions. DRP – delayed response paradigm, TYP – typical visual feedback, MR – mirror-reversed visual feedback, Switch – switching between typical and mirror-reversed visual feedback. The delayed version of the task was always performed in the scanner.*

Participants moved the cursor controlled by the robot manipulandum from a central fixation cross to and from a target 8cm from the central fixation cross, which appeared in 1 of 6 equally spaced locations (30°, 90°, 150°, 210°, 270°, 330°) in a circle around the central fixation cross. There was a speeded and delayed response version of the task (see Figure 4.2 for schematic). In the speeded version of the task, the target was green when it initially appeared on the screen, signalling to participants to commence their movement as quickly as

possible. In the delayed version of the task, the target initially appeared on the screen in red, and then turned green following a period of 600ms, signalling to the participant to move. The speeded version of the task was designed to encourage participants to automatize the task, whereas the delayed sessions were to train participants to complete the task without making excessive jerking movements which would result in head motion in the scanner. The task was completed both without any manipulation on the visual feedback, and when the visual feedback was mirror-reversed (i.e. flipped across an axis from the top to the bottom of the screen, running through the fixation point). Thus to reach to a target at 30°, participants had to make an arm movement towards the 270° target, which they would observe on-screen as a movement towards the 30° target. Participants were exposed to the mirror-reversed mapping on day 2 prior to the scanning session to ensure they were sufficiently familiar with it to be able to perform it with a reasonable degree of accuracy in the scanner. To avoid sleep dependent consolidation of the mirror-reversed mapping, we did not expose participants to this mapping on the first day.

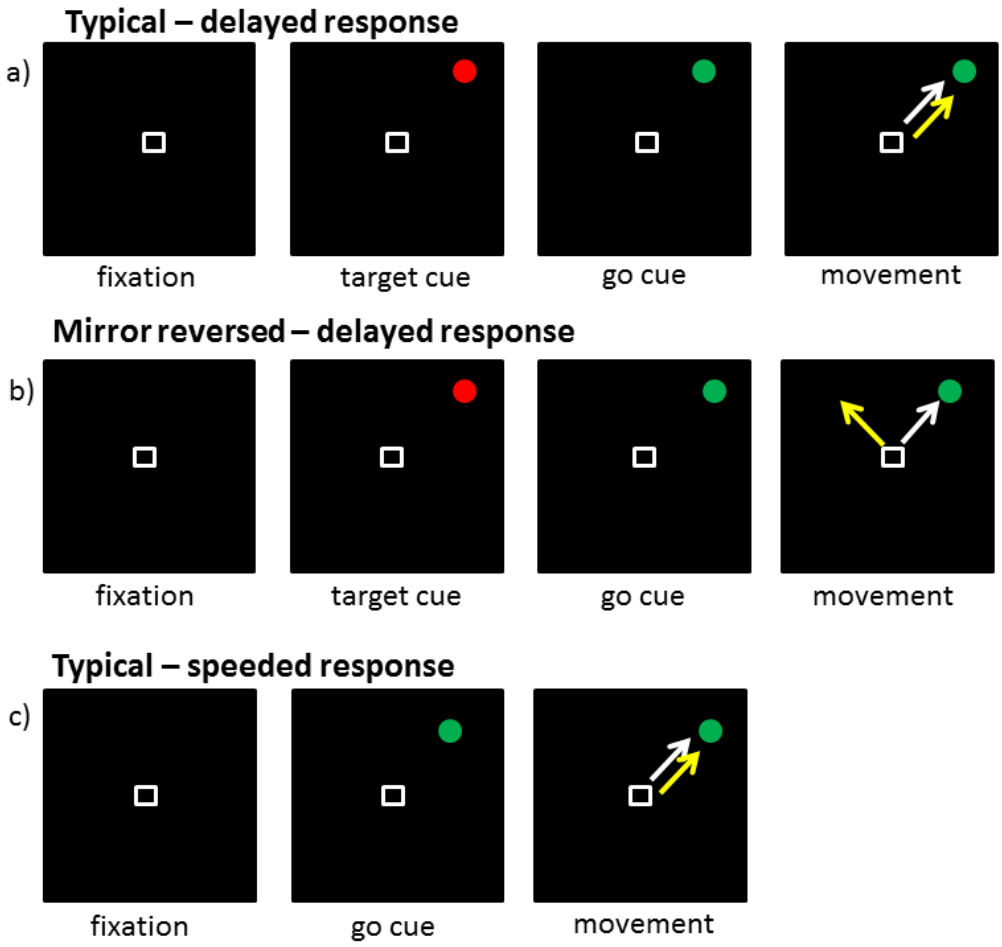

Figure 4.2: *Schematic of the task. Fixation point is denoted with a white box and was present throughout each trial, red circles denote the target cue, and when these turned green the participant had to move. During the speeded version of the task, the target immediately appeared on the screen as red and participants had to move immediately. The white arrow corresponds to the visual feedback, and the yellow arrow corresponds to the arm movement participants were required to make to cause the cursor to move into the target. The conditions displayed are as follows; A) delayed response paradigm with typical visual feedback, B) delayed response paradigm with mirror-reversed visual feedback, C) speeded paradigm with typical visual feedback.*

Training sessions consisted of 10 blocks of 72 arm movements, which were one of typical reaching, mirror-reversed reaching, or switching between these 2 mappings mid-run. Switching between the visual mappings was announced on the screen with the word 'swap'.

Scanning sessions consisted of 6-8 blocks of 72 arm movements, each block requiring the participant to switch between mirror-reversed and typical reaching. Typically 8 blocks were acquired, however, due to technical failure and time constraints, for 2 participants only 6

blocks were acquired in the first session, and one participant had only 7 blocks in the second session. For one participant, only 6 blocks were acquired in the second session. During scanning, if a participant finished a block in the mirror-reversed visual feedback mapping they would commence the next block in this mapping also, as was the case for the typical mapping. Pilot work demonstrated that participants exhibited a 'switch cost' when moving between the two mappings, therefore we blocked as many of these trials together as possible to maximise the number of correctly executed arm movements.

During training sessions, starting when the green target appeared, participants had to commence their movement within 600ms and complete this movement within 1000ms, otherwise they would receive error feedback (specifically a blue fixation cross and an irritating tone). When the participant returned the cursor to the initial fixation cross a new trial was initiated. The movement time completion criterion was relaxed to 7000ms during fMRI scanning (the same as the trial length) which provided ample time for participants to complete the movements, even during trials in which they made extensive online corrections. Movements were considered to be started when tangential velocity exceeded 2.5 cm/s for at least 200ms. A yellow fixation cross was displayed when the maximum radius of the movement exceeded 14cms. A green fixation cross signified that the movement speed was accurate, but that the accuracy of the movement was poor. A red visual explosion and pleasant tone was used to indicate that the movement was correct and participants would be awarded a point. Feedback was provided for each movement. During the training sessions, a points counter was displayed below the fixation cross to motivate participants'. This counter was not present in the scanner, but for motivational purposes, participants were informed of their points total at the end of each run.

Imaging Parameters

As in chapters 2 and 3, imaging took place at the Birkbeck UCL Centre for Neuroimaging using a 1.5 Tesla Siemens Avanto MRI scanner (Erlangen, Germany) with a 32

channel head coil. A multiband sequence with multiband accelerator factor of 4 was used, such that 4 non-adjacent slices were excited simultaneously. We used 36 contiguous slices rotated at ~45° from the AC-PC line. This allows coverage of motor regions, parietal and visual cortex, as well as the most superior part of the cerebellum. There was no coverage of the inferior prefrontal lobes, or the inferior or anterior temporal lobes. Voxel size was 2.3x2.3x2.3 mm, with TR=1000ms, TE=55ms, with a flip angle of 75°, and BW=1628Hz/pix. For each scanning run, 532 volumes were acquired, the first 10 of which were discarded to ensure magnetisation stabilisation transfer.

An MPRAGE structural sequence with voxel size of 1mm³, flip angle of 7°, T1=1000ms, TR=8.4ms, TE=3.57ms and BW=190 Hz/pix was acquired, also using the 32 channel head coil.

Imaging Pre-processing

SPM 8 was used to realign and unwarp the functional images (http://www.fil.ion.ucl.ac.uk/spm/software/spm8/), and to coregister the volumes with the anatomical scan. Data was neither spatially smoothed nor normalised to an anatomical template at this stage.

Cortical reconstruction of the anatomical scan was completed in FreeSurfer version 5.0.0. (http://freesurfer.net/fswiki/FreeSurferWiki). Details of this procedure are provided in chapter 2. Both hemispheres from each participant were registered to the same, symmetric surface-based template brain using FreeSurfer (fsaverage_sym). This data was transferred into CARET (http://brainvis.wustl.edu/wiki/index.php/Main_Page).

Surface-based searchlight

We used a surface based searchlight to perform the pattern component analyses. Around each vertex generated during the cortical reconstruction in FreeSurfer, a circle was defined and slowly grown, until it included 300 voxels between the pial and the white-gray surfaces. The average resultant radius was approximately 17.5mm. Analyses were performed

on the data from each of these searchlights, and the results were assigned to the central vertex, creating a full surface map of information content (Oosterhof et al., 2011).

Region of Interest

For ROI analyses we used 16 regions of interest which were defined symmetrically in both hemispheres. These regions included primary somatosensory cortex (BA 2,3 and 1 – 2.5cm above and below the hand knob), the hand region of primary motor cortex (BA4 -2.5cm above and below the hand knob), dorsal pre-motor cortex (lateral aspect of BA 6 – superior to the middle frontal gyrus), ventral pre-motor cortex, supplementary motor area (medial aspect of BA6), intra-parietal sulcus (areas medial to the fundus of the intraparietal sulcus) and the occipital parietal junction in both hemispheres. These regions of interest were based on a cytoarchitectonic atlas aligned to the FreeSurfer atlas surface (Fischl et al., 2008). These regions were initially defined in the symmetric group template, and projected into each participant's native space image via their individual surface.

Imaging Analysis

Data analysis was performed using SPM8 and custom-written MATLAB (MathWorks) routines. A general linear model (GLM) was used to estimate how much each voxel was activated by the 12 conditions (6 target angles x 2 visual feedback conditions) in each of the runs. When appropriate, a 13^{th} regressor was used to model error trials made in all conditions (see results section for criteria for error trials). Boxcar functions were used as regressors which were equal to one when the trial type was present, and zero otherwise. As such, each regressor was the average of the activity for all trials of that condition (unique visual mapping x target angle combination) in each run. These boxcar functions were then convolved with the canonical haemodynamic response function in SPM8. GLMs were estimated using the robust weighted least squares (RWLS) toolbox (Diedrichsen and Shadmehr, 2005). This divides each image by the estimated noise variance in the image, which means that images were there are movements or other potential sources of artefact (corresponding to high variance in the

image) are effectively down-weighted to approximately zero in terms of their contribution to the time series. Low frequency trends were removed from the data. For each participant, a GLM was constructed for either session. The data for each of these sessions was realigned to the first image of the first session, so that there was a voxel-to-voxel correspondence between sessions.

Multivariate Analyses

Multivariate analyses can be used to investigate how a variable is encoded within a cortical region. The approach we used here consisted of 2 main stages. Initially we estimated variance-covariance matrices (G matrix) of the patterns associated with each of the 12 conditions (6 target directions x 2 visual feedback conditions) from the beta estimates from general linear models (GLM) calculated for each scanning session individually (see above for the description of how the GLMs were constructed). Several pre-processing stages were completed on these beta estimates before estimating the G matrices. We used estimates of noise based on each run to spatially pre-whiten the data. There were different numbers of trials of each movement type used to estimate the betas as a result of different numbers of these trials being excluded from the analysis. To account for this, we took the root of the variance-covariance matrix of the parameter estimates multiplied by the residual mean squares of the parameter estimates. We then performed mean subtraction for each run on these betas. The estimation of the G matrix was performed using cross-validation, rendering unbiased estimates (Walther, in prep).

As a second step, we then modelled the estimated G-matrix as a mixture of visual directional encoding, motor directional encoding and directional encoding that was unique to the visual feedback condition (that is, no information was shared between visual and motor coordinates). Figure 4.3 provides a graphical description of the visual, motor and unique parameters in this regression model. For the quadrants corresponding to the covariance between the typical and mirror-reversed reaching conditions, motor encoding is the flipped

version of the visual matrix. For the 30° target, when there is visual encoding, we would expect the highest covariance between movements 1 and 7, as this produces the same visual stimulus of moving towards the 30° target, despite the difference in the movement required to generate this cursor movement. On the other hand, for motor encoding, covariance would be highest between movements 1 and 12 as these are matched movements, although the on-screen cursor movement they generate is different. When there is unique encoding, there would be no covariance between any of the movements between the different visual feedback conditions, as there is no shared information in either visual or motor coordinates.

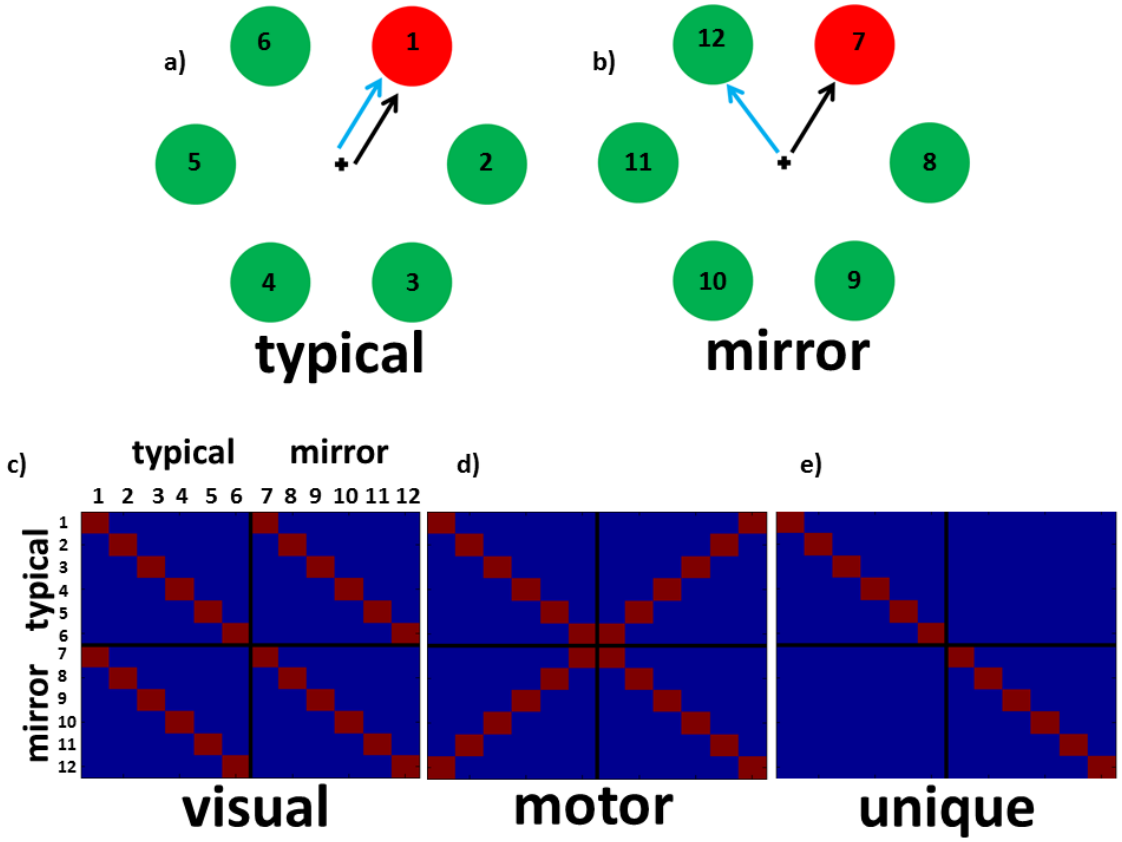

Figure 4.3: Experimental task and design. *a) schematic illustrating the task in the typical reaching condition. Participants made reaching movements with a robot manipulandum towards the highlighted target. The black arrow indicates the cursor movement, and the blue arrow indicates the arm movement that should be made to generate the cursor movement. b) In the mirror-reversed condition, the movement required to generate the same cursor movement towards the highlighted target is rotated around an axis through the centre of the screen. In both a and b, the additional targets and numbers are shown for illustrative purposes, however, these were not present during the scanning or training sessions. We used a pattern*

component model to estimate a cross-validated variance-covariance matrix for these 12 conditions (6 reaching direction X 2 visual feedback). This is demonstrated schematically in the 12x12 matrices depicted in c-e. Target directions and visual feedback conditions are indicated in c. c) directional encoding in visual coordinates. Between the typical and mirror-reversed, movements to target 1 would have the highest correlation as they share the same on-screen cursor movement despite differing in movements required to produce this on-screen cursor movement. d) directional encoding in motor coordinates. Movements to target 1 in typical and target 6 in the mirror-reversed condition have the highest correlation as they share a movement, though the on-screen cursor movement differs. e) directional encoding in unique coordinates. There is no covariance between the two visual mapping conditions.

In addition to these directional-specific terms, we included terms to model the covariance between the typical and mirror-reversed reaching conditions, and the mean patterns for the typical and mirror-reversed conditions.

In sum, the G matrix can be expressed as a weighted sum of 5 component matrices:

$$G=\text{sum}(\eta_{1\text{-}5} * G_{1\text{-}5}) \quad (4.1)$$

One complication, however, is that the covariance matrix for the typical condition was not purely diagonals. Rather, there was evidence for a cross-diagonal (for example, movements to 30° and -30° targets) were more similar to one another than other movements made by participants (see Figure 4.6). As this was present in the typical reaching condition, we know this was not an artefact of the participant simulating the target on the other side of the screen, as the visual and motor information were aligned in this condition. We had to estimate the strength of this cross-diagonal, otherwise in the mirror-reversed conditions we would attribute all variance explained on the off-diagonal to the motor code. More broadly, we needed to estimate simultaneously the strength of directional encoding (diagonal) and the elevated covariance on the cross-diagonal (γ) and the strength of the visual, motor and unique encoding (η). This becomes a dual estimation problem were G can be expressed either as a linear function of η or γ.

$$G=X(\eta) * \gamma + noise \quad (4.2)$$

$$G=X(\gamma) * \eta + noise \quad (4.3)$$

This bivariate regression problem can be solved by alternating between estimating formula 4.2 and 4.3, until convergence. The strength of the directional encoding (corrected for the strength of the cross-diagonal) was then $\eta * \gamma 1$.

Behavioural Confounds

The behavioural exclusion criteria meant that different numbers of trials were used to estimate the strength of typical and mirror-reversed directional encoding in sessions 1 and 2. We correlated these parameters in each participant with the number of trials the estimation was based upon to determine whether there was a dependency between these two factors.

Motor learning by definition involves changes in behavioural performance of a task. Therefore it can be a problem to disentangle effects of learning with those associated with task performance, such as a reduced amount of time spent on the task. We wanted to determine whether these behavioural differences between sessions accounted for the differences observed in the MRI data. To do this, we correlated each participant's peak t statistic in the clusters identified in the contrasts between session 1 and 2 in the BOLD activity analysis and the directional encoding analysis, with the differences between session 1 and 2 in their kinematic data for the potential behavioural confounds of reaction time, movement time, maximum speed and early error.

In addition to between-session changes in kinematic parameters averaged across all movement directions correlating with between-session differences in BOLD activation or directional encoding strength, it is also possible that the encoding analysis is sensitive to differences in a combination of kinematic parameters between different movement directions within a session. To test for this possibility, we performed the same analysis as used on the imaging data on the kinematic parameters of reaction time, movement time out, maximum

speed, end radius, movement time out and back, absolute error 100ms and 200ms into the movement, absolute error from the target, and absolute error 100ms from when the movement ended.

We calculated a pre-whitened cross-validated variance-covariance matrix on this data, and then used a dual estimation method to simultaneously estimate the parameters of η and γ. More information on these methods is provided above. From this behavioural data, we calculated an estimate of the systematic differences between movement direction, which are preserved in visual, motor and unique coordinates for each participant for each participant in each session, and correlated this with the t statistic at the peak of each cluster for visual, motor and unique encoding in each session.

Results

For this chapter, participants made reaching movements towards six visually presented targets while the visual feedback presented to them was typical and when it was mirror-reversed. Participants were scanned both when they were novice and expert at the task (see methods for further details). The purpose of this experiment was twofold. First, we dissociated the visual and motor aspects of visually guided reaching behaviour. Following this, we investigated the neural representation of sensorimotor skill learning.

Trial exclusion criteria

Often participants made an early error, which they rapidly corrected. However, in some instances participants made an entirely mirror-reversed movement. Alternatively some participants initially executed a correct movement towards the target, but began their movement back to the target in the other mapping from what they should be using, causing the cursor to move out again rather than towards the inner fixation cross. We sought to remove these trials as they would be a confounding factor in our analysis. We excluded all trials in which the error was greater than 60° at 150ms, or greater than 45° at 200ms, or greater than 40° at 300ms, or greater than 90° within 100ms of the trial ending. We applied

additional exclusion criteria to remove very atypical trials. We excluded all trials for which the maximum radius was greater than 15cm, the minimum radius was less than 4cm, the speed was higher than 100m/s, or lower than 15m/s. Often participants developed a strategy of making curved movements, passing through the target rather than using the target to turn around in. We excluded all trials in which the cursor was more than 3cm perpendicularly displaced from the mid-point (4cm) on the line connecting the fixation cross and the target, both on the movement out towards the target and the movement home. These exclusion criteria resulted on average of 7.96% (SD: 3.2%) of typical trials being excluded in the session 1, and 6.4% (SD: 3.31%) of typical trials being excluded in the session 2. For mirror-reversed trials, and average of 18.54% (SD: 14.55%) were excluded in session 1, and 14.54% (SD: 3.07%) if trials were excluded from session 2.

fMRI data analysis

How is visual, motor and unique encoding represented throughout the cortex?

Figure 4.4 shows average BOLD activity and directional encoding of all visual mapping conditions for both sessions.

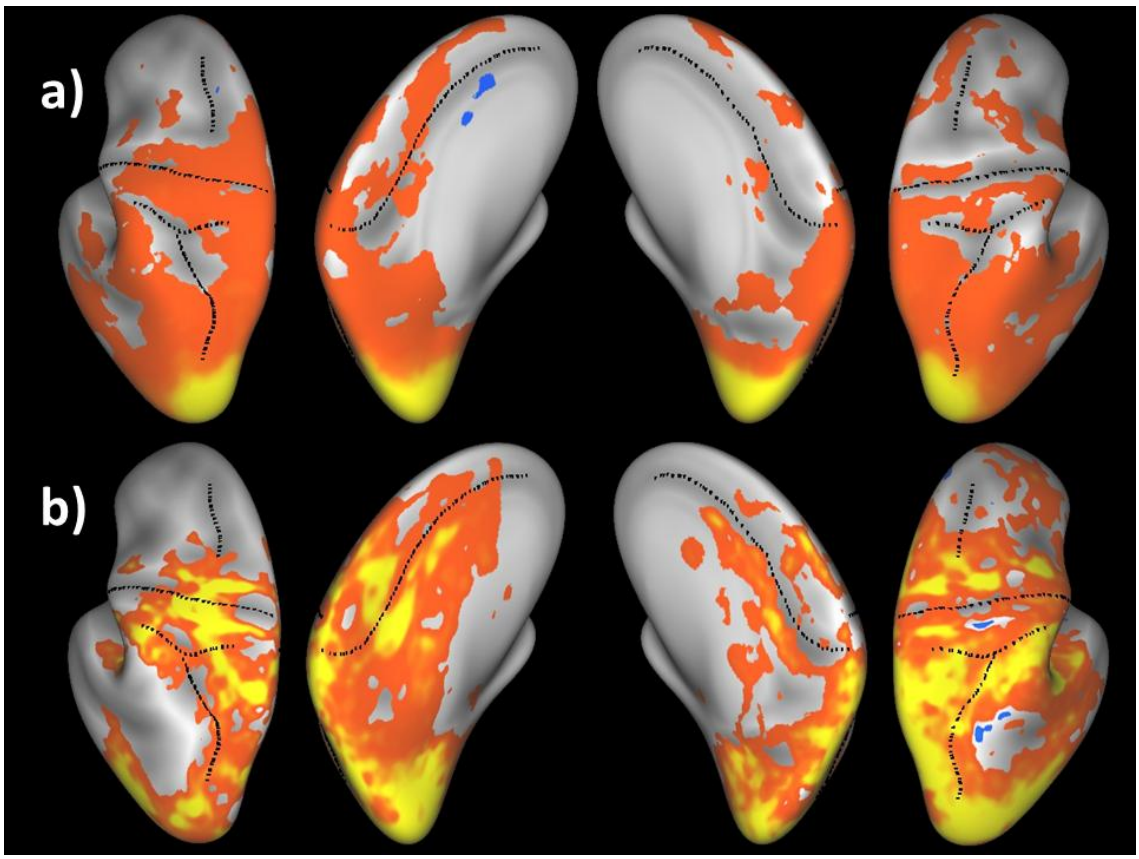

Figure 4.4: *a)Mean directional encoding (thresholded at +/-0.05 a.u.) and (b)mean BOLD percentage signal change (thresholded at +/-0.05%) for all movement directions (i.e. main effect of 12 condition regressors) averaged across scanning sessions. These maps were used as masks for further analyses. The left hemisphere is presented on the left hand side.*

Figure 4.4 demonstrates that BOLD is modulated throughout most cortical areas in the field of view used, including occipital, temporal, parietal and frontal lobes. A more restricted set of regions focussed on the occipital lobe, extending into superior parietal and inferior parietal regions, as well as contralateral motor and sensorimotor cortex exhibit directional encoding. These maps were used as functional masks for subsequent BOLD percentage signal change and multivariate analyses, respectively.

We asked participants to complete the reaching task to the 6 different targets with both typical and mirror-reversed visual feedback conditions to be able to dissociate the visual and motor components of making visually guided reaching movements (see figure 4.3). This

means that within these regions exhibiting directional encoding, we can determine how much of this is constituted by visual, motor or unique encoding. Unique encoding corresponds to directional information which cannot be accounted for by the visual or motor aspects of the task. As described above, we computed a cross-validated variance-covariance matrix that expressed the similarity of these 12 activity patterns.

Figure 4.5 below demonstrates variance-covariance matrices in eight left hemisphere cortical regions, so contralateral to the arm which was used for task performance. Data was averaged across sessions (see supplementary information table 4.1 for between session contrasts). From the structure of the covariances between activity patterns we can determine the type of encoding. Visual inspection suggests there is evidence of visual encoding in V1/2, motor encoding in S1 and M1. Regions such as PMv show evidence for both mixed visual and motor codes, whereas in regions PMv and SMA there is less evidence for directional encoding. Unfortunately the structure of the variance-covariance matrix does not only contain simple diagonals as outlined in Figure 4.3. Instead, the cross-diagonal has more covariance in comparison to the background; movements to the 30° and -30° directions are more similar to each other than other movements. This cross-diagonal needs to be considered in the analysis, otherwise we cannot distinguish it from motor encoding. Hence we used a bivariate regression method to simultaneously estimate the hyperparameters corresponding to visual, motor and unique encoding (η), as well as the underlying directional tuning function present in the network (γ) (see methods for more complete details on this method).

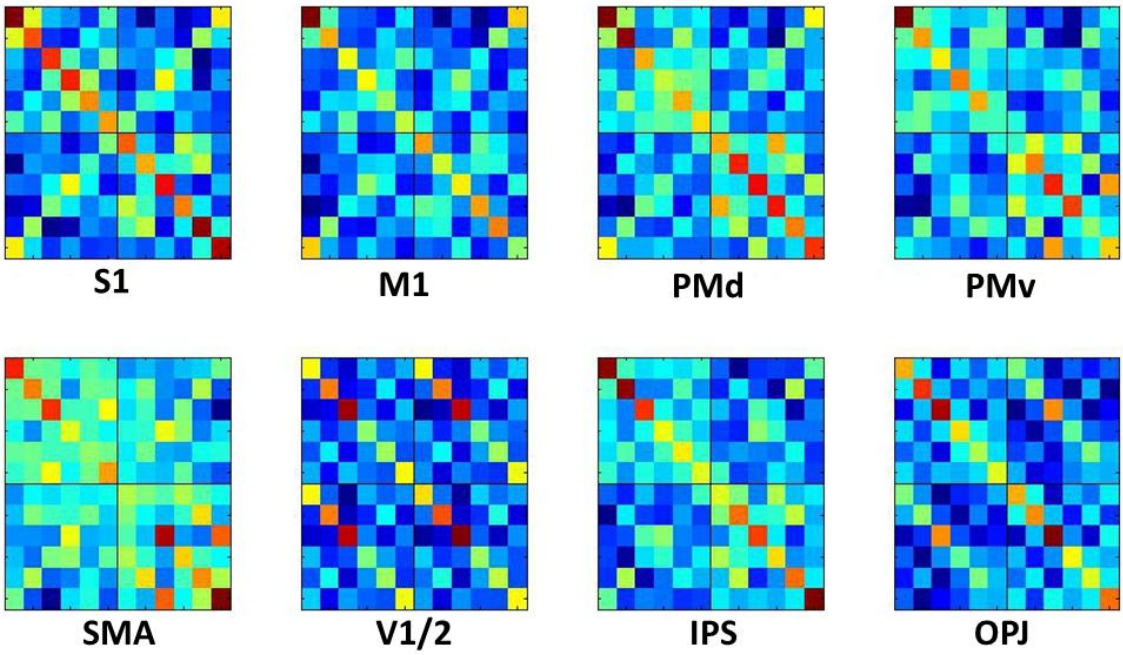

Figure 4.5: *Variance-covariance matrices for contralateral regions of interest. The following abbreviations have been used. S1 – primary somatosensory cortex, M1 – primary motor cortex, PMd – dorsal premotor cortex, PMv – ventral premotor cortex, SMA – supplementary motor area, V1/2 – visual area 1 and 2, IPS – intraparietal sulcus, OPJ – occipito-parietal junction. In regions S1, M1, PMd, PMv and V1/2 there is evidence of a cross-diagonal, whereby in the quadrant corresponding to typical reaching the diagonal opposite to directional encoding is brighter than the background.*

Throughout the rest of this section, visual, motor and unique encoding will be averaged across sessions (see supplementary information table 4.1 for between-session comparisons). Figure 4.6 shows regions of visual, motor and unique encoding, and tables 4.2, 4.3 and 4.4 detail significant clusters of activation in these maps.

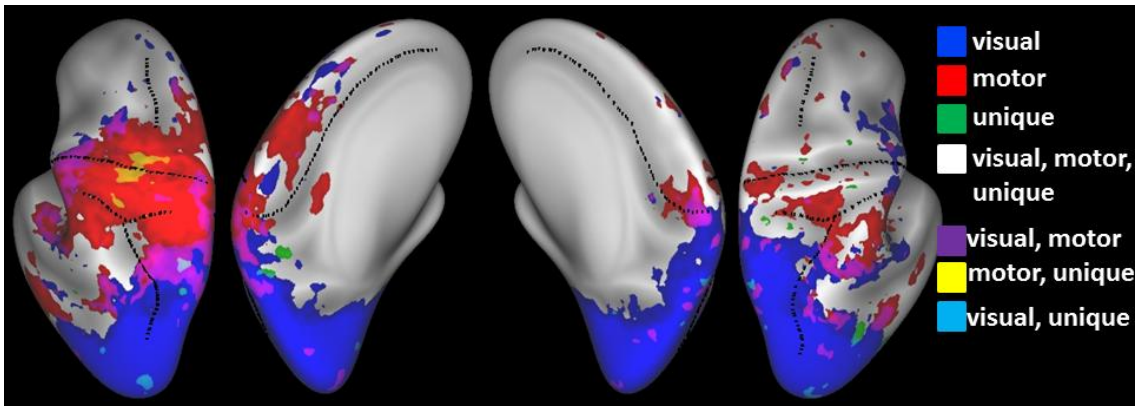

Figure 4.6: *Mean encoding parameters (thresholded at 0.1 a.u.) Visual encoding predominates throughout visual cortex, whereas motor encoding is found throughout motor cortex. Superior parietal cortex displays a high degree of overlap between visual and motor encoding. The left hemisphere is presented on the left hand side.*

Region	H	Area	p(cl)	Max (t)	X	Y	Z
Inferior parietal, pericalcarine, cuneas, precuneas, lingual gyrus, lateral occipital gyrus, fusiform gyrus	L	17580.39	<0.001	14.96	-45.35	-67.73	34.26
Paracentral	L	696.68	<0.001	8.64	-11.25	-29.90	56.91
Precentral	L	658.28	<0.001	6.84	-57.64	-5.33	29.96
Superior temporal	L	425.19	<0.001	7.20	-51.43	-30.32	4.06
Precentral	L	344.87	0.001	11.92	-47.77	-4.32	35.08
Superior temporal sulcus	L	233.68	0.013	4.53	-54.17	-46.97	9.49
Precentral	L	181.72	0.046	5.85	-14.62	-30.59	58.95
Pericalcarine, inferior parietal, cuneas, precuneas, lingual gyrus, lateral occipital gyrus, fusiform gyrus	R	18560.15	<0.001	17.42	7.34	-79.73	16.71
Superior temporal, transverse temporal gyrus and sulcus	R	1697.20	<0.001	13.25	56.94	-41.91	26.42
Caudal middle frontal	R	914.07	<0.001	7.76	25.17	-0.98	40.78
Postcentral	R	323.15	0.002	6.00	56.57	-13.38	31.43
Superior frontal	R	186.12	0.045	5.57	9.19	7.92	59.28

Table 4.2: *Significant clusters of visual encoding with height threshold of T=3.01, p=0.005. p(cl) corresponds to the cluster corrected p value, H corresponds to hemisphere, area is measured in millimetres and (X,Y,Z) correspond to FreeSurfer coordinates.*

Region	H	Area	p(cl)	Max (t)	X	Y	Z
Precentral, postcentral, premotor cortex, supramarginal, superior parietal, transverse temporal sulcus & gyrus, superior temoral sulcus, insula	L	12106.96	<0.001	21.38	-41.14	-2.97	42.98
Inferior temporal, middle temporal	L	1399.41	<0.001	21.38	-47.59	-53.31	5.06
Superior temporal	L	635.16	<0.001	6.96	-53.18	-28.57	2.65
Inferior parietal	L	446.42	<0.001	11.41	-44.01	-54.53	15.77
Inferior temporal	L	163.97	0.038	4.08	-36.76	-60.74	2.60
Supramarginal, superior temporal gyrus, transverse temporal sulcus and gyrus, insula	R	1561.15	<0.001	9.51	54.62	-25.63	42.86
Postcentral	R	887.33	<0.001	7.19	32.44	-24.40	53.14
Postcentral	R	859.06	<0.001	6.94	9.75	-30.85	54.81
Lateral occipital	R	629.13	<0.001	5.59	44.48	-64.61	5.36
Middle temporal	R	570.83	<0.001	8.91	54.49	-52.37	21.51
Inferior parietal	R	506.53	<0.001	7.56	42.43	-62.34	34.53
Superior temporal sulcus	R	452.40	<0.001	6.86	53.02	-39.43	14.98
Superior parietal	R	288.37	<0.001	6.63	10.66	-61.37	51.84
Superior frontal	R	210.17	<0.001	7.41	6.47	6.11	60.56
Inferior parietal	R	204.71	<0.001	5.95	35.74	-75.72	29.62
Rostral middle frontal	R	169.69	<0.001	4.50	18.87	43.43	32.70
Pars opercularis	R	163.36	0.001	4.05	48.92	14.78	29.04

Table 4.3: *Significant clusters of motor encoding with height threshold of T=3.01, p=0.005. p(cl) corresponds to the cluster corrected p value, H corresponds to hemisphere, area is measured in millimetres and (X,Y,Z) correspond to FreeSurfer coordinates.*

Region	H	Area	p(cl)	Max (t)	X	Y	Z
Precentral	L	206.16	0.031	3.97	-37.60	-20.65	52.91
Lingual	L	189.71	0.046	4.57	-15.42	-71.93	2.44
Lateral occipital	R	210.72	0.044	4.70	23.72	-90.44	2.37

Table 4.4: *Significant clusters of unique encoding with height threshold of T=3.01, p=0.005. p(cl) corresponds to the cluster corrected p value, H corresponds to hemisphere, area is measured in millimetres and (X,Y,Z) correspond to FreeSurfer coordinates.*

From figure 4.6, a clear pattern is evident of visual encoding throughout the occipital lobe, motor encoding throughout motor cortical regions, including dorsal premotor cortex and extending into the supplementary area. Compared to visual and motor encoding, there is a smaller amount of unique encoding throughout the cortex. Unique encoding appears to be strongest in left hemisphere primary motor cortex and also in precuneus cortex. Small patches of unique encoding are observed in the right hemisphere throughout the motor cortex, and also at the temporo-parietal occipital junction. In both superior and inferior parietal regions, and in more ventral motor regions, there is evidence of both visual and motor encoding.

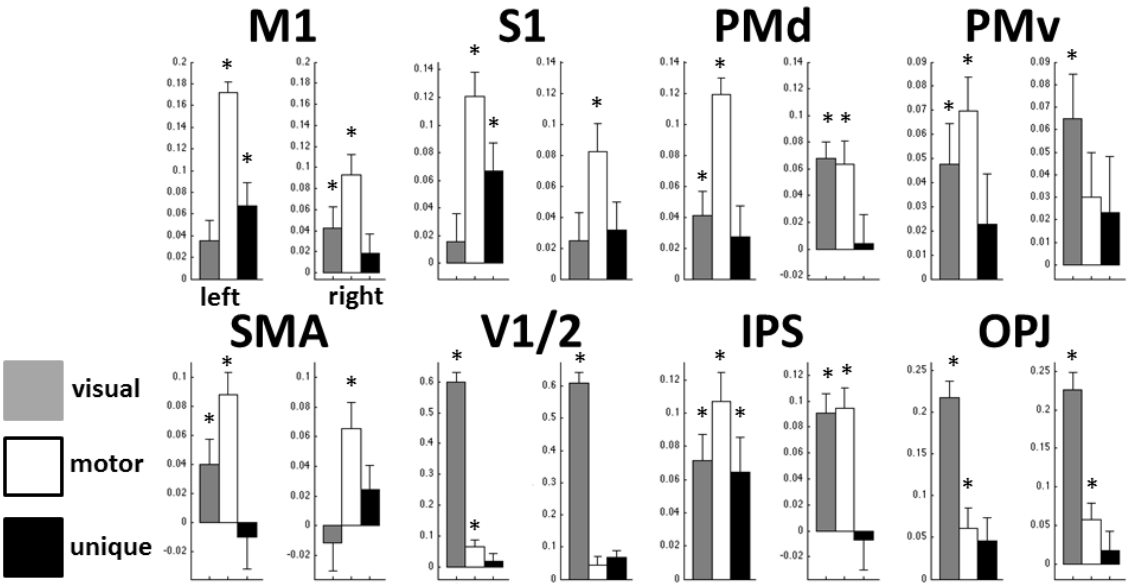

Figure 4.7: *Averaged across the two sessions, we report the η parameters of visual, motor and unique encoding in arbitrary units. Left (contralateral) hemisphere is displayed to the left of the right (ipsilateral) hemisphere. Abbreviations are as for figure 4.5 and details of the ROI are provided in the methods section. An asterisk has been used to denote when the parameter is significantly different from zero. Axes are the same for each ROI in either hemisphere, but differ between ROIs. Error bars correspond to the S.E.M.*

Figure 4.7 displays η parameters in each ROI. There is evidence for visual encoding throughout motor cortex, in regions including right M1, bilateral PMd, left PMv and left SMA. We replicate Eisenberg et al., (2011) in finding evidence for visual encoding in M1, though the strength of motor encoding here is greater (left: $t(27)=5.8433$, $p<0.001$). Motor encoding is

significantly greater than visual encoding in PMd in the left hemisphere ($t(27)=4.299$, $p<0.001$), but not right PMd ($t(27)=0.1288$, $p=0.90$), or left PMv ($t(27)=0.7429$, $p=0.46$). Additionally, there is evidence for motor encoding in the V1/2 ROI. Unsurprisingly, the strength of this motor encoding is vastly reduced in comparison to visual encoding (left: $t(27)=10.6097$, $p<0.001$). Compared to the visual and motor encoding, the amount of unique encoding throughout the brain is substantially smaller. It is of note, however, that all the primary sensory cortices (V1/2, M1, S1) display evidence of unique encoding. The role of the parietal cortex in visuomotor transformations is well established. The left IPS is the only region where there is evidence of all 3 types of encoding. There are no differences between the strength of visual and motor encoding ($t(27)=1.8517$, $p=0.08$), motor and unique encoding ($t(27)=1.499$, $p=0.15$), or visual and unique encoding ($t(27)=0.0696$, $p=0.95$) in the left hemisphere; similarly there are no differences between the strength of visual and motor encoding ($t(27)=0.3674$, $p=0.72$) in the right hemisphere. The results in OPJ demonstrate that although this region is capable of simultaneously representing both motor and visual coordinates, visual encoding in this region is stronger (left: $t(27)=5.576$, $p<0.001$, right: $t(27)=5.5237$, $p<0.001$). Reiterating figure 4.6, these results provide evidence for gradients of visual and motor information throughout the cortex, rather than a single area which is responsible for the coordinate transformation.

Learning Effects

The second question addressed in this chapter, concerns whether we could detect changes in the representation of a sensorimotor task with learning. To address this, we scanned participants at the beginning and end of an 8 day training paradigm.

Training

We had to determine that participants learnt during the course of the training to ensure that we were studying the difference between novice and expert neural representations. It has been suggested that one key characteristic of skill learning are shifts in

speed-accuracy trade-offs, which are not present during visuomotor adaptation to rotations (Telgen et al., 2014). Speed accuracy trade-offs are the dependence of accuracy on reaction time, whereby at shorter RTs, movements become less accurate. Furthermore, the authors observed offline gains, which are overnight improvements or at least resistance to forgetting which occurs during motor skill learning (Telgen et al., 2014).

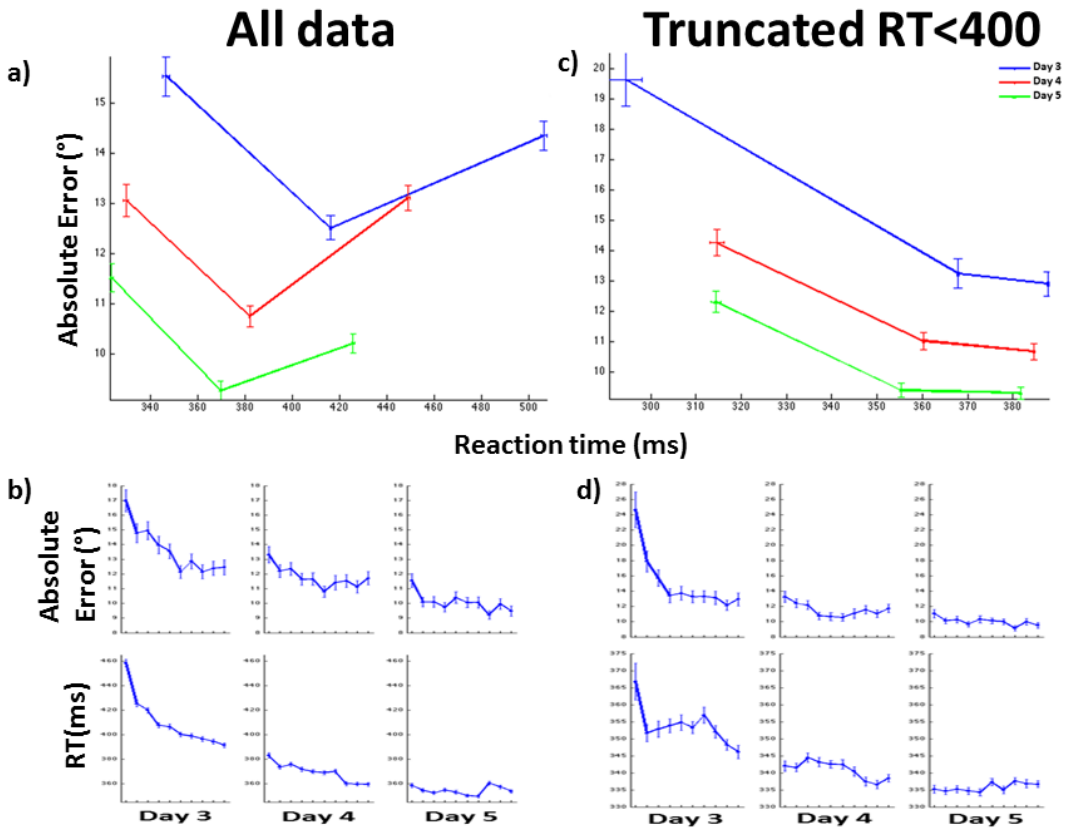

Figure 4.8: *Training data from days 3-5, when participants completed a speeded version of the task. a)speed accuracy trade-off with all data, b) offline gains for absolute error and reaction time for all data, c)speed accuracy trade-off for trials with RT<400ms, d) offline gains for trials with RT<400ms. Error bars indicate S.E.M.*

On days 3-5 of the training paradigm we completed a speeded version of the task, to assess whether these behavioural markers of skilled performance were present. We predicted that short RTs would be associated with larger errors, indicative of a speed-accuracy trade-off, as demonstrated by Telgen et al., (2014). However, figure 4.8a demonstrates a u-shaped relationship between speed and accuracy. Reaction times reported in this chapter are slower

than those observed by Telgen et al., (2014). There were differences between the set up and purpose of these experiments which may have contributed to this discrepancy. In the current experiment, participants were exposed to the delayed response conditions, and the importance of accuracy was emphasized whereas Telgen et al. (2014) emphasized both accuracy and speed in their instructions to participants. To equate the data sets from these two experiments, we truncated data analysis to include only trials with an RT of less than 400ms.

The pattern of results which emerges from the truncated data is more comparable with the results of Telgen et al. (2014). Figure 4.8d displays the results for offline gains. We used a mixed model ANOVA with random effects of participants and fixed effects of day to test the difference between the final block on one day and the first block on the consecutive day. For RT data, there was a significant reduction between the final block of day 3 and the first block of day 4 ($F(1,13)=8.316$, $p=0.01$), but there was no significant reduction between the final block of day 4 and the first block of day 5 ($F(1,13)=0.074$, $p=0.79$). For error data, there was no significant difference between the final block of day 3 and the first block of day 4 ($F(1,13)=1.347$, $p=0.27$), nor between the final block of day 4 and the first block of day 5 ($F(1,13)=2.37$, $p=0.15$). Therefore there is evidence of resistance to forgetting overnight, which suggests motor skill learning is taking place. Figure 4.8c displays the speed accuracy trade-off. We found a negative regression slope between RT and accuracy on each day; day three (beta=-0.2094, 95% CI: -0.2780 -0.1409), day four (beta=-0.1049, 95% CI: -0.1656 -0.0442), day five (beta=-0.2332, 95% CI: -0.2966 -0.1697). Taken together, these analyses strongly suggest motor skill learning occurred.

Task Performance in scanner

Most participants found the task challenging; the mean number of points awarded in the first session was 9.73 (SD: 8.26) in the typical reaching condition and 5.14 (SD: 7.13) in the

mirror-reversed condition. The mean during the second session was 18.8 (SD: 7.19) in the typical reaching condition and 13.02 (SD: 7.28) in the mirror-reversed reaching condition.

Participants may have developed an expert representation of the task on the days in which they performed the speeded version of the task, but did not recruit this representation during the easier delayed version of the task which is performed in the scanner. This may affect one visual feedback condition more than the other. Here, to determine whether participants recruited the expert representation of the task which they acquired during the training days, we contrasted task performance between the 2 sessions on key performance variables. These results are shown in table 4.5. For the early error in both reaching conditions and movement time in the mirror-reversed feedback condition, there are significant improvements between sessions, which suggest participants were making more accurate movements with fewer time-consuming online corrections. It was emphasized to participants throughout the experiment to prioritise the spatial accuracy of the movement above the speed, which is likely to be the reason we do not observe differences in either reaction time or maximum speed. These results suggest participants were recruiting these learned representations. However, this introduces the issue that any differences in the fMRI data between sessions may be a result of behavioural differences (for example, a region is more active in the first session because the participants spent more time overall making the movement) rather than because of learning affecting the neural representation of the task. These potential confounds will be addressed in greater detail below.

	Typical Reaching			**Mirror-Reversed Reaching**		
	Mean(SD)		**F test**	**Mean (SD)**		**F test**
	Sess 1	**Sess 2**		**Sess 1**	**Sess 2**	
RT (ms)	182.64 (77.02)	167.96 (55.60)	F(1,13)=4.405, P=0.0559	179.01 (87.97)	166.55 (58.83)	F(1,13)=2.592, P=0.1314
Early Error (°)	17.95 (27.11)	12.95 (18.86)	F(1,13)=9.782, P=0.0078	24.79 (31.49)	14.93 (20.53)	F(1,13)=15.748, P=0.0016
Max Speed (m/s)	35.35 (13.46)	33.51 (10.70)	F(1,13)=1.739, p=0.2101	34.26 (13.71)	33.12 (10.20)	F(1,13)=0.356, P=0.5612
MT (ms)	629.78 (316.75)	571.05 (258.43)	F(1,13)=3.566, p=0.0815	747.17 (394.44)	612.62 (284.44)	F(1,13)=16.787, P=0.0013

Table 4.5: *Mean and standard deviations of task performance for Reaction time (RT), Early Error(absolute amount of error from the target trajectory at 150ms), Maximum speed (Max speed), and Movement time(MT). A mixed model ANOVA with random effects of participants and a fixed effect of session was used to test for differences between the first and second session.*

BOLD Percentage Signal Change Analysis

Previous studies into motor skill learning have used absolute change in the BOLD signal to characterise learning. For motor learning, interpretation of the BOLD signal is problematic. Motor skill learning has been argued to result in increased BOLD activation in motor cortices, as a result of increased neural recruitment with learning (Grafton et al., 1995, Karni et al., 1995, Hazeltine et al., 1997, Karni et al., 1998, Penhune and Doyon, 2002, Debaere et al., 2004a, Floyer-Lea and Matthews, 2005, Penhune and Doyon, 2005). Alternatively a region may not be recruited for the performance of a task once this task has been learnt. Decreases in BOLD activation have also been reported, which have been interpreted as demonstrating learning creates neural efficiency in the neuronal populations underpinning the movement (Toni et al., 1998, Ungerleider et al., 2002). Increased neural recruitment and neural efficiency will have an antagonistic effect on the BOLD signal, and so it is possible both these processes may occur within the same region in a way which makes it invisible to the mass action BOLD signal. Here we have completed percentage signal change analysis to make our analyses comparable to previous literature, and to use as an adjunct to interpreting the representation similarity analyses reported below. It should be noted however, that as we used different functional masks for the BOLD and directional encoding analyses, direct statistical comparison between these analyses is not viable.

We contrasted the typical reaching movements between novice and expert sessions, and following this, mirror-reversed movements between novice and expert sessions. These results are displayed in table 4.6, and shown in figure 4.9.

Contrast	Region	H	P(cl)	Area	Max(t)	X	Y	Z
				increases				
Typ	Precuneas	L	0.035	203.76	4.48	-9.50	-48.00	-40.00
Typ	Postcentral	R	0.001	375.51	4.40	35.63	-14.73	40.34
				decreases				
MR	Precentral	L	0.001	340.55	4.27	-29.90	-15.92	53.93
				Increases				
MR	Lateral occipital	L	0.005	283.42	5.2	-26.47	-89.81	-1.71
MR	Lateral occipital	R	<0.001	465.53	5.26	28.37	-88.08	8.39

***Table 4.6**: Learning effects: Differences between session 1 and 2 in BOLD percentage signal change (significance determined as exceeding a height threshold of T=+/-2.65 (p=0.01). p(cl) corresponds to the cluster corrected p value, H corresponds to hemisphere, area is measured in millimetres and (X,Y,Z) correspond to FreeSurfer coordinates.*

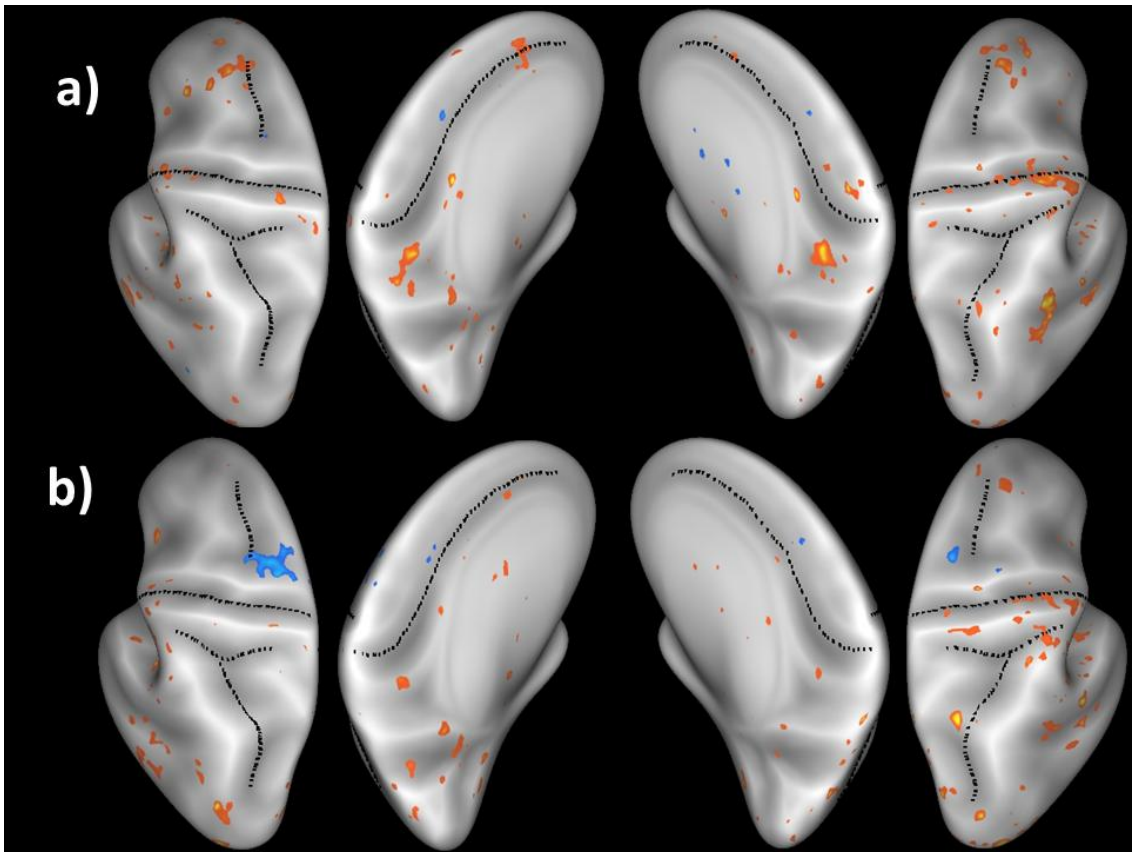

***Figure 4.9:** BOLD percentage signal change for (a) typical and (b) mirror-reversed reaching conditions between sessions 1 and 2. T statistic map with height threshold t=2.65, p=0.01. Increases/decreases indicate activity was greater/less in the expert session. The left hemisphere is presented on the left hand side.*

Directional Encoding Analysis

In addition to BOLD percentage signal change analysis, we used a pattern component model to investigate the strength of directional encoding in typical and mirror-reversed reaching conditions. We contrasted directional encoding strengths between sessions to see if the learning effects were evident in the strength of directional encoding. These results are displayed in figure 4.10 and table 4.7 below.

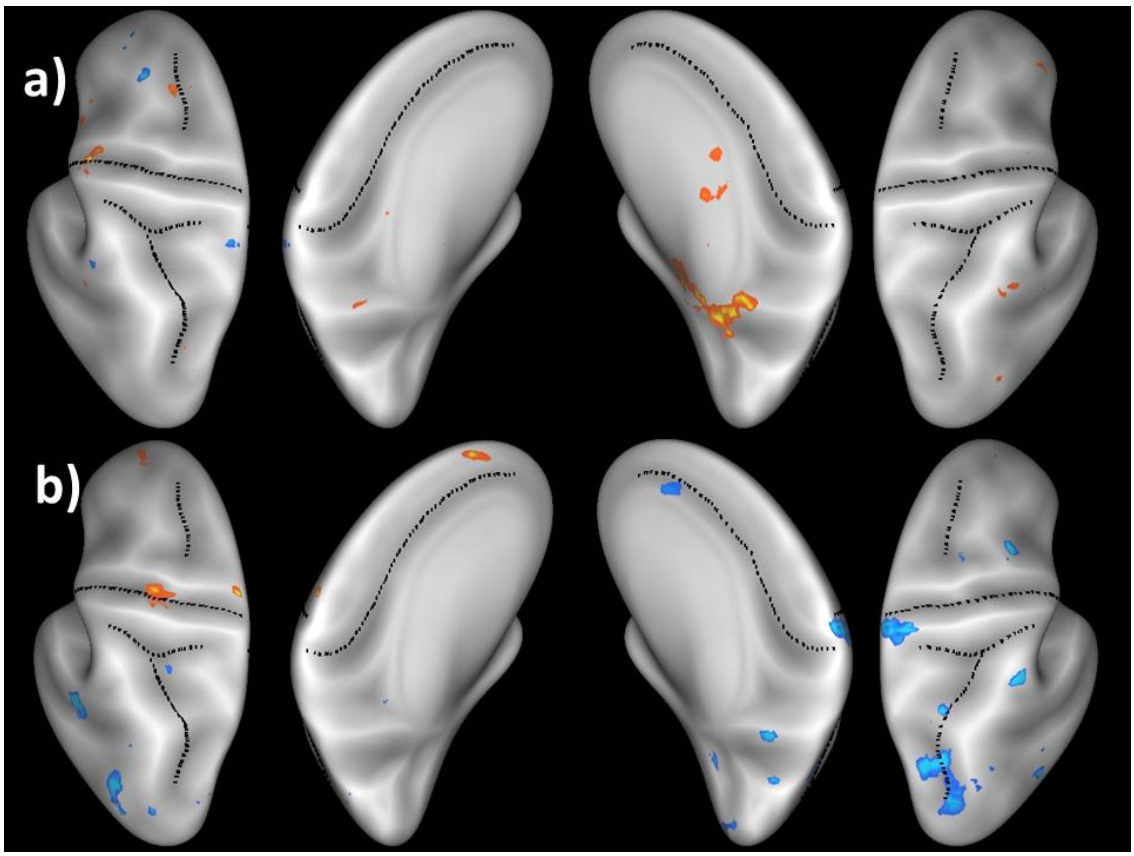

Figure 4.10: *Directional encoding change for (a)typical and (b)mirror-reversed reaching movements between sessions 1 and 2. T statistic map with height threshold t=2.65, p=0.01. The left hemisphere is presented on the left hand side.*

Contrast	H	Region	p(cl)	Area	Max (t)	X	Y	Z
				increases				
Typ	R	Isthmus Cingulate	0.003	568.65	5.93	17.37	-50.10	13.38
				decreases				
MR	R	Inferior parietal	<0.001	746.97	6.07	26.02	-57.65	35.13
MR	R	Post central	0.040	320.03	6.02	-3.35	-37.98	67.82

Table 4.7: *Learning effects – differences between sessions 1 and 2 in typical and mirror-reversed directional encoding. Height threshold t=2.65, p=0.01. p(cl) corresponds to the cluster*

corrected p value, H corresponds to hemisphere, area is measured in millimetres and (X,Y,Z) correspond to FreeSurfer coordinates.

Figure 4.11 demonstrates plots of BOLD percentage signal change and directional encoding in each of the previously described cortical ROIs for both visual feedback conditions.

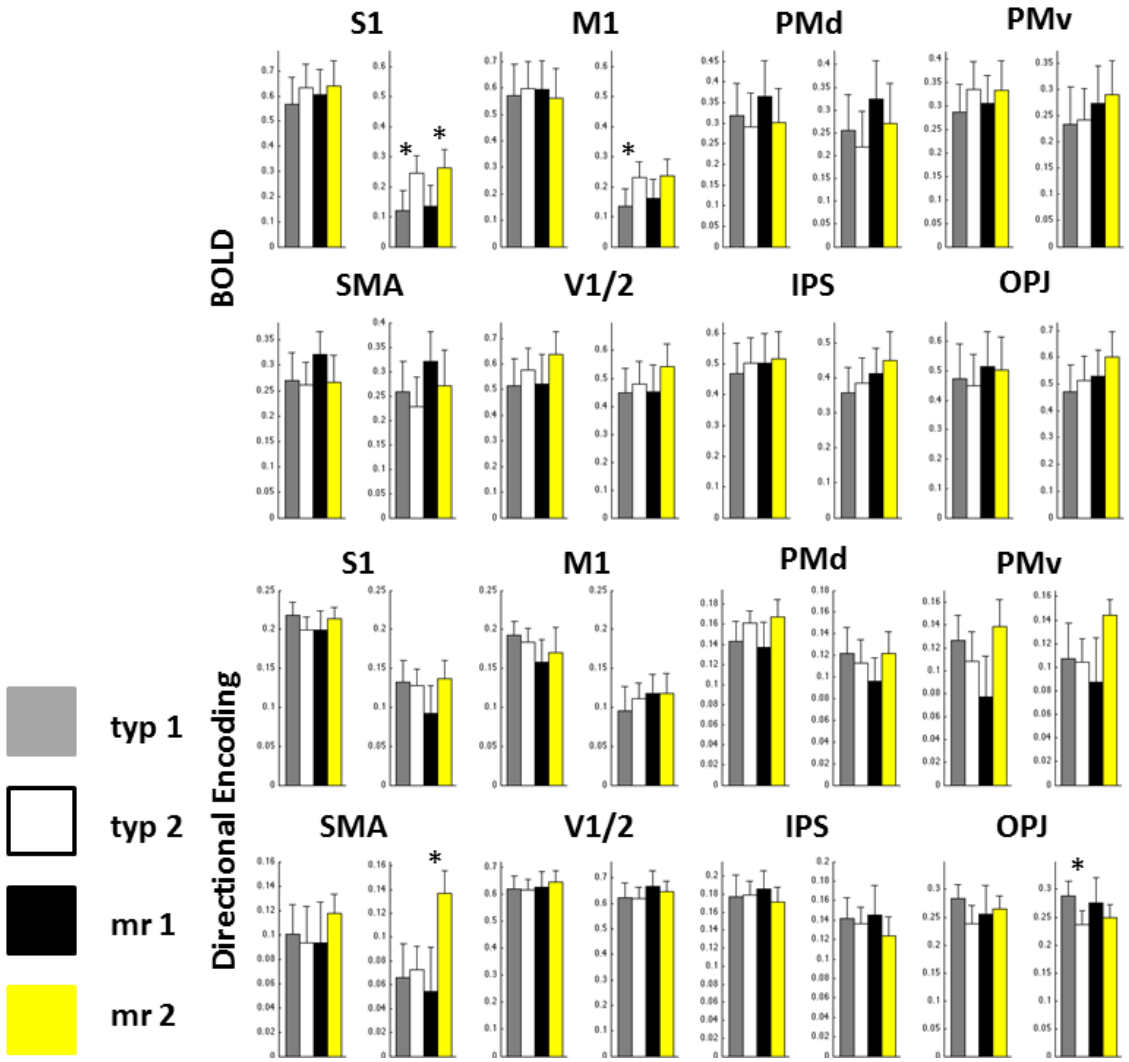

Figure 4.11: *For each cortical ROI, BOLD percentage signal change and directional encoding are plotted for both typical and mirror-reversed reaching conditions in both sessions. Abbreviations are as described in figure 4.5, and definitions of these ROIs are provided in the methods section. Asterisks are used to denote when there are significant differences between session 1 and 2. Axes are the same for each ROI in either hemisphere, but differ between ROIs. Error bars indicate S.E.M.*

Figure 4.11 shows that between session BOLD signal increases are focused in right (ipsilateral) M1/S1, whereas the right occipito-parietal junction and supplementary motor area show differences in directional coding between sessions. From this analysis, it appears that there is not a lot of convergence between the BOLD percentage signal changes analysis and the directional encoding analysis in terms of the areas which are highlighted as contributing to learning. It is interesting to note that in both the searchlight and ROI analysis, changes in the strength of directional encoding are found only in the right hemisphere. This might suggest there is a role for either right or ipsilateral cortex in skill learning.

Interaction analysis

We then investigated the interaction between visual feedback condition and session. We hypothesised that because participants were vastly more familiar with typical visual feedback, there would be less learning for these trials between sessions, but for mirror-reversed visual feedback, there would be more learning. This learning may cause the mirror-reversed mapping to look more like the typical mapping, either in terms of the kinematic parameters or neural data.

	Session	Visual Feedback	Interaction
RT (ms)	F(1,13)=6.531, p=0.0239	F(1,13)=0.292, p=0.5979	F(1,13)=0.087, p=0.7728
Early Error (°)	F(1,13)=10.626, p=0.0062	F(1,13)=13.963, p=0.0025	F(1,13)=2.796, p=0.1184
Max speed (m/s)	F(1,13)=1.328, p=0.2699	F(1,13)=2.314, p=0.1521	F(1,13)=0.347, p=0.5662
MT (ms)	F(1,13)=7.535, p=0.0167	F(1,13)=38.03, p<0.0001	**F(1,13)=10.635, p=0.0062**

Table 4.8: *A mixed model ANOVA with within subjects factors session (1 or 2) and visual feedback condition (typical or mirror-reversed), as well as an interaction term between these two factors was used to explore movement parameters of reaction time (RT), early error(absolute amount of error from the target trajectory at 150ms), maximum speed (Max speed), and movement time(MT).Significant results are denoted in bold typeface.*

The results of a mixed model ANOVA are displayed in table 4.8. Perhaps surprisingly, this interaction is significant only for the movement time (MT) parameter. Inspection of table 4.4 suggests this is driven by the reduction in MT in session 2 for mirror-reversed movements.

Figure 4.12 below displays the neural data for this interaction. The accompanying statistics are presented in table 4.9.

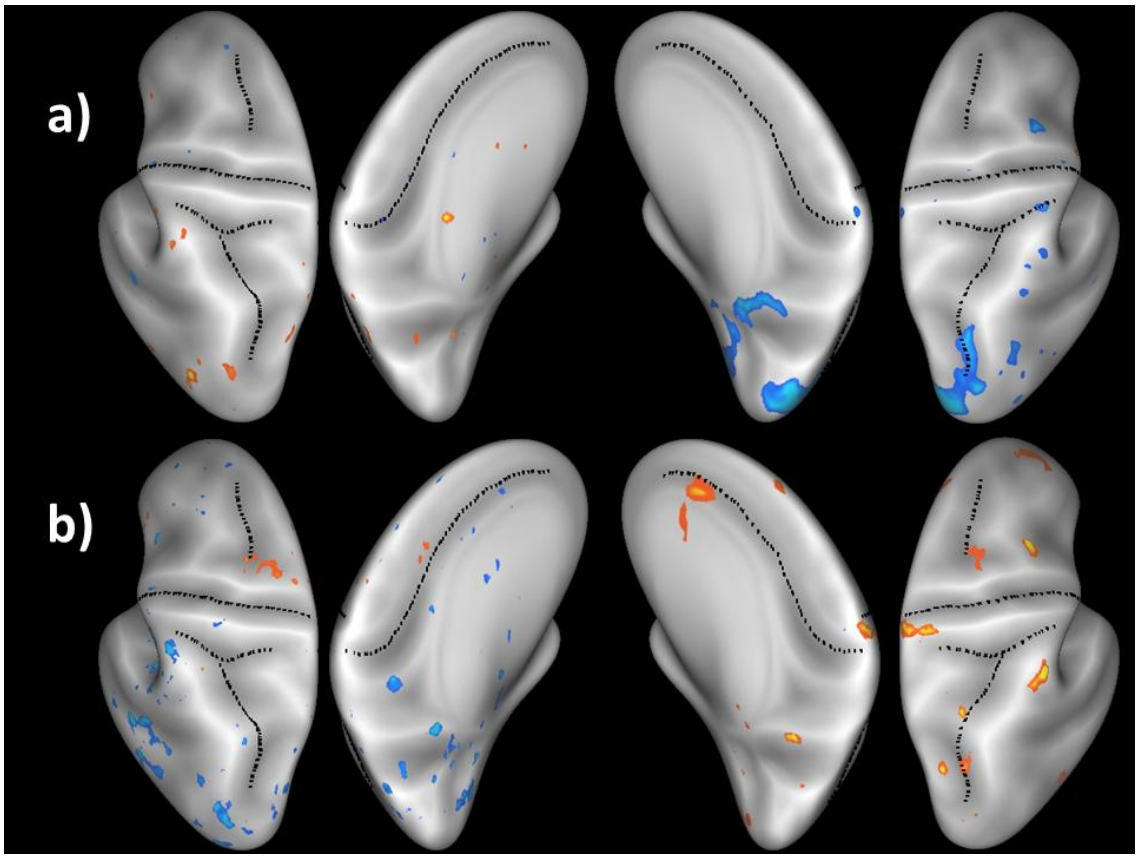

Figure 4.12: *Interaction between visual feedback condition (typ/mr) and session(1/2) for (a) BOLD percentage signal change and (b)directional encoding strength. T statistic map with height threshold t=2.65, p=0.01. The left hemisphere is presented on the left hand side.*

Region	Hemi	Area	p(cl)	Max(t)	X	Y	Z
BOLD - decreases							
Lateral Occipital	R	1697.13	<0.001	6.4	18.59	-89.54	19.77
Corpus callosum	R	1352.85	<0.001	4.75	6.35	-45.22	13.59
Directional encoding strength - decreases							
Superior temporal sulcus	L	272.60	0.001	7.73	-51.94	-48.10	3.87
Supramarginal	L	220.15	0.005	5.23	-49.06	-15.60	20.52
Lingual	L	212.77	0.006	4.62	-3.85	-74.76	2.92
Lateral Occipital	L	189.86	0.013	8.45	-27.18	-89.90	-1.12
Lateral Occipital	L	185.92	0.014	8.97	-33.74	-77.18	14.05
Inferior Temporal	L	154.81	0.040	4.92	-46.75	-50.29	0.82

Table 4.9: *Interaction between visual feedback condition (typ/mr) and session(1/2) for BOLD percentage signal change and directional encoding strength. Height extent threshold T=2.65, p=0.01. p(cl) corresponds to the cluster corrected p value, hemi corresponds to hemisphere, area is measured in millimetres and (X,Y,Z) correspond to FreeSurfer coordinates.*

For the directional encoding analysis there is evidence for an interaction between visual feedback condition and session in some regions in occipital and temporal cortex. This is driven by a reduction in the amount of directional encoding in the mirror-reversed condition in session 2. As is the case with the between-session contrasts, there is no evidence of convergence between the results from the BOLD activation analysis and the directional encoding analysis. In figure 4.12b there appears to be increases in directional encoding in PMd, however, this does not reach statistical significance with a height extent threshold of T=2.65 (p=0.01). When the height extent threshold is relaxed to T=1.77 (p=0.05), this region becomes significant (p=0.04, cluster corrected), which suggests there may be a trend for an interaction in this region, specifically whereby the extent of directional encoding increases more in the mirror-reversed condition.

We used a mixed model ANOVA with random effects of participant and fixed effects of visual feedback condition and session to investigate this interaction further in the ROIs. None

of these statistical tests of the interaction were significant. However, trends were found in right hemisphere V1/2 ($F(1,13)=4.589$, $p=0.05$) and in SMA ($F(1,13)=4.095$, $p=0.06$). Inspection of supplementary figure 4.2 reveals this is driven by decreased directional encoding in the mirror-reversed condition in session 2 early visual cortex, whereas there is increased directional encoding in motor regions including the SMA.

Behavioural Confounds

The number of trials upon which the encoding model was based differed between participants and within participants between the first and second scanning session due to time limitations on the scanning sessions meaning less runs were completed in the scanner for some participants, and because the elimination criteria meant a different number of trials are excluded for each experimental session. We accounted for the variance with which betas were estimated during the analysis (see methods). However, it is still possible that the differences in strengths of encoding between sessions are driven by the number of trials used to estimate these parameters. To test whether there is a relationship between the amount of data and the parameters of the encoding model, we correlated the number of trials which were used for analysis and directional encoding strength in typical and mirror-reversed reaching conditions separately for each participant in each session. This was completed by extracting the t statistic at the peak of each cluster reported for typical and mirror-reversed directional encoding for each participant, and then correlating this with the number of trials used to estimate the amount of directional encoding. There were 28 clusters identified from contrasting typical and mirror-reversed directional encoding in sessions 1 and 2 to baseline, and so 28 correlational analyses were performed. Only the correlation between number of trials and typical directional encoding in lateral occipital cortex in session 1 was significant ($R^2=0.5535$, $p=0.04$). However, is not more than the number of correlations we would anticipate to be significant by chance. Therefore it is unlikely that the number of trials used to estimate directional encoding strength was having an undue influence on parameter estimation.

Motor skill learning by definition involves changes in behavioural performance. These changes are demonstrated in table 4.4. To discern whether the learning effects we observed between sessions were actually a result of differences in the movement kinematics, we correlated the t statistic at the peak of each reported cluster in tables 4.6, 4.7, 4.9 and 4.10, with the potential behavioural confounds of reaction time, movement time, early error and maximum speed. For the BOLD percentage signal change analysis, 28 correlations were performed (7 clusters x 4 potential confounds). For the directional encoding analyses, 36 correlations were performed (9 clusters x 4 potential confounds). These results are shown below in table 4.11, however, none of these correlations survive a Bonferroni correction (α=0.00179 for BOLD, α=0.00139 for directional encoding), and the same number are significant as we would expect by chance with performing this number of correlations. As such, there is no cause for concern that the results reported here are only driven by behavioural confounds.

Confound	MRI measure	Region	Hemi	Correlation
Reaction time	PSC TYP 2>1	Postcentral	R	R^2=0.6269, p=0.0164
Maximum speed	DIR TYP 2>1	Isthmus cingulate	R	R^2=0.6581, p=0.0105
Maximum speed	DIR MR 2>1	Inferior parietal	R	R^2=-0.5799, p=0.0297

Table 4.10: *Significant correlations between the differences in potential behavioural confounds between session 1 and 2, and the peak t statistic for significant clusters of differences between session 1 and 2 for BOLD activations and directional encoding strength. Data are averaged across all movement directions.*

We also tested for the possibility that within a session, the pattern component modeling analysis was sensitive to differences between movement directions in a combination of kinematic parameters. We calculated a variance-covariance matrix on 9 kinematic parameters, and using the dual estimation procedure calculated an estimate of the systematic differences between movement direction, which are preserved in visual, motor and unique coordinates for each participant in each session. We correlated this with the t statistic at the peak of each cluster for visual, motor and unique encoding in sessions 1 and 2. We found 47

clusters, and so 47 correlational analyses were performed. Of these, only the relationship between motor encoding in session 2 estimated from the behavioural data and motor encoding in session 2 in the supramarginal gyrus were correlated (R^2=0.7417, p=0.0024). Similar to these previous analyses, this result is no longer significant following a Bonferroni correction, and is less than the number of correlations we would anticipate to be significant by chance with this number of statistical tests. Therefore we can conclude that there is no evidence that any regions is sensitive to a combination of the movement parameters, which is unique for each movement direction, and has therefore been mistaken for visual, motor or unique encoding.

Discussion

How is visual and motor information represented throughout the brain?

Our findings provide evidence that there are gradients of visual and motor information throughout the cortex, arguing against a model in which a restricted set of regions bear sole responsibility for coordinate transformations. Unsurprisingly, visual information predominated throughout the visual cortex and into parietal cortex. Regions in parietal cortex including superior parietal occipital cortex (Gallivan et al., 2009), V6a (Pitzalis et al., 2013) and parietal reach regions (Andersen and Buneo, 2002, Buneo et al., 2002, Buneo and Andersen, 2006, Cui and Andersen, 2011) have been highlighted as contributing to visuomotor transformations which specifically underpin visually guided reaching movements. Here we show mixtures of visual, motor and unique coordinate frames in these regions, which are more balanced than in other parts of the cortex, reiterating these regions privileged, but not unique, role in coordinate transformation.

The ROI analysis confirmed visual encoding was also evident in numerous regions in sensorimotor cortex, including somatosensory cortex, premotor cortex and supplementary motor area. However, its strength was drastically reduced in comparison to motor encoding. We replicated previous fMRI (Eisenberg et al., 2011), and electrophysiological (Martin and

Ghez, 1985, Kakei et al., 1999, 2003) findings regarding the representation of visual information in M1. Additionally, there was evidence for motor encoding in the left hemisphere V1/2 ROI (figure 4.7). Inspection of the cortical map (figure 4.6) reveals this is in the anterior calcarine sulcus, which corresponds to foveal V1. Recently there has been an increasing interest in possible 'higher cognitive functions' performed in V1 (Gavornik and Bear, 2014a). V1 is capable of learning spatiotemporal sequences (Gavornik and Bear, 2014b). V1 neurons can predict the time course of anticipated rewards by responding to visual inputs with dynamics reflecting the stimulus-reward intervals established during a training period and not those of the visual stimuli actually evoking their activity (Shuler and Bear, 2006). In the introduction to this thesis, V1's role in visual illusions, including size (Murray et al., 2006) and motion (Muckli et al., 2005, Larsen et al., 2006, Sterzer et al., 2006) illusions was highlighted. In these studies, V1 activity represents anticipated rather than actual sensory stimuli. Therefore it is a possibility that in this chapter, the motor information we report in V1 is a prediction or simulation of the visual consequences of actions.

Alternatively, participants could have used a strategy for the mirror-reversed movements in which they imagined a target on the other side of the screen and executed their reaching movement towards this. As such, visual attention may have been focused on an imagined target in the mirror-reversed position, and the effects we observe are a result of this reorganisation of visual attention. fMRI responses in V1 have been previously shown to be strongly modulated by attention (Ress et al., 2000, Silver et al., 2007). If participants were consciously using this strategy, we would anticipate learning effects; either the participants learn to use this strategy effectively during the course of the training or become less dependent on this strategy as they learnt the transformation. Early visual cortices were not highlighted as regions which changed in strength of motor encoding, or in strength of directional encoding between sessions. However, from the interaction analysis, there is some evidence that directional encoding is more strongly reduced in the mirror-reversed condition for the second session. Therefore learning the mirror-reversal means participants become less

dependent on early visual cortex to reorient their attention. Unfortunately with the current experimental design, it is problematic to distinguish this explanation from the explanation in which V1 is predicting the visual consequences of motor actions. We might also expect learning effects if this was a predictive signal as the forward model became more accurate with time. Completing this paradigm with a different imaging methodology such as magnetoencephalography (MEG) would provide time course information regarding this signal, which may help to disambiguate between these two competing explanations.

Inspection of figure 4.6 shows that in early visual cortex, visual and motor encoding overlap mainly in V1. V1 is considerably better vascularised in comparison with other regions in visual cortex, making it much easier to record signal from this region. As such, it is possible that the combined visual and motor encoding we observe in V1 is actually a result of feedback either from higher visual or parietal areas which represent information in both visual and motor coordinates, but the motor information is too weak for detection in these regions.

Telgen et al. (2014) have argued that mirror-reversed reaching is an example of motor skill learning which requires learning a new internal model. M1 has been identified as a candidate region for the encoding of motor memories (Reis et al., 2009, Galea et al., 2011). It is interesting therefore to speculate that the unique encoding exhibited in this region is the neural correlate of this internal model for switching between motor and visual coordinate frames.

Sensorimotor Skill Learning

We were interested in determining whether pattern component modeling could be used to detect changes in the representation of sensorimotor skills which occur with learning. Participants were scanned on day 2 and day 8 of an 8 day training paradigm so that novice and expert task performance could be compared. Previous work in our lab has demonstrated that the neural activity patterns associated with trained finger sequences are more easily distinguished from one another in compared to the neural activity patterns associated with

untrained sequences (Wiestler et al., 2013). With learning, instead of representing single finger movements, participants develop neural representations for the execution of multiple finger movements, including the transition between two or more movements (chunks). Sequences which are executed as combinations of these different chunks are more different than those which are simply a shuffled combination of each finger press, which is reflected in the increased classification accuracy of the neural patterns. Here, we have used a sensorimotor task rather sequence learning task. In the motor skill learning literature a distinction has been drawn between motor sequence learning tasks in which sequential movements are formulated through learning into a well-articulated behaviour, and sensorimotor tasks in which participants have to learn novel movement kinematics (Hardwick et al., 2013). It is not yet clear how the neural representation of a sensorimotor task changes with learning.

In the mirror-reversed reaching condition, decreased BOLD activation in the expert session was found in precentral gyrus extending into dorsal premotor cortex. This region was highlighted by Hardwick et al (2014) as common to all motor skill learning tasks. There was increased BOLD activation between sessions for the typical reaching condition in the precuneus and postcentral gyrus, in regions corresponding to the cingulate default area (Raichle and Snyder, 2007), and the mouth representation of motor cortex. It is unclear whether and how these regions contribute to sensorimotor skill learning. However, it is possible that these activations reflect that following extensive training, the task was less demanding of the participant's attention, allowing their mind to wander and perhaps making them more aware of the bite bar.

The pattern of results which emerges from the changes in directional encoding analyses is different. The isthmus cingulate increases in directional encoding strength with learning for the typical reaching condition. Activity in the cingulate cortex region has been shown to be modulated by task complexity in a bimanual coordination task, which was interpreted as reflecting its role in the planning and execution of complex movements (Debaere et al., 2004a,

b, Wenderoth et al., 2005). This region also overlaps with the retrosplenial cortex, which is involved in tasks using visuospatial cues for navigation and movement (Hindley et al., 2014), specifically by encoding spatial information (Czajkowski et al., 2014). However, its role here is unclear as for both these explanations we would anticipate greater effects in the more complex mirror-reversed reaching condition.

There is evidence for decreases in directional encoding strength in inferior parietal and post central regions in mirror-reversed reaching, and in the occipito-parietal junction for typical reaching. The parietal cortex has been repeatedly shown to be involved in visuomotor transformations (Kalaska and Crammond, 1992, Graziano et al., 1994, Graziano and Gross, 1998, Snyder, 2000, Andersen and Buneo, 2002, Buneo et al., 2002, Merriam et al., 2003, Buneo and Andersen, 2006, Graziano, 2006). In the first section it was argued that whilst there is evidence of a gradient of visual and motor information throughout the cortex, our observation of proportionally equal encoding for visual and motor information in parietal regions corroborates the importance of these regions in visuomotor transformations. It is possible the reduction in encoding strength between these sessions reflects how learning the visuomotor transformation makes performance of this task less demanding upon these regions. The region of interest analysis demonstrates the strength of directional encoding for mirror-reversed movements increases in the supplementary motor area (SMA) between sessions. The role of the SMA in motor planning and readiness (Deecke et al., 1969, Deecke et al., 1976, Lang et al., 1991, Cunnington et al., 1996), suggests that with learning, this region prepares these mirror-reversed movements more reliably.

Based on previous studies highlighting a role for PMd in motor skill learning (Hardwick et al., 2013), we have interpreted BOLD modulation and trends of changes in directional encoding strength in this region as being a result of motor skill learning. However, this region is adjacent to and densely interconnected with the frontal eye fields, a key gaze control area (Hutchison et al., 2012). The frontal eye fields have been argued to control gaze movements in terms of

visual target location (Sajad et al., 2014), and as such can act as an attentional priority map (Thompson and Bichot, 2005). Participants in this study were instructed and trained to fixate centrally. During training sessions, this was monitored and participants received feedback at the end of each run. Recording of eye movements in the scanner was unreliable for many reasons including that the bite bar often fixed participants in a position in which the head coil cast a shadow on their eye. Whilst participants were likely to have maintained good fixation throughout the experiment, we cannot entirely rule out the possibility that during the course of the training participants were able to fixate better which account for these results. However, even if we were able to monitor and equate eye movements between the two sessions, differences in the effort required to suppress saccades to the target between sessions may still be evident in these regions, owing to the obligatory coupling between attention and saccades (Dhawan et al., 2013).

As the mirror-reversed condition is harder than the typical condition, we predicted that there would be an interaction between visual feedback condition and session. We anticipated that the representation of typical reaching would remain more stable over time, whereas the representation of mirror-reversed reaching would change more drastically between novice and expert sessions, perhaps converging on a representation more similar to typical reaching. From the BOLD activation analysis, there was evidence of decreases in lateral occipital regions and corpus callosum, which are indicative of a greater amount of BOLD reduction in the mirror-reversed condition with learning. The directional encoding analyses similarly show that regions in lateral occipital cortex are decreased, as well as regions in temporal cortex, including the superior temporal sulcus, supramarginal gyrus, lingual gyrus and inferior temporal cortex. Again, these changes are indicative of a greater decrease in directional encoding strength in the mirror-reversed condition in the second session. There is also evidence of a trend towards increased directional encoding in PMd, which reflects the increases in directional encoding in the mirror-reversed condition with learning.

Supplementary figure 4.2b shows that in the mean change in directional encoding strength for mirror-reversed reaching there is a pattern in the left hemisphere of decreased encoding strength in visual and parietal cortices, but increased encoding strength in motor cortices. This pattern of decreased encoding strength in the early visual cortex and increased encoding strength in motor cortex is less pronounced in the typical reaching condition (supplementary information figure 4.2a) in the left hemisphere, and entirely absent in the right hemisphere which seems to show increased encoding with learning throughout the cortex. This pattern of results is reiterated in the interaction analysis for directional encoding strength (supplementary figure 4.3b) which demonstrates that the learning of the visuomotor transformation results in decreased encoding in left hemisphere visual regions and increased encoding in motor areas. It is tempting therefore to speculate that learning the mirror-reversal visuomotor transformation results in less dependence on visual and parietal cortices to perform remapping operations, as motor cortex learns a model for this transformation. The converse appears to be true for the right hemisphere. Further research would be needed to determine whether these effects are a result of hemispheric specific roles in sensorimotor skill learning, whether they are due to being contralateral and ipsilateral to the hand performing the reaching action, or as is more likely, a combination of these effects. To better understand the neural network underpinning both mirror reversed and typical reaching, and how these change with learning, Granger causality mapping could be used to assess the directed influence of different neural structures on one another when switching between these two mappings (Roebroeck et al., 2004).

Whilst there is some evidence of a shift from visual and parietal encoding to motor encoding with sensorimotor skill learning, these effects often fail to reach an acceptable level of significance, and as such the evidence is not overwhelming. There are many possible reasons why this might be the case. Firstly, this experiment was performed on a 1.5T scanner, and it may have been the case that the signal to noise ratio (SNR) at this level may have been insufficient to detect these effects. Both strength of encoding and BOLD activation analyses

are computed on a per session basis, and as such will be influenced by the amount of scanner noise during each session. It is possible that the variance introduced by this is greater than any changes we would observe between sessions in learning. Whilst we aligned data from both sessions, it is possible that there is some error in this process which meant there was not an exact voxel-to-voxel correspondence. Note that to investigate sequence learning, Wiestler et al. (2013) compared trained and untrained sequences within the same session. It is possible a more powerful experimental design to investigate sensorimotor skill learning would be to compare trained and untrained visuomotor transformations within the same scanning session. For example, mirror-reversal could be compared with a visual rotation of 90° placed on the visual feedback.

As discussed in the introduction to this chapter, there is debate as to whether motor skill learning results in BOLD activation increases or decreases, and the functional significance of these. For the BOLD activation and directional encoding strength analyses, we developed separate functional masks to perform subsequent statistical analyses, preventing direct statistical comparison between these two analyses. Nevertheless, similar regions were captured by both these functional masks, and as such we will consider these results alongside one another with caution. Comparison of suprathreshold clusters between the two metrics for contrasts highlights little overlap, which is likely to be a result of there being few significant results. However, a significant positive correlation was observed between the mean unthresholded map for the differences between sessions 1 and 2 in typical reaching for BOLD and directional encoding strength (left hemisphere: R^2=0.1794, p<0.001, right hemisphere R^2=0.1969, p<0.001), and for the differences between sessions 1 and 2 in mirror reversed reaching for BOLD and directional encoding strength (left hemisphere: R^2=-0.2363, p<0.001, right hemisphere R^2=-0.1751, p<0.001), and for the interaction between visual feedback condition and session (left hemisphere: R^2 =-0.5225, p<0.001, right hemisphere: R^2=-0.6604, p<0.001). Taken together these results suggest that during the learning of the mirror reversal, increased encoding strength is associated with decreases in BOLD activity. Visual motion

imagery has previously been shown to be associated with negative BOLD in V1 (Kaas et al., 2009), and this may suggest that reduced BOLD activation in these regions is associated with either mental imagery or attention of imagining the target in the mirror reversed position. Further analyses would be required to substantiate these preliminary results, and further experimentation is necessary to understand the relationship between BOLD, encoding, and cognitive processes in early visual cortex.

In summary, we have used a pattern component model to dissociate visual and motor information in a visually guided reaching task with typical and mirror-reversed visual feedback. We have shown that there is a gradient of motor information throughout sensorimotor, parietal and occipital cortex, which is strongest in motor cortex and weakest in visual cortex. The same is true of visual encoding, which is strongest in visual cortex, but maintains a weak representation even into primary motor cortex. These results strongly support a model of visuomotor coordinate transformation that occurs throughout these regions, rather than is subscribed to a single neural locus. The neural representation of sensorimotor skill learning proved more elusive. There was evidence that learning the mirror-reversal caused decreased directional encoding in lateral occipital cortex, with a trend towards this skilled representation having stronger encoding in premotor cortex. We interpreted this as demonstrating sensorimotor skill learning reducing the demands on visual and parietal cortices to perform remapping operations, as motor cortex learns a model for task execution.

Chapter 5: Discussion

In this thesis I used magnetic resonance imaging to examine experience dependent neuroplasticity in three complementary studies. The first two of these studies focused on changes which have occurred over a long period of time in the congenitally deaf brain, and the third study focused on more rapid changes associated with motor skill learning. In chapter 2, I used diffusion weighted imaging to assess how congenital auditory deprivation affects the microstructural properties of the thalamus and thalamo-cortical afferents. In chapter 3, I used population receptive field modeling to examine how the functional architecture of early visual cortex is affected by congenital deafness. The final study presented in chapter 4 was a training paradigm designed to isolate the visual and motor aspects of a sensorimotor task. A pattern component model was used to determine the extent of visual and motor encoding throughout the cortex, and how the neural representation of sensorimotor skill changes with learning. These more recent methods for analysing fMRI data attempt to obviate the problems associated with the interpretation of changes in the mass action BOLD signal. When studying experience dependent plasticity, interpretation of the BOLD signal can be problematic as many factors additional to the experimental factor of interest will differ between groups and with learning.

Chapters 2 and 3 of this thesis focused on experience dependent plasticity which occurs as a result of congenital deafness. As highlighted in the introduction, the altered way in which the senses are used in congenital deafness acts as a driver for plastic change alongside the absence of auditory input. To date, there have been few Diffusion Weighted Imaging (DWI) studies of the neuroanatomical consequences of congenital deafness (Kim et al., 2009, Li et al., 2012, Hribar et al., 2014). These studies have used whole brain approaches to compare deaf and hearing brains. Whole brain approaches have many benefits. Firstly, they do not require the researcher to define anatomical regions of interest, the accuracy of which is dependent on their level of expertise, and could be biased by the experimental hypothesis should the

delineation be completed without appropriate blinding (Jones and Cercignani, 2010). Also, whole brain analyses do not require *a priori* hypotheses, which may limit or bias findings. However, during procedures to test for the statistically significant differences between groups, a family wise error correction is also applied across the whole brain. With smaller groups, as is often the case in studies with special populations, there is a risk that the approach will be statistically underpowered. Communication between two structures in the brain relies on the integrity of the entire tract between the two structures in question. It is biologically plausible that in conditions such as congenital deafness which are not associated with a focal injury or pathology, small cumulative changes over the length of a tract of interest may occur which drastically effect communication between regions. With a FWE correction applied at a whole brain level, the magnitude of these differences in each voxel may not be detectable. Further, in many analysis pipelines for whole brain data, sub-cortical structures are not considered. In this thesis, I was interested the thalamus and thalamo-cortical connections. As discussed in the introduction to chapter 2, this structure is immensely important for modulating the flow of information throughout the brain. Determining whether and how the thalamus and its afferents are altered by congenital deafness could provide critical insight into understanding the patterns of crossmodally reorganised activation in response to visual and somatosensory stimuli observed at the level of the cortex.

Co-morbid neurological and psychiatric concerns are highly prevalent in deaf populations, as are cochlear implants, which are contra-indicated for MRI studies. Recruiting a group of healthy congenitally deaf participants who are homogenous in terms of the extent of their hearing loss and sign language characteristics, as well as comparable to a hearing control group in terms of their sign language characteristics and educational/occupational attainment was very difficult. In the end, only 15 deaf participants were scanned. For various reasons, we could not use data from all of these participants. As such, the diffusion weighted imaging analysis reported in chapter 2 most likely lacked sufficient statistical power to be able to detect effects at a whole brain level. Fortunately, the use of probabilistic tractography to segment the

thalamus and to trace the thalamo-cortical connections was sufficient to answer the experimental question of interest. Somewhat surprisingly, alterations were found in the visual and frontal thalamic parcellation, as well as in all thalamo-cortical tracts throughout the brain, save for the temporal thalamo-cortical tract. This is evidence that communication throughout the brain is altered by deafness and the resulting compensatory strategies. The widespread nature of these findings emphasize the importance of considering all possible connections which may contribute to plastic processes in the brain, and not simply plastic mechanisms that operate at a cortical level.

These surprising findings also highlight several additional lines of research which would need to be addressed to develop a clearer picture of the anatomical consequences of deafness. First of all, it is not clear the extent to which later or less severe deafening would have on the thalamus and thalamo-cortical connections, or how early in development these differences arise. Multisensory cortices undergo a more protracted period of development in comparison to primary sensory cortices (Gogtay et al., 2004, Shaw et al., 2008). This extended opportunity for re-weighting of the various inputs into these structures is thought to contribute to plastic reorganisation in these areas (Bavelier and Neville, 2002, Fine et al., 2005). In contrast, areas such as primary sensory cortices are thought to mature earlier in development. For example, it has been estimated that Heschl's gyrus reaches peak synaptogenesis at three months of age (Huttenlocher and Dabholkar, 1997). It is possible that later deafening will not be associated with such drastic sub-cortical reorganisation. Later deafened individuals may exhibit a different pattern of plasticity, depending on the developmental profiles of structures they can exploit to achieve reorganisation of the brain which better adapts them to the loss of the auditory modality. Following contrasting congenitally and early deafened participants who also differed in terms of duration of deafness, Li et al., (2012) have argued the age of onset of deafness has a greater impact on auditory cortex than the duration of deafness. However, the effect on subcortical structures was not investigated. The connectivity between different remote brain areas increases

dramatically in the first year of life (Wallace et al., 2006, Knickmeyer et al., 2008), which suggests that auditory deprivation during this period may have a disproportionate effect on neurodevelopment. Studying cohorts of people deafened at different ages would illuminate the developmental time course of these changes. The changes observed in these studies could become very pronounced following early auditory deprivation, or they could become continuously reinforced and strengthened through a lifetime of using the brain in a different way. Understanding the developmental trajectory of these changes could have important implications for assistive technologies for hearing loss, particularly for cochlear implants were there are substantial risks associated with the surgical procedure to implant the device. Specifically, plastic reorganisation of sub-cortical structures could be maladaptive in terms of causing changes which are detrimental to restoring functional hearing. Subsequent to establishing whether this plasticity is maladaptive, it could be used as a biomarker for determining the likelihood of regaining functional hearing following cochlear implantation.

A critical question is how different levels of hearing loss are associated with the extent of these anatomical changes. The effects of different levels of hearing loss on neuroanatomy have not yet been fully explored. It is possible that there would be non-linearities in the relationship between extent of hearing loss and anatomical reorganisation. In cases of milder hearing loss, it is possible that other anatomical connections are re-organised to potentiate the diminished auditory signal, rather than adopting a strategy of enhancing other modalities such as the visual modality as evidenced in the population tested here.

As noted in the introduction to this thesis, animal studies have provided evidence for direct connections between the primary sensory cortices. At present, there are problems associated with investigating these crossmodal connections (particularly those between primary sensory cortices) in humans. Post-mortem studies cannot be used as active transport mechanisms are no longer available to transport tracer injections over long-range connections. Diffusion weighted imaging (DWI) is the only method for *in vivo* assessment of anatomical

connections. However, there is still immense debate about the extent to which the 'crossing fibres' issue has been resolved. This relates to the extent to which fibres from different anatomical tracts which either cross or kiss within a voxel can be reliably distinguished from one another. The sequence acquisition time for diffusion tensor models which are better able to resolve this 'crossing fibres' issue can be prohibitively long for use with special populations. The strength of connections between primary cortices such as visual and auditory cortices are drastically diminished in comparison to those which exist between association areas of visual and auditory cortices (Falchier et al., 2002). Tract geometry influences the ease with which tracts can be traced. Both primary auditory and primary visual cortex are positioned in way in which makes probabilistic tractography to these regions difficult. All these factors conspire to make establishing whether these tracts are present in humans, never mind deaf humans, a non-trivial matter. However, it is likely that in the next few years, advances will be made in terms of scanning sequences and the modeling of diffusion profiles which make it possible to assess whether these tracts are present in humans, and how they are affected by congenital deafness. It is possible these crossmodal projections are potentiated at some levels of hearing loss in order to facilitate communication between the senses.

As noted in the introduction to chapter 2, this study was exploratory, as the effect of congenital deafness on sub-cortical structures had not previously been studied. Future research in this area would benefit from acquiring several relevant behavioural measures, such as tactile discrimination thresholds or tests of executive function which may help the interpretation of these findings.

In Chapter 3, I presented findings of increased population receptive field sizes in the cortical representation of the visual periphery of congenitally deaf participants, which is interpreted as compensatory experience dependent plasticity. This study provides an important piece of the puzzle in terms of understanding the compensatory changes which occur in the visual system of congenitally deaf people. Prior to this thesis, studies have argued

changes in auditory cortex (Lomber et al., 2010, 2011), as well as higher visual areas (MT+) (Finney et al., 2001), contribute to enhanced peripheral visual perception observed in deaf people. Retinal changes have also been shown (Codina et al., 2011). Chapters 2 and 3 of this thesis strongly suggest that changes can be found throughout the visual system. Previous studies of compensatory visual peripheral advantages in deaf populations attempted to rule out a role for changes to early visual cortex in contributing to the observed plasticity, suggesting that these regions are too highly specialised for their visual function (Fine et al., 2005). However, there is a clear hierarchical structure in the visual system. As such, explanations based on the changes in auditory cortex or changes emerging in higher visual cortex are likely to be preceded by changes lower down the visual processing hierarchy. Chapter 3 also demonstrated that the mass-univariate framework for analysing fMRI can be misleading. Both here, and in Finney et al., (2005) there were no changes in the absolute amount of BOLD signal across primary visual cortex. Differences were only apparent with population receptive field modeling, which studies properties of the activation at a voxel level. This reiterates the importance of more recent computational imaging methods, in which analyses are more comparable to those conducted in the neurophysiology literature, helping to make these two methods of enquiry more comparable.

Several questions remain regarding the nature of the effects reported in chapter 3, some of which echo those outlined in response to chapter 2. For example, would comparable effects be found in later deafened people, or people with less severe hearing loss? Furthermore, would temporary methods for removing auditory input (for example, using ear plugs in humans or surgical methods in animals) cause experience dependent changes in adults, and over what timescale could we expect these to occur? More generally, this study demonstrates the utility of pRF modeling to examine the factors affecting visual experience. Action video gamers have been studied alongside deaf people as they engage in intense training of their visual attention to continuously monitor dynamically changing stimuli throughout the visual scene (Buckley et al., 2010). As yet, the functional architecture of visual

cortex in gamers has not been studied with population receptive field modeling. It is a possibility that experience dependent plasticity due to intense training in this group would also result in changes to primary visual cortex. Both visuospatial attention and attentional load have been shown to affect pRF properties of early visual cortex (de Haas et al., 2014, Klein et al., 2014). Therefore it is not implausible that changes in pRF properties in gamers could be observed.

The purpose of chapter 4 was twofold. First of all, I wanted to determine how visual and motor information were represented throughout the cortex. Secondly, I wanted to determine whether pattern component modeling could be used to detect changes in the neural representation of a sensorimotor skill that occur with learning.

From the first question, perhaps the most surprising finding is that motor information is present in early visual cortex, including primary visual cortex. Several questions regarding the nature of this finding arise. Eisenberg et al., (2011) show visual information is present in motor cortex by showing that the correlations between two movements which cause the same visual feedback are higher than we would expect by chance, even though the movements used to produce the visual feedback differed (a rotation was applied to the visual feedback in one instance). However, when participants passively viewed videos of these movement trajectories, there were no correlations between activation caused by the visual traces of movements to the same target (Eisenberg et al., 2011). The authors interpreted this as demonstrating active control is required for the motor system to represent visual information. Similarly, above chance classification accuracy on images of different object categories can be achieved on the neural activity patterns from early somatosensory cortex, though only when familiar rather than arbitrary object categories were presented (Smith & Goodale, 2013). These studies suggest action and experience is a prerequisite for motor and somatosensory cortices to represent visual information. Here, it would be instructive to see if when the hand was passively moved in these different directions, or if participants simply viewed the

movement trajectories (after having had experience of completing the task in both the typical and mirror-reversed reaching conditions) whether motor information was present in early visual cortex. The studies of Eisenberg et al., 2011 and Smith and Goodale 2013 suggest that passive viewing alone would be insufficient for motor information to be represented in early visual cortex.

From research with mice, there is evidence that locomotion speed information is integrated in V1 (Saleem et al., 2013). Here we show evidence of directional encoding in V1. This raises several questions; is movement speed also represented in V1 in humans? What other motor properties are represented in V1? Locomotion speed and movement direction both have visual analogues. It is possible that this visuomotor crossmodal processing is linked to the supramodal hypothesis of crossmodal plasticity, whereby sensory deafferentation causes a cortical area to lose its typical input but maintain its typical function. As discussed in the introduction to this thesis, this is thought to be mediated by already existing multimodal representations in these regions. Previous examples of these non-dominant representations (for example, auditory and somatosensory motion in visual motion areas) have only been demonstrated between the sensory modalities. Therefore, it is a novel finding of this thesis that the concept of crossmodal plasticity and processing may also apply to motor information. More broadly, the gradients of visual and motor information demonstrated throughout the cortex suggests we should eschew notions of coordinate transformations occurring in a single region in favour of a model in which there are multimodal representations throughout the cortex, though these representations differ in their relative strength.

For the second question in Chapter 4, I was interested in whether I could determine how the neural representation of sensorimotor skill changed with learning. There was some evidence that learning a mirror-reversal was associated with decreased directional encoding strength in lateral occipital cortex, and increased directional encoding strength in PMd. Between session changes in BOLD activity were negatively correlated with between session

changes in directional encoding strength, which could suggest that more efficient task encoding with learning creates less metabolic demands. However, these results were far from conclusive. It is possible that a design which compares trained and untrained movement kinematics within a session would be more informative regarding the difference between novel and expert sensorimotor skill.

This thesis has addressed three quite different questions from the field of experience dependent plasticity. However, common to all these projects was the idea that crossmodal processing, and so the potential for plasticity is present throughout the entire brain. In chapter 2, I examined for the first time the neuroanatomical sequelae of congenital deafness on the thalamus and it's afferent. The widespread nature of alterations that were found emphasizes that loss of the auditory modality does not merely affect the auditory cortex, but instead can influence communication throughout the entire brain. This point was reinforced in chapter 3 were I demonstrated that auditory deprivation is capable of altering the functional and structural properties of the earliest stage of the cortical visual processing stream. Finally, in chapter 3, I dissociated visual and motor encoding throughout the cortex, which led to the surprising finding that motor encoding is present in early visual cortex. Again, this underscores the extent of crossmodal processing in the brain.

A second theme common to the analysis of the fMRI data, was that the mass action BOLD signal may not always be appropriate for studying plasticity. In chapter 3, the extent of BOLD activation in V1 was shown not to differ between deaf and hearing groups across eccentricity. However, when a difference-of-Gaussian model was fitted – differences in the receptive field profile became apparent. Similarly in chapter 4, using a pattern component model we were able to decompose the contributions of visual, motor and unique encoding throughout the cortex. This would not have been possible with activation analyses alone. Therefore it is hoped that this thesis demonstrates the utility of more recent methods of

analysing fMRI data, including population receptive field modeling and pattern component modeling, for the field of experience dependent neuroplasticity.

Chapter 6: Supplementary Information

Supplementary Information from chapter 3

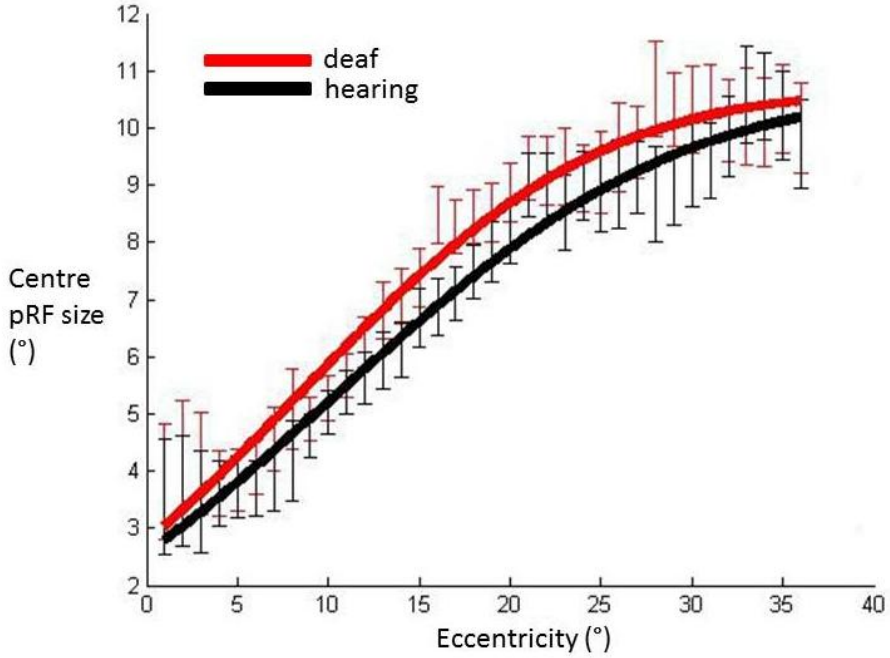

Supplementary Figure 3.1: *pRF centre sizes averaged across participants in each group, plotted against eccentricity in V1 All participants are included in the analysis and no outlier removal procedures have been applied to the data. Red: Deaf participants, Black: Control group. Error bars denote +/- standard error of the mean.*

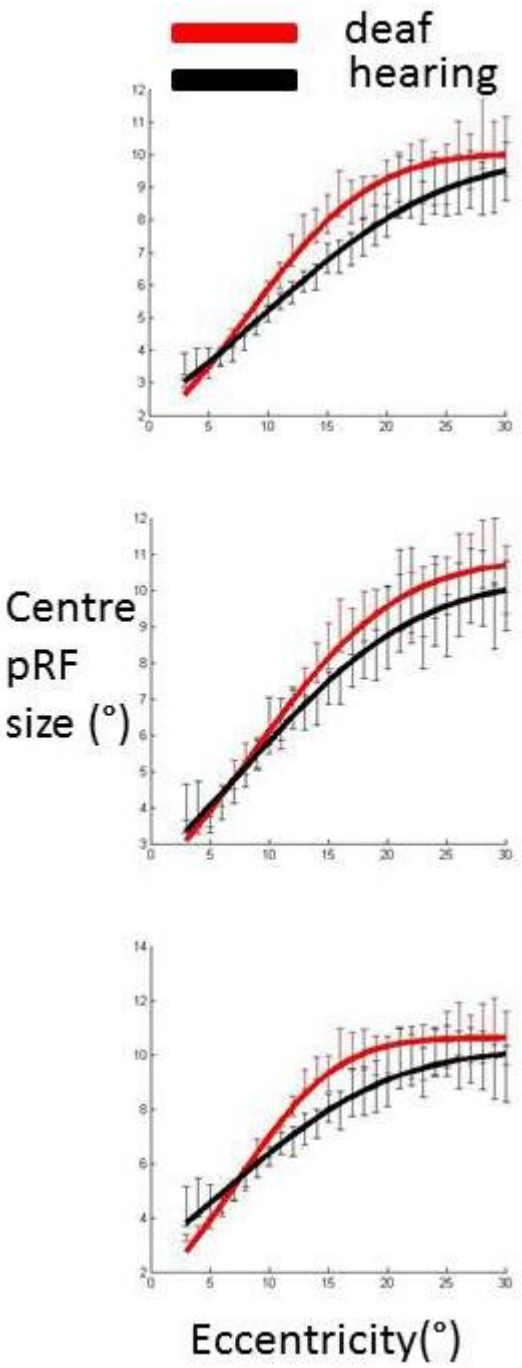

Supplementary Figure 3.2: *pRF centre sizes averaged across hemispheres for participants in each group with the same data exclusion procedures as reported in the main analysis for visual areas V1/V2/V3. Red: Deaf participants, Black: Control group. Error bars denote +/- standard error of the mean. Direct comparison of the size of the difference between deaf and hearing groups demonstrates that this difference is largest in V1.*

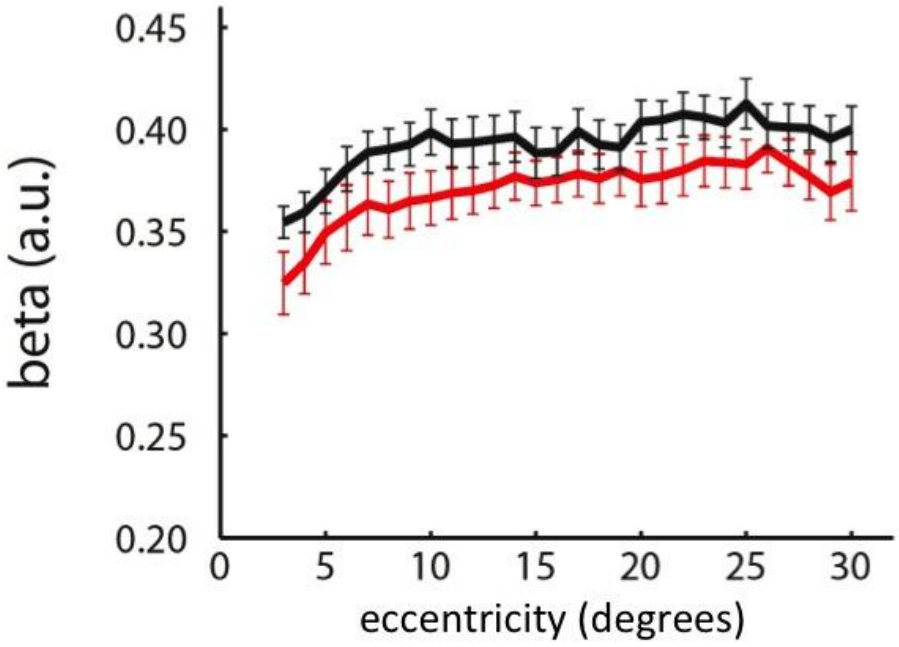

Supplementary Figure 3.3: *Betas values averaged across hemispheres for participants in each group with the same data exclusion procedures as reported in the main analysis for visual areas V1. Red: Deaf participants, Black: Control group. Error bars denote +/- standard error of the mean. Though it appears that the deaf group have lower beta values across eccentricities in comparison to the hearing group, neither the main effect in the bootstrapping curve fitting analysis was significant, nor the independent samples t-tests at each eccentricity.*

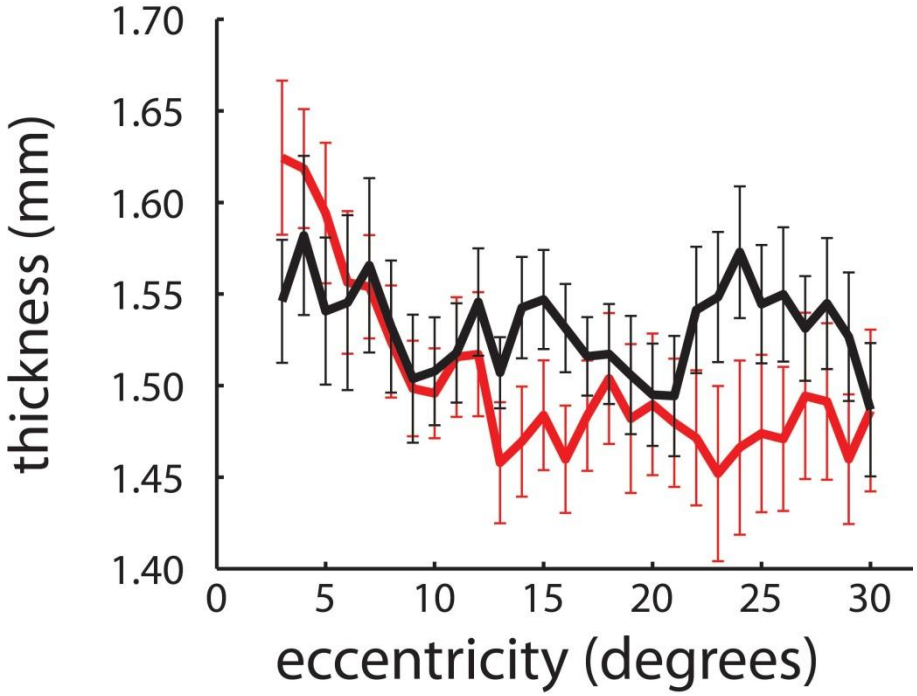

Supplementary Figure 3.4: *Cortical thickness for both hemispheres for participants in each group with the same data exclusion procedures as reported in the main analysis for visual areas V1. Red: Deaf participants, Black: Control group. Error bars denote +/- standard error of the mean. A trend is observed in the visual periphery where the deaf group appear to have thinner visual cortex in comparison to the hearing group.*

Supplementary Information from chapter 4

Visual, motor and unique encoding throughout the brain

In the main analyses, visual, motor and unique encoding were averaged across the 2 sessions. Below in table 4.1, we present the between sessions contrast for this data.

Region	Hemi	Area	p(cl)	Max (t)	X	Y	Z
Visual - decreases							
Superior parietal	R	281.04	0.024	4.15	26.59	-64.33	34.11
Motor - decreases							
Fusiform	R	315.53	0.011	4.84	29.69	-62.91	1.86

Supplementary Table 4.1: *Between session differences for encoding (with height extent T=2.65, p=0.01).*

Learning Effects

In the main analysis, t statistic maps for BOLD percentage signal change maps and directional encoding strength were presented for the difference between session 1 and 2, and the interaction between visual feedback condition and session. Here we present unthresholded maps of mean parameter change.

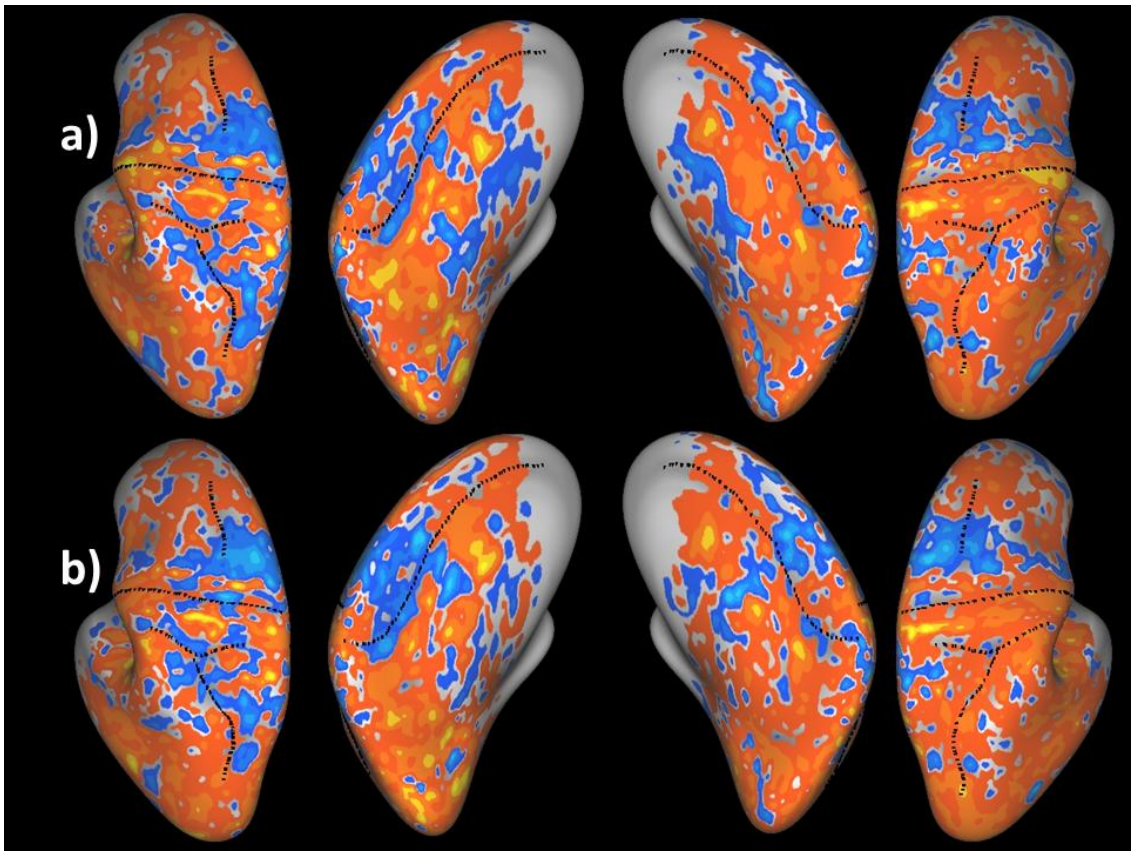

Supplementary Figure 4.1: *Mean BOLD percentage signal change for (a)typical and (b)mirror-reversed reaching conditions between sessions 1 and 2. The left hemisphere is presented on the left hand side.*

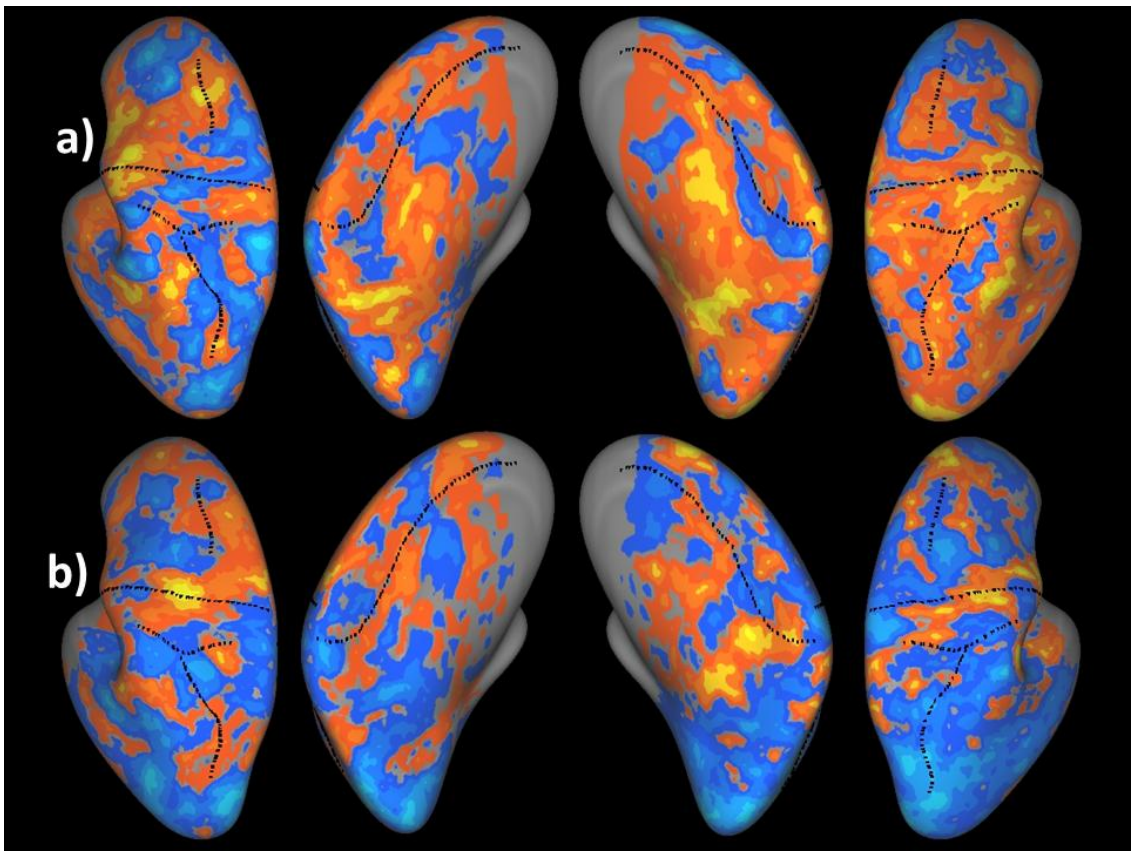

Supplementary Figure 4.2: *Mean directional encoding change for (a)typical and (b)mirror-reversed reaching movements between sessions 1 and 2. The left hemisphere is presented on the left hand side.*

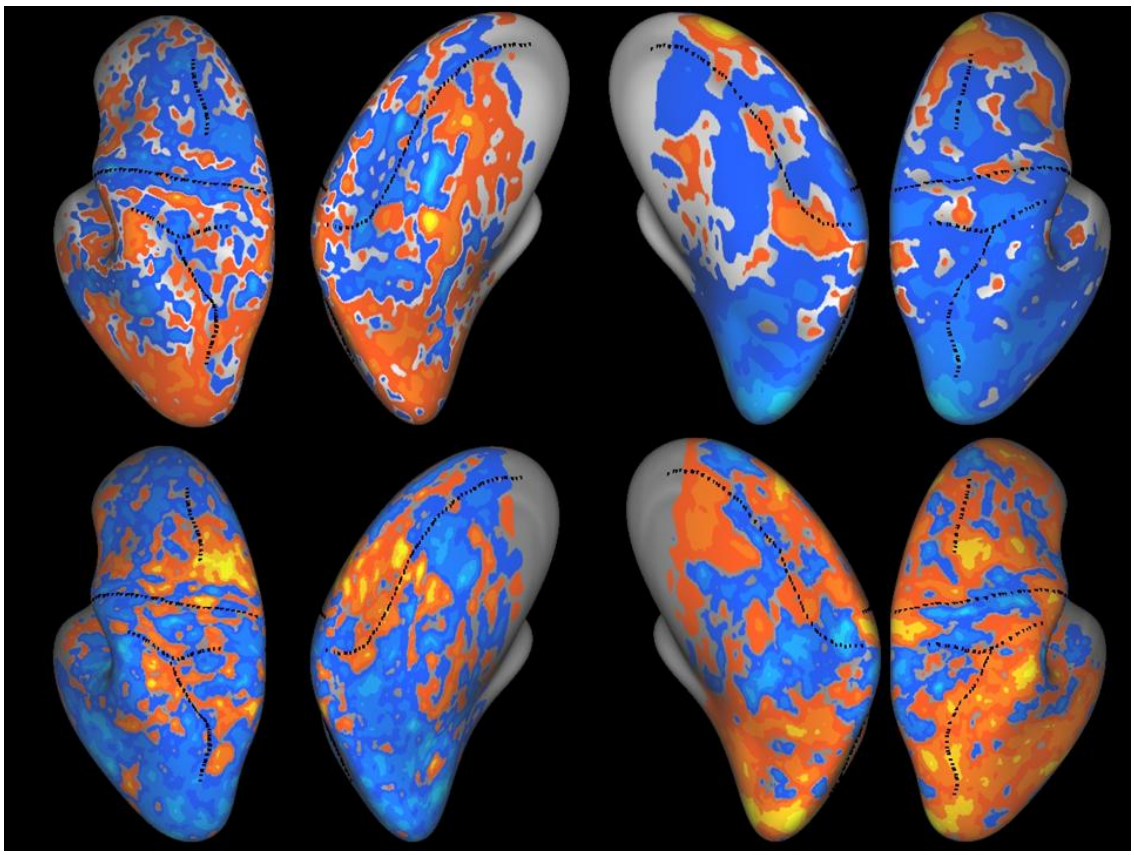

Supplementary Figure 4.3: *Unthresholded maps of interaction between visual feedback condition (typical/mirror-reversed) and session (1/2) (a)mean BOLD percentage signal change and (b)mean directional encoding strength. Decreases indicate mirror-reversed reaching was more decreased in the second session. The left hemisphere is presented on the left hand side.*

References

Alexander GE, Crutcher MD (1990) Neural representations of the target (goal) of visually guided arm movements in three motor areas of the monkey. J Neurophysiol 64:164-178.

Allen JS, Emmorey K, Bruss J, Damasio H (2013) Neuroanatomical differences in visual, motor, and language cortices between congenitally deaf signers, hearing signers, and hearing non-signers. Front Neuroanat 7:00026.

Allman BL, Keniston LP, Meredith MA (2009) Adult deafness induces somatosensory conversion of ferret auditory cortex. Proc Natl Acad Sci U S A 106:5925-5930.

Amano K, Wandell BA, Dumoulin SO (2009) Visual Field Maps, Population Receptive Field Sizes, and Visual Field Coverage in the Human MT plus Complex. Journal of Neurophysiology 102:2704-2718.

Amedi A, Malach R, Hendler T, Peled S, Zohary E (2001) Visuo-haptic object-related activation in the ventral visual pathway. Nat Neurosci 4:324-330.

Amedi A, Stern WM, Camprodon JA, Bermpohl F, Merabet L, Rotman S, Hemond C, Meijer P, Pascual-Leone A (2007) Shape conveyed by visual-to-auditory sensory substitution activates the lateral occipital complex. Nat Neurosci 10:687-689.

Andersen RA, Buneo CA (2002) Intentional maps in posterior parietal cortex. Annu Rev Neurosci 25:189-220.

Andersson JL, Hutton C, Ashburner J, Turner R, Friston K (2001) Modeling geometric deformations in EPI time series. Neuroimage 13:903-919.

Anton-Erxleben K, Carrasco M (2013) Attentional enhancement of spatial resolution: linking behavioural and neurophysiological evidence. Nat Rev Neurosci 14:188-200.

Anton-Erxleben K, Stephan VM, Treue S (2009) Attention reshapes center-surround receptive field structure in macaque cortical area MT. Cereb Cortex 19:2466-2478.

Antonini A, Stryker MP (1993) Rapid remodeling of axonal arbors in the visual cortex. Science 260:1819-1821.

Auer ET, Bernstein LE, Sungkarat W, Singh M (2007) Vibrotactile activation of the auditory cortices in deaf versus hearing adults. Neuroreport 18:645-648.

Bandettini PA, Wong EC, Hinks RS, Tikofsky RS, Hyde JS (1992) Time course EPI of human brain function during task activation. Magn Reson Med 25:390-397.

Bartolo MJ, Gieselmann MA, Vuksanovic V, Hunter D, Sun L, Chen X, Delicato LS, Thiele A (2011) Stimulus-induced dissociation of neuronal firing rates and local field potential gamma power and its relationship to the resonance blood oxygen level-dependent signal in macaque primary visual cortex. Eur J Neurosci 34:1857-1870.

Baseler HA, Gouws A, Haak KV, Racey C, Crossland MD, Tufail A, Rubin GS, Cornelissen FW, Morland AB (2011) Large-scale remapping of visual cortex is absent in adult humans with macular degeneration. Nature Neuroscience 14:649-U148.

Bavelier D, Brozinsky C, Tomann A, Mitchell T, Neville H, Liu G (2001) Impact of early deafness and early exposure to sign language on the cerebral organization for motion processing. J Neurosci 21:8931-8942.

Bavelier D, Neville HJ (2002) Cross-modal plasticity: where and how? Nat Rev Neurosci 3:443-452.

Beauchamp MS (2005) See me, hear me, touch me: multisensory integration in lateral occipital-temporal cortex. Curr Opin Neurobiol 15:145-153.

Beer AL, Plank T, Greenlee MW (2011) Diffusion tensor imaging shows white matter tracts between human auditory and visual cortex. Experimental Brain Research 213:299-308.

Behrens TE, Berg HJ, Jbabdi S, Rushworth MF, Woolrich MW (2007) Probabilistic diffusion tractography with multiple fibre orientations: What can we gain? Neuroimage 34:144-155.

Behrens TE, Jenkinson M, Robson MD, Smith SM, Johansen-Berg H (2006) A consistent relationship between local white matter architecture and functional specialisation in medial frontal cortex. Neuroimage 30:220-227.

Behrens TE, Johansen-Berg H, Woolrich MW, Smith SM, Wheeler-Kingshott CA, Boulby PA, Barker GJ, Sillery EL, Sheehan K, Ciccarelli O, Thompson AJ, Brady JM, Matthews PM (2003) Non-invasive mapping of connections between human thalamus and cortex using diffusion imaging. Nat Neurosci 6:750-757.

Binda P, Thomas JM, Boynton GM, Fine I (2013) Minimizing biases in estimating the reorganization of human visual areas with BOLD retinotopic mapping. J Vis 13:13.

Bisley JW, Goldberg ME (2010) Attention, intention, and priority in the parietal lobe. Annu Rev Neurosci 33:1-21.

Blakemore C, Van Sluyters RC (1974) Reversal of the physiological effects of monocular deprivation in kittens: further evidence for a sensitive period. J Physiol 237:195-216.

Bosworth RG, Dobkins KR (2002) The effects of spatial attention on motion processing in deaf signers, hearing signers, and hearing nonsigners. Brain Cogn 49:152-169.

Bosworth RG, Wright, C.E., Bartlett, M.S., Corina, D.P., Dobkins, K.R. (2000) Characterisation of the visual properties of signs in ASL. . In: Theoretical Issues in Sign Language Research Seventh Biannual Conference Amsterdam.

Bottari D, Caclin A, Giard MH, Pavani F (2011) Changes in early cortical visual processing predict enhanced reactivity in deaf individuals. PLoS One 6:29.

Bridge H, von dem Hagen EAH, Davies G, Chambers C, Gouws A, Hoffmann M, Morland AB (2012) Changes in brain morphology in albinism reflect reduced visual acuity. Cortex.

Bross M (1979) Response bias in deaf and hearing subjects as a function of motivational factors. Perceptual and Motor Skills 49:779-782.

Bross M, Sauerwein H (1980) Signal detection analysis of visual flicker in deaf and hearing individuals. Perceptual and Motor Skills 51:839-843.

Brozinsky CJ, Bavelier D (2001) Does early deafness alter motion processing? Society for Neuroscience Abstracts 27:2555.

Buchel C, Price C, Frackowiak RS, Friston K (1998) Different activation patterns in the visual cortex of late and congenitally blind subjects. Brain 121:409-419.

Buckley D, Codina C, Bhardwaj P, Pascalis O (2010) Action video game players and deaf observers have larger Goldmann visual fields. Vision Res 50:548-556.

Budinger E, Heil P, Hess A, Scheich H (2006) Multisensory processing via early cortical stages: Connections of the primary auditory cortical field with other sensory systems. Neuroscience 143:1065-1083.

Buneo CA, Andersen RA (2006) The posterior parietal cortex: sensorimotor interface for the planning and online control of visually guided movements. Neuropsychologia 44:2594-2606.

Buneo CA, Jarvis MR, Batista AP, Andersen RA (2002) Direct visuomotor transformations for reaching. Nature 416:632-636.

Burkhalter A, Van Essen DC (1986) Processing of color, form and disparity information in visual areas VP and V2 of ventral extrastriate cortex in the macaque monkey. J Neurosci 6:2327-2351.

Burton H, Diamond JB, McDermott KB (2003) Dissociating cortical regions activated by semantic and phonological tasks: a FMRI study in blind and sighted people. J Neurophysiol 90:1965-1982.

Burton H, Snyder AZ, Conturo TE, Akbudak E, Ollinger JM, Raichle ME (2002) Adaptive changes in early and late blind: a fMRI study of Braille reading. J Neurophysiol 87:589-607.

Buschman TJ, Miller EK (2007) Top-down versus bottom-up control of attention in the prefrontal and posterior parietal cortices. Science 315:1860-1862.

Calvert GA, Bullmore ET, Brammer MJ, Campbell R, Williams SC, McGuire PK, Woodruff PW, Iversen SD, David AS (1997) Activation of auditory cortex during silent lipreading. Science 276:593-596.

Calvert GA, Campbell R (2003) Reading Speech from Still and Moving Faces: The Neural Substrates of Visible Speech. J Cognitive Neurosci 15:57-70.

Calvert GA, Campbell R, Brammer MJ (2000) Evidence from functional magnetic resonance imaging of crossmodal binding in the human heteromodal cortex. Curr Biol 10:649-657.

Capek CM, MacSweeney M, Woll B, Waters D, McGuire PK, David AS, Brammer MJ, Campbell R (2008) Cortical circuits for silent speechreading in deaf and hearing people. Neuropsychologia 46:1233-1241.

Capek CM, Woll B, MacSweeney M, Waters D, McGuire PK, David AS, Brammer MJ, Campbell R (2010) Superior temporal activation as a function of linguistic knowledge: insights from deaf native signers who speechread. Brain Lang 112:129-134.

Cappe C, Barone P (2005) Heteromodal connections supporting multisensory integration at low levels of cortical processing in the monkey. Eur J Neurosci 22:2886-2902.

Cappe C, Morel A, Barone P, Rouiller EM (2009a) The thalamocortical projection systems in primate: an anatomical support for multisensory and sensorimotor interplay. Cereb Cortex 19:2025-2037.

Cappe C, Rouiller EM, Barone P (2009b) Multisensory anatomical pathways. Hear Res 258:28-36.

Carandini M, Demb JB, Mante V, Tolhurst DJ, Dan Y, Olshausen BA, Gallant JL, Rust NC (2005) Do we know what the early visual system does? J Neurosci 25:10577-10597.

Cardin V, Orfanidou E, Ronnberg J, Capek CM, Rudner M, Woll B (2013) Dissociating cognitive and sensory neural plasticity in human superior temporal cortex. Nat Commun 4.

Carlo CN, Stevens CF (2013) Structural uniformity of neocortex , revisited. Proc Natl Acad Sci U S A 110:1488-1493.

Carrera E, Bogousslavsky J (2006) The thalamus and behavior: effects of anatomically distinct strokes. Neurology 66:1817-1823.

Cavanaugh JR, Bair W, Movshon JA (2002) Nature and interaction of signals from the receptive field center and surround in macaque V1 neurons. J Neurophysiol 88:2530-2546.

Clavagnier S, Falchier A, Kennedy H (2004) Long-distance feedback projections to area V1: Implications for multisensory integration, spatial awareness, and visual consciousness. Cognitive Affective & Behavioral Neuroscience 4:117-126.

Codina C, Pascalis O, Mody C, Toomey P, Rose J, Gummer L, Buckley D (2011) Visual Advantage in Deaf Adults Linked to Retinal Changes. PLoS One 6:e20417.

Collignon O, Vandewalle G, Voss P, Albouy G, Charbonneau G, Lassonde M, Lepore F (2011) Functional specialization for auditory-spatial processing in the occipital cortex of congenitally blind humans. Proc Natl Acad Sci U S A 108:4435-4440.

Corina D, Chiu YS, Knapp H, Greenwald R, San Jose-Robertson L, Braun A (2007) Neural correlates of human action observation in hearing and deaf subjects. Brain Res 4:111-129.

Cui H, Andersen RA (2011) Different representations of potential and selected motor plans by distinct parietal areas. J Neurosci 31:18130-18136.

Cunnington R, Iansek R, Bradshaw JL, Phillips JG (1996) Movement-related potentials associated with movement preparation and motor imagery. Exp Brain Res 111:429-436.

Czajkowski R, Jayaprakash B, Wiltgen B, Rogerson T, Guzman-Karlsson MC, Barth AL, Trachtenberg JT, Silva AJ (2014) Encoding and storage of spatial information in the retrosplenial cortex. Proc Natl Acad Sci U S A 111:8661-8666.

Dale AM, Fischl B, Sereno MI (1999) Cortical surface-based analysis. I. Segmentation and surface reconstruction Neuroimage 9:179-194.

de Haas B, Schwarzkopf DS, Anderson EJ, Rees G (2014) Perceptual load affects spatial tuning of neuronal populations in human early visual cortex. Current Biology 24.

de la Mothe LA, Blumell S, Kajikawa Y, Hackett TA (2006) Thalamic connections of the auditory cortex in marmoset monkeys: core and medial belt regions. J Comp Neurol 496:72-96.

Debaere F, Wenderoth N, Sunaert S, Van Hecke P, Swinnen SP (2004a) Cerebellar and premotor function in bimanual coordination: parametric neural responses to spatiotemporal complexity and cycling frequency. Neuroimage 21:1416-1427.

Debaere F, Wenderoth N, Sunaert S, Van Hecke P, Swinnen SP (2004b) Changes in brain activation during the acquisition of a new bimanual coodination task. Neuropsychologia 42:855-867.

Deecke L, Grozinger B, Kornhuber HH (1976) Voluntary finger movement in man: cerebral potentials and theory. Biol Cybern 23:99-119.

Deecke L, Scheid P, Kornhuber HH (1969) Distribution of readiness potential, pre-motion positivity, and motor potential of the human cerebral cortex preceding voluntary finger movements. Exp Brain Res 7:158-168.

Destrieux C, Fischl B, Dale A, Halgren E (2010) Automatic parcellation of human cortical gyri and sulci using standard anatomical nomenclature. Neuroimage 53:1-15.

Dhawan S, Deubel H, Jonikaitis D (2013) Inhibition of saccades elicits attentional suppression. J Vis 13:9.

Diedrichsen J, Shadmehr R (2005) Detecting and adjusting for artifacts in fMRI time series data. Neuroimage 27:624-634.

Dorman MF, Sharma A, Gilley P, Martin K, Roland P (2007) Central auditory development: evidence from CAEP measurements in children fit with cochlear implants. J Commun Disord 40:284-294.

Doyon J, Bellec P, Amsel R, Penhune V, Monchi O, Carrier J, Lehericy S, Benali H (2009) Contributions of the basal ganglia and functionally related brain structures to motor learning. Behav Brain Res 199:61-75.

Driver J, Noesselt T (2008) Multisensory interplay reveals crossmodal influences on 'sensory-specific' brain regions, neural responses, and judgments. Neuron 57:11-23.

Dumoulin SO, Wandell BA (2008) Population receptive field estimates in human visual cortex. Neuroimage 39:647-660.

Duncan RO, Boynton GM (2003) Cortical magnification within human primary visual cortex correlates with acuity thresholds. Neuron 38:659-671.

Eisenberg M, Shmuelof L, Vaadia E, Zohary E (2011) The representation of visual and motor aspects of reaching movements in the human motor cortex. J Neurosci 31:12377-12384.

Emmorey K, Allen JS, Bruss J, Schenker N, Damasio H (2003) A morphometric analysis of auditory brain regions in congenitally deaf adults. Proc Natl Acad Sci U S A 100:10049-10054.

Emmorey K, McCullough S (2009) The bimodal bilingual brain: effects of sign language experience. Brain Lang 109:124-132.

Emmorey K, Xu J, Braun A (2011) Neural responses to meaningless pseudosigns: evidence for sign-based phonetic processing in superior temporal cortex. Brain Lang 117:34-38.

Eurich CW, Schwegler H (1997) Coarse coding: calculation of the resolution achieved by a population of large receptive field neurons. Biol Cybern 76:357-363.

Fabbri S, Strnad L, Caramazza A, Lingnau A (2014) Overlapping representations for grip type and reach direction. Neuroimage 94:138-146.

Falchier A, Clavagnier S, Barone P, Kennedy H (2002) Anatomical evidence of multimodal integration in primate striate cortex. Journal of Neuroscience 22:5749-5759.

Falchier A, Renaud L, Barone P, Kennedy H (2001) Extensive projections from the primary auditory cortex and polysensory area STP to peripheral area V1 in the macaque. Society for Neuroscience Abstracts 27:1342.

Felleman DJ, Van Essen DC (1987) Receptive field properties of neurons in area V3 of macaque monkey extrastriate cortex. J Neurophysiol 57:889-920.

Fine I, Finney EM, Boynton GM, Dobkins KR (2005) Comparing the effects of auditory deprivation and sign language within the auditory and visual cortex. J Cogn Neurosci 17:1621-1637.

Finney EM, Fine I, Dobkins KR (2001) Visual stimuli activate auditory cortex in the deaf. Nature Neuroscience 4:1171-1173.

Fischl B, Dale AM (2000) Measuring the thickness of the human cerebral cortex from magnetic resonance images. Proc Natl Acad Sci U S A 97:11050-11055.

Fischl B, Liu A, Dale AM (2001) Automated manifold surgery: constructing geometrically accurate and topographically correct models of the human cerebral cortex. IEEE Transactions on Medical Imaging 20:70-80.

Fischl B, Rajendran N, Busa E, Augustinack J, Hinds O, Yeo BT, Mohlberg H, Amunts K, Zilles K (2008) Cortical folding patterns and predicting cytoarchitecture. Cereb Cortex 18:1973-1980.

Fischl B, Salat DH, Busa E, Albert M, Dietrich M, Haselgrove C, van der Kouwe A, Killany R, D. K, Klaveness S, Montillo A, Makris N, Rosen B, Dale AM (2002) Whole brain segmentation: automated labeling of neuroanatomical structures in the human brain. Neuron 33:341-355.

Fischl B, Salat DH, van der Kouwe AJ, Makris N, Segonne F, Quinn BT, Dale AM (2004) Sequence-independent segmentation of magnetic resonance images. Neuroimage 23:69-84.

Fischl B, Sereno MI, Tootell RBH, Dale AM (1999) High-resolution intersubject averaging and a coordinate system for the cortical surface. Human Brain Mapping 8:272-284.

Fischl B, Sereno, M.I., Dale, A.M. (1999) Cortical surface based analysis. II: Inflation, flattening, and a surface-based coordinate system. Neuroimage 9:195-207.

Floyer-Lea A, Matthews PM (2005) Distinguishable brain activation networks for short- and long-term motor skill learning. J Neurophysiol 94:512-518.

Fregnac Y, Imbert M (1978) Early development of visual cortical cells in normal and dark-reared kittens: relationship between orientation selectivity and ocular dominance. J Physiol 278:27-44.

Furmanski CS, Schluppeck D, Engel SA (2004) Learning strengthens the response of primary visual cortex to simple patterns. Curr Biol 14:573-578.

Galea JM, Vazquez A, Pasricha N, de Xivry JJ, Celnik P (2011) Dissociating the roles of the cerebellum and motor cortex during adaptive learning: the motor cortex retains what the cerebellum learns. Cereb Cortex 21:1761-1770.

Gallivan JP, Cavina-Pratesi C, Culham JC (2009) Is that within reach? fMRI reveals that the human superior parieto-occipital cortex encodes objects reachable by the hand. J Neurosci 29:4381-4391.

Gattass R, Gross CG, Sandell JH (1981) Visual topography of V2 in the macaque. J Comp Neurol 201:519-539.

Gattass R, Sousa AP, Rosa MG (1987) Visual topography of V1 in the Cebus monkey. J Comp Neurol 259:529-548.

Gavornik JP, Bear MF (2014a) Higher brain functions served by the lowly rodent primary visual cortex. Learn Mem 21:527-533.

Gavornik JP, Bear MF (2014b) Learned spatiotemporal sequence recognition and prediction in primary visual cortex. Nat Neurosci 17:732-737.

Georgopoulos AP, Merchant H, Naselaris T, Amirikian B (2007) Mapping of the preferred direction in the motor cortex. Proc Natl Acad Sci U S A 104:11068-11072.

Georgopoulos AP, Schwartz AB, Kettner RE (1986) Neuronal population coding of movement direction. Science 233:1416-1419.

Ghazanfar AA, Schroeder CE (2006) Is neocortex essentially multisensory? Trends Cogn Sci 10:278-285.

Gilbert CD, Sigman M (2007) Brain states: top-down influences in sensory processing. Neuron 54:677-696.

Gogtay N, Giedd JN, Lusk L, Hayashi KM, Greenstein D, Vaituzis AC, Nugent TF, 3rd, Herman DH, Clasen LS, Toga AW, Rapoport JL, Thompson PM (2004) Dynamic mapping of human cortical development during childhood through early adulthood. Proc Natl Acad Sci U S A 101:8174-8179.

Gougoux F, Zatorre RJ, Lassonde M, Voss P, Lepore F (2005) A functional neuroimaging study of sound localization: visual cortex activity predicts performance in early-blind individuals. PLoS Biol 3:25.

Grafton ST, Hazeltine E, Ivry R (1995) Functional mapping of sequence learning in normal humans. J Cogn Neurosci 7:497-510.

Graziano MS (2006) Progress in understanding spatial coordinate systems in the primate brain. Neuron 51:7-9.

Graziano MS, Gandhi S (2000) Location of the polysensory zone in the precentral gyrus of anesthetized monkeys. Exp Brain Res 135:259-266.

Graziano MS, Gross CG (1998) Spatial maps for the control of movement. Curr Opin Neurobiol 8:195-201.

Graziano MS, Yap GS, Gross CG (1994) Coding of visual space by premotor neurons. Science 266:1054-1057.

Hall AJ, Lomber SG (2008) Auditory cortex projections target the peripheral field representation of primary visual cortex. Experimental Brain Research 190:413-430.

Hall CN, Reynell C, Gesslein B, Hamilton NB, Mishra A, Sutherland BA, O'Farrell FM, Buchan AM, Lauritzen M, Attwell D (2014) Capillary pericytes regulate cerebral blood flow in health and disease. Nature 508:55-60.

Han X, Jovicich J, Salat D, van der Kouwe A, Quinn B, Czanner S, Busa E, Pacheco J, Albert M, Killiany R, Maguire P, Rosas D, Makris N, Dale A, Dickerson B, Fischl B (2006) Reliability of MRI-derived measurements of human cerebral cortical thickness: the effect of field strength, scanner upgrade and manufacturer Neuroimage 32:180-194.

Hardwick RM, Rottschy C, Miall RC, Eickhoff SB (2013) A quantitative meta-analysis and review of motor learning in the human brain. Neuroimage 67:283-297.

Harrison SA, Tong F (2009) Decoding reveals the contents of visual working memory in early visual areas. Nature 458:632-635.

Harvey BM, Dumoulin SO (2011) The Relationship between Cortical Magnification Factor and Population Receptive Field Size in Human Visual Cortex: Constancies in Cortical Architecture. J Neurosci 31:13604-13612.

Hazeltine E, Grafton ST, Ivry R (1997) Attention and stimulus characteristics determine the locus of motor-sequence encoding. A PET study. Brain 120:123-140.

Hindley EL, Nelson AJ, Aggleton JP, Vann SD (2014) The rat retrosplenial cortex is required when visual cues are used flexibly to determine location. Behav Brain Res 263:98-107.

Hribar M, Suput D, Carvalho AA, Battelino S, Vovk A (2014) Structural alterations of brain grey and white matter in early deaf adults. Hear Res 28:00153-00151.

Hua T, Bao P, Huang CB, Wang Z, Xu J, Zhou Y, Lu ZL (2010) Perceptual learning improves contrast sensitivity of V1 neurons in cats. Curr Biol 20:887-894.

Hubel DH, Wiesel TN (1970) The period of susceptibility to the physiological effects of unilateral eye closure in kittens. J Physiol 206:419-436.

Hubel DH, Wiesel TN (1977) Ferrier lecture. Functional architecture of macaque monkey visual cortex. Proc R Soc Lond B Biol Sci 198:1-59.

Huk AC, Dougherty RF, Heeger DJ (2002) Retinotopy and functional subdivision of human areas MT and MST. J Neurosci 22:7195-7205.

Hulme OJ, Whiteley L, Shipp S (2010) Spatially distributed encoding of covert attentional shifts in human thalamus. J Neurophysiol 104:3644-3656.

Hutchison RM, Gallivan JP, Culham JC, Gati JS, Menon RS, Everling S (2012) Functional connectivity of the frontal eye fields in humans and macaque monkeys investigated with resting-state fMRI. J Neurophysiol 107:2463-2474.

Huttenlocher PR, Dabholkar AS (1997) Regional differences in synaptogenesis in human cerebral cortex. J Comp Neurol 387:167-178.

Jenkins IH, Brooks DJ, Nixon PD, Frackowiak RS, Passingham RE (1994) Motor sequence learning: a study with positron emission tomography. J Neurosci 14:3775-3790.

Jiang J, Zhu W, Shi F, Liu Y, Li J, Qin W, Li K, Yu C, Jiang T (2009) Thick visual cortex in the early blind. J Neurosci 29:2205-2211.

Johansen-Berg H, Behrens TE, Robson MD, Drobnjak I, Rushworth MF, Brady JM, Smith SM, Higham DJ, Matthews PM (2004) Changes in connectivity profiles define functionally distinct regions in human medial frontal cortex. Proc Natl Acad Sci U S A 101:13335-13340.

Johansen-Berg H, Behrens TEJ (2006) Just pretty pictures? What diffusion tractography can add in clinical neuroscience. Current Opinion in Neurology 19:379-385.

Johansen-Berg H, Rushworth MFS (2009) Using Diffusion Imaging to Study Human Connectional Anatomy. In: Annual Review of Neuroscience, vol. 32, pp 75-94 Palo Alto: Annual Reviews.

Johnson JA, Zatorre RJ (2005) Attention to simultaneous unrelated auditory and visual events: behavioral and neural correlates. Cereb Cortex 15:1609-1620.

Jones DK, Cercignani M (2010) Twenty-five pitfalls in the analysis of diffusion MRI data. NMR Biomed 23:803-820.

Jones DK, Knosche TR, Turner R (2013) White matter integrity, fiber count, and other fallacies: the do's and don'ts of diffusion MRI. Neuroimage 73:239-254.

Jones EG (1985) The Thalamus. New York: Plenum Press.

Jones EG (2009) Synchrony in the interconnected circuitry of the thalamus and cerebral cortex. Ann N Y Acad Sci.

Jones EG, Pons TP (1998) Thalamic and brainstem contributions to large-scale plasticity of primate somatosensory cortex. Science 282:1121-1125.

Jones EG, Powell TP (1970) An anatomical study of converging sensory pathways within the cerebral cortex of the monkey. Brain 93:793-820.

Jovicich J, Czanner S, Greve D, Haley. E, van der Kouwe A, Gollub R, Kennedy D, Schmitt F, Brown G, Macfall J, Fischl B, Dale A (2006) Reliability in multi-site structural MRI studies: effects of gradient non-linearity correction on phantom and human data. Neuroimage 30:436-443.

Kaas A, Weigelt S, Roebroeck A, Kohler A, Muckli L (2010) Imagery of a moving object: The role of occipital cortex and human MT/V5+. Neuroimage 49:794-804.

Kakei S, Hoffman DS, Strick PL (1999) Muscle and movement representations in the primary motor cortex. Science 285:2136-2139.

Kakei S, Hoffman DS, Strick PL (2003) Sensorimotor transformations in cortical motor areas. Neurosci Res 46:1-10.

Kalaska JF, Crammond DJ (1992) Cerebral cortical mechanisms of reaching movements. Science 255:1517-1523.

Karni A, Meyer G, Jezzard P, Adams MM, Turner R, Ungerleider LG (1995) Functional MRI evidence for adult motor cortex plasticity during motor skill learning. Nature 377:155-158.

Karni A, Meyer G, Rey-Hipolito C, Jezzard P, Adams MM, Turner R, Ungerleider LG (1998) The acquisition of skilled motor performance: fast and slow experience-driven changes in primary motor cortex. Proc Natl Acad Sci U S A 95:861-868.

Karni A, Sagi D (1993) The time course of learning a visual skill. Nature 365:250-252.

Karns CM, Dow MH, Neville HJ (2012) Altered cross-modal processing in the primary auditory cortex of congenitally deaf adults: a visual-somatosensory fMRI study with a double-flash illusion. Journal of Neuroscience 32:9626-9638.

Kim D-J, Park S-Y, Kim J, Lee DH, Park H-J (2009) Alterations of white matter diffusion anisotropy in early deafness. Neuroreport 20:1032-1036.

Kim JK, Zatorre RJ (2011) Tactile-auditory shape learning engages the lateral occipital complex. J Neurosci 31:7848-7856.

Klein BP, Harvey BM, Dumoulin SO (2014) Attraction of Position Preference by Spatial Attention throughout Human Visual Cortex. Neuron 84:227-237.

Knickmeyer RC, Gouttard S, Kang C, Evans D, Wilber K, Smith JK, Hamer RM, Lin W, Gerig G, Gilmore JH (2008) A structural MRI study of human brain development from birth to 2 years. J Neurosci 28:12176-12182.

Knudsen EI (2004) Sensitive periods in the development of the brain and behavior. J Cogn Neurosci 16:1412-1425.

Kok MA, Chabot N, Lomber SG (2014) Cross-modal reorganization of cortical afferents to dorsal auditory cortex following early- and late-onset deafness. J Comp Neurol 522:654-675.

Kral A (2007) Unimodal and cross-modal plasticity in the 'deaf' auditory cortex. International Journal of Audiology 46:479-493.

Kral A, Hartmann R, Tillein J, Heid S, Klinke R (2002) Hearing after congenital deafness: central auditory plasticity and sensory deprivation. Cereb Cortex 12:797-807.

Kral A, Sharma A (2012) Developmental neuroplasticity after cochlear implantation. Trends in Neurosciences 35:111-122.

Kujala T, Palva MJ, Salonen O, Alku P, Huotilainen M, Jarvinen A, Naatanen R (2005) The role of blind humans' visual cortex in auditory change detection. Neurosci Lett 379:127-131.

Kwong KK, Belliveau JW, Chesler DA, Goldberg IE, Weisskoff RM, Poncelet BP, Kennedy DN, Hoppel BE, Cohen MS, Turner R, et al. (1992) Dynamic magnetic resonance imaging of human brain activity during primary sensory stimulation. Proc Natl Acad Sci U S A 89:5675-5679.

Lagarias JC, Reeds, J.A., Wright, M.H., Wright, P.E. (1998) Convergence Properties of the Nelder-Mead Simplex Methods in Low Dimensions. SIAM Journal of Optimization 9:112-147.

Lane B, Sullivan EV, Lim KO, Beal DM, Harvey RL, Jr., Meyers T, Faustman WO, Pfefferbaum A (1996) White matter MR hyperintensities in adult patients with congenital rubella. AJNR Am J Neuroradiol 17:99-103.

Lang W, Cheyne D, Kristeva R, Beisteiner R, Lindinger G, Deecke L (1991) Three-dimensional localization of SMA activity preceding voluntary movement. A study of electric and magnetic fields in a patient with infarction of the right supplementary motor area. Exp Brain Res 87:688-695.

Larsen A, Madsen KH, Lund TE, Bundesen C (2006) Images of illusory motion in primary visual cortex. J Cogn Neurosci 18:1174-1180.

Las L, Shapira AH, Nelken I (2008) Functional gradients of auditory sensitivity along the anterior ectosylvian sulcus of the cat. J Neurosci 28:3657-3667.

Laurienti PJ, Burdette JH, Wallace MT, Yen YF, Field AS, Stein BE (2002) Deactivation of sensory-specific cortex by cross-modal stimuli. J Cogn Neurosci 14:420-429.

Lavie N (1995) Perceptual load as a necessary condition for selective attention. Journal of Experimental Psychology-Human Perception and Performance 21:451-468.

Law CT, Gold JI (2008) Neural correlates of perceptual learning in a sensory-motor, but not a sensory, cortical area. Nat Neurosci 11:505-513.

Lee H, Noppeney U (2011) Physical and Perceptual Factors Shape the Neural Mechanisms That Integrate Audiovisual Signals in Speech Comprehension. The Journal of Neuroscience 31:11338-11350.

Levanen S, Hamdorf D (2001) Feeling vibrations: enhanced tactile sensitivity in congenitally deaf humans. Neurosci Lett 301:75-77.

Levanen S, Jousmaki V, Hari R (1998) Vibration-induced auditory-cortex activation in a congenitally deaf adult. Curr Biol 8:869-872.

Levin N, Dumoulin SO, Winawer J, Dougherty RF, Wandell BA (2010) Cortical maps and white matter tracts following long period of visual deprivation and retinal image restoration. Neuron 65:21-31.

Li Y, Ding G, Booth JR, Huang R, Lv Y, Zang Y, He Y, Peng D (2012) Sensitive Period for White Matter Connectivity of Superior Temporal Cortex in Deaf People. Human Brain Mapping 33:349-359.

Logothetis NK (2003) The underpinnings of the BOLD functional magnetic resonance imaging signal. J Neurosci 23:3963-3971.

Logothetis NK (2008) What we can do and what we cannot do with fMRI. Nature 453:869-878.

Lohse KR, Wadden K, Boyd LA, Hodges NJ (2014) Motor skill acquisition across short and long time scales: a meta-analysis of neuroimaging data. Neuropsychologia 59:130-141.

Loke WH, Song S (1991) Central and peripheral visual processing in hearing and nonhearing individuals. Bulletin of the Psychonomic Society 29:437-440.

Lomber SG, Meredith MA, Kral A (2010) Cross-modal plasticity in specific auditory cortices underlies visual compensations in the deaf. Nat Neurosci 13:1421-1427.

Lomber SG, Meredith MA, Kral A (2011) Adaptive crossmodal plasticity in deaf auditory cortex: areal and laminar contributions to supranormal vision in the deaf. Prog Brain Res 191:251-270.

Lyness CR, Woll B, Campbell R, Cardin V (2013) How does visual language affect crossmodal plasticity and cochlear implant success? Neurosci Biobehav Rev 37:2621-2630.

Ma L, Wang B, Narayana S, Hazeltine E, Chen X, Robin DA, Fox PT, Xiong J (2010) Changes in regional activity are accompanied with changes in inter-regional connectivity during 4 weeks motor learning. Brain Res 8:64-76.

MacSweeney M, Campbell R, Woll B, Giampietro V, David AS, McGuire PK, Calvert GA, Brammer MJ (2004) Dissociating linguistic and nonlinguistic gestural communication in the brain. Neuroimage 22:1605-1618.

MacSweeney M, Capek CM, Campbell R, Woll B (2008a) The signing brain: the neurobiology of sign language. Trends Cogn Sci 12:432-440.

MacSweeney M, Waters D, Brammer MJ, Woll B, Goswami U (2008b) Phonological processing in deaf signers and the impact of age of first language acquisition. Neuroimage 40:1369-1379.

MacSweeney M, Woll B, Campbell R, McGuire PK, David AS, Williams SC, Suckling J, Calvert GA, Brammer MJ (2002) Neural systems underlying British Sign Language and audio-visual English processing in native users. Brain 125:1583-1593.

Martin JH, Ghez C (1985) Task-related coding of stimulus and response in cat motor cortex. Exp Brain Res 57:427-442.

Matsuzaka Y, Picard N, Strick PL (2007) Skill representation in the primary motor cortex after long-term practice. J Neurophysiol 97:1819-1832.

Mayberry RI, Chen JK, Witcher P, Klein D (2011) Age of acquisition effects on the functional organization of language in the adult brain. Brain Lang 119:16-29.

McGettigan C, Faulkner A, Altarelli I, Obleser J, Baverstock H, Scott SK (2012) Speech comprehension aided by multiple modalities: behavioural and neural interactions. Neuropsychologia 50:762-776.

Mechelli A, Crinion JT, Noppeney U, O'Doherty J, Ashburner J, Frackowiak RS, Price CJ (2004) Neurolinguistics: structural plasticity in the bilingual brain. Nature 431:757.

Merabet LB, Pascual-Leone A (2010) Neural reorganization following sensory loss: the opportunity of change. Nat Rev Neurosci 11:44-52.

Meredith MA, Allman BL (2012) Early hearing-impairment results in crossmodal reorganization of ferret core auditory cortex. Neural Plast 601591:19.

Meredith MA, Clemo HR (1989) Auditory cortical projection from the anterior ectosylvian sulcus (Field AES) to the superior colliculus in the cat: an anatomical and electrophysiological study. J Comp Neurol 289:687-707.

Meredith MA, Keniston LP, Allman BL (2012) Multisensory dysfunction accompanies crossmodal plasticity following adult hearing impairment. Neuroscience 214:136-148.

Meredith MA, Kryklywy J, McMillan AJ, Malhotra S, Lum-Tai R, Lomber SG (2011) Crossmodal reorganization in the early deaf switches sensory, but not behavioral roles of auditory cortex. Proc Natl Acad Sci U S A 108:8856-8861.

Meredith MA, Lomber SG (2011) Somatosensory and visual crossmodal plasticity in the anterior auditory field of early-deaf cats. Hear Res 280:38-47.

Merriam EP, Genovese CR, Colby CL (2003) Spatial updating in human parietal cortex. Neuron 39:361-373.

Meyer K, Kaplan JT, Essex R, Webber C, Damasio H, Damasio A (2010) Predicting visual stimuli on the basis of activity in auditory cortices. Nature Neuroscience 13:667-668.

Miao W, Li J, Tang M, Xian J, Li W, Liu Z, Liu S, Sabel BA, Wang Z, He H (2013) Altered white matter integrity in adolescents with prelingual deafness: a high-resolution tract-based spatial statistics imaging study. AJNR Am J Neuroradiol 34:1264-1270.

Mills CB (1985) Perception of visual temporal patterns by deaf and hearing adults. Bulletin of the Psychonomic Society 23:483-486.

Mitchell TV, Armstrong BA, Hillyard SA, Neville HJ (1997) Effects of auditory deprivation on the processing of motion and color. Society for Neuroscience Abstracts 23:1585.

Moran J, Desimone R (1985) Selective attention gates visual processing in the extrastriate cortex. Science 229:782-784.

Morel A, Magnin M, Jeanmonod D (1997) Multiarchitectonic and stereotactic atlas of the human thalamus. J Comp Neurol 387:588-630.

Morzaria S, Westerberg BD, Kozak FK (2004) Systematic review of the etiology of bilateral sensorineural hearing loss in children. International Journal of Pediatric Otorhinolaryngology 68:1193-1198.

Muckli L (2010) What are we missing here? Brain imaging evidence for higher cognitive functions in primary visual cortex V1. International Journal of Imaging Systems and Technology 20:131-139.

Muckli L, Kohler A, Kriegeskorte N, Singer W (2005) Primary visual cortex activity along the apparent-motion trace reflects illusory perception. PLoS Biol 3:19.

Murray SO, Boyaci H, Kersten D (2006) The representation of perceived angular size in human primary visual cortex. Nat Neurosci 9:429-434.

Nair A, Treiber JM, Shukla DK, Shih P, Muller RA (2013) Impaired thalamocortical connectivity in autism spectrum disorder: a study of functional and anatomical connectivity. Brain 136:1942-1955.

Neville HJ, Lawson D (1987) Attention to central and peripheral visual space in a movement detection task: An event-related potential and behavioural study II. Congenitally deaf adults. Brain Research 405:268-283.

Nishimura H, Hashikawa K, Doi K, Iwaki T, Watanabe Y, Kusuoka H, Nishimura T, Kubo T (1999) Sign language 'heard' in the auditory cortex. Nature 397:116.

Ogawa S, Lee TM (1990) Magnetic resonance imaging of blood vessels at high fields: in vivo and in vitro measurements and image simulation. Magn Reson Med 16:9-18.

Ogawa S, Tank DW, Menon R, Ellermann JM, Kim SG, Merkle H, Ugurbil K (1992) Intrinsic signal changes accompanying sensory stimulation: functional brain mapping with magnetic resonance imaging. Proc Natl Acad Sci U S A 89:5951-5955.

Olulade OA, Koo DS, LaSasso CJ, Eden GF (2014) Neuroanatomical profiles of deafness in the context of native language experience. J Neurosci 34:5613-5620.

Oosterhof NN, Wiestler T, Downing PE, Diedrichsen J (2011) A comparison of volume-based and surface-based multi-voxel pattern analysis. Neuroimage 56:593-600.

Park HJ, Lee JD, Kim EY, Park B, Oh MK, Lee S, Kim JJ (2009) Morphological alterations in the congenital blind based on the analysis of cortical thickness and surface area. Neuroimage 47:98-106.

Passingham RE, Stephan KE, Kotter R (2002) The anatomical basis of functional localization in the cortex. Nat Rev Neurosci 3:606-616.

Pekkola J, Ojanen V, Autti T, Jaaskelainen IP, Mottonen R, Tarkiainen A, Sams M (2005) Primary auditory cortex activation by visual speech: an fMRI study at 3 T. Neuroreport 16:125-128.

Penhune VB, Doyon J (2002) Dynamic cortical and subcortical networks in learning and delayed recall of timed motor sequences. J Neurosci 22:1397-1406.

Penhune VB, Doyon J (2005) Cerebellum and M1 interaction during early learning of timed motor sequences. Neuroimage 26:801-812.

Penhune VB, Steele CJ (2012) Parallel contributions of cerebellar, striatal and M1 mechanisms to motor sequence learning. Behav Brain Res 226:579-591.

Penicaud S, Klein D, Zatorre RJ, Chen JK, Witcher P, Hyde K, Mayberry RI (2012) Structural brain changes linked to delayed first language acquisition in congenitally deaf individuals. Neuroimage 11:42-49.

Petitto LA, Zatorre RJ, Gauna K, Nikelski EJ, Dostie D, Evans AC (2000) Speech-like cerebral activity in profoundly deaf people processing signed languages: implications for the neural basis of human language. Proc Natl Acad Sci U S A 97:13961-13966.

Philibert B, Collet L, Vesson JF, Veuillet E (2002) Intensity-related performances are modified by long-term hearing aid use: a functional plasticity? Hear Res 165:142-151.

Pietrini P, Furey ML, Ricciardi E, Gobbini MI, Wu WH, Cohen L, Guazzelli M, Haxby JV (2004) Beyond sensory images: Object-based representation in the human ventral pathway. Proc Natl Acad Sci U S A 101:5658-5663.

Pitzalis S, Sereno MI, Committeri G, Fattori P, Galati G, Tosoni A, Galletti C (2013) The human homologue of macaque area V6A. Neuroimage 82:517-530.

Poirier C, Collignon O, Scheiber C, Renier L, Vanlierde A, Tranduy D, Veraart C, De Volder AG (2006) Auditory motion perception activates visual motion areas in early blind subjects. Neuroimage 31:279-285.

Poldrack RA (2000) Imaging brain plasticity: conceptual and methodological issues--a theoretical review. Neuroimage 12:1-13.

Poldrack RA (2014) Is "efficiency" a useful concept in cognitive neuroscience? Dev Cogn Neurosci 13:00041-00043.

Poldrack RA, Sabb FW, Foerde K, Tom SM, Asarnow RF, Bookheimer SY, Knowlton BJ (2005) The neural correlates of motor skill automaticity. J Neurosci 25:5356-5364.

Proksch J, Bavelier D (2002) Changes in the spatial distribution of visual attention after early deafness. J Cogn Neurosci 14:687-701.

Ptito M, Matteau I, Gjedde A, Kupers R (2009) Recruitment of the middle temporal area by tactile motion in congenital blindness. Neuroreport 20:543-547.

Raemaekers M, Bergsma DP, van Wezel RJA, van der Wildt GJ, van den Berg AV (2011) Effects of Vision Restoration Training on Early Visual Cortex in Patients With Cerebral Blindness Investigated With Functional Magnetic Resonance Imaging. Journal of Neurophysiology 105:872-882.

Raggio MW, Schreiner CE (1999) Neuronal responses in cat primary auditory cortex to electrical cochlear stimulation. III. Activation patterns in short- and long-term deafness. J Neurophysiol 82:3506-3526.

Raichle ME, Snyder AZ (2007) A default mode of brain function: a brief history of an evolving idea. Neuroimage 37:1083-1090.

Ramachandran VS, Kupperman B (1986) Reversal of the physiological effects of monocular deprivation in adult dark-reared cats. Brain Res 367:309-313.

Reale RA, Calvert GA, Thesen T, Jenison RL, Kawasaki H, Oya H, Howard MA, Brugge JF (2007) Auditory-visual processing represented in the human superior temporal gyrus. Neuroscience 145:162-184.

Rees G, Friston K, Koch C (2000) A direct quantitative relationship between the functional properties of human and macaque V5. Nat Neurosci 3:716-723.

Reis J, Schambra HM, Cohen LG, Buch ER, Fritsch B, Zarahn E, Celnik PA, Krakauer JW (2009) Noninvasive cortical stimulation enhances motor skill acquisition over multiple days through an effect on consolidation. Proc Natl Acad Sci U S A 106:1590-1595.

Renier LA, Anurova I, De Volder AG, Carlson S, VanMeter J, Rauschecker JP (2010) Preserved functional specialization for spatial processing in the middle occipital gyrus of the early blind. Neuron 68:138-148.

Ress D, Backus BT, Heeger DJ (2000) Activity in primary visual cortex predicts performance in a visual detection task. Nat Neurosci 3:940-945.

Roder B, Stock O, Bien S, Neville H, Rosler F (2002) Speech processing activates visual cortex in congenitally blind humans. Eur J Neurosci 16:930-936.

Roebroeck A, Formisano E, Goebel R (2005) Mapping directed influence over the brain using Granger causality and fMRI. Neuroimage 25: 230-242.

Rosa MG, Sousa AP, Gattass R (1988) Representation of the visual field in the second visual area in the Cebus monkey. J Comp Neurol 275:326-345.

Rushworth MF, Behrens TE, Johansen-Berg H (2006) Connection patterns distinguish 3 regions of human parietal cortex. Cereb Cortex 16:1418-1430.

Sadato N, Okada T, Honda M, Matsuki K, Yoshida M, Kashikura K, Takei W, Sato T, Kochiyama T, Yonekura Y (2005) Cross-modal integration and plastic changes revealed by lip movement, random-dot motion and sign languages in the hearing and deaf. Cereb Cortex 15:1113-1122.

Sadato N, Pascual-Leone A, Grafman J, Deiber MP, Ibanez V, Hallett M (1998) Neural networks for Braille reading by the blind. Brain 121:1213-1229.

Sadato N, Pascual-Leone A, Grafman J, Ibanez V, Deiber MP, Dold G, Hallett M (1996) Activation of the primary visual cortex by Braille reading in blind subjects. Nature 380:526-528.

Sadato N, Yamada H, Okada T, Yoshida M, Hasegawa T, Matsuki K, Yonekura Y, Itoh H (2004) Age-dependent plasticity in the superior temporal sulcus in deaf humans: a functional MRI study. BMC Neurosci 5:56.

Sajad A, Sadeh M, Keith GP, Yan X, Wang H, Crawford JD (2014) Visual-Motor Transformations Within Frontal Eye Fields During Head-Unrestrained Gaze Shifts in the Monkey. Cereb Cortex 9.

Saleem AB, Ayaz A, Jeffery KJ, Harris KD, Carandini M (2013) Integration of visual motion and locomotion in mouse visual cortex. Nat Neurosci 16:1864-1869.

Saygin AP, Sereno MI (2008) Retinotopy and Attention in Human Occipital, Temporal, Parietal, and Frontal Cortex. Cerebral Cortex 18:2158-2168.

Saygin ZM, Osher DE, Koldewyn K, Reynolds G, Gabrieli JD, Saxe RR (2011) Anatomical connectivity patterns predict face selectivity in the fusiform gyrus. Nat Neurosci 15:321-327.

Schoups A, Vogels R, Qian N, Orban G (2001) Practising orientation identification improves orientation coding in V1 neurons. Nature 412:549-553.

Scott GD, Karns CM, Dow MW, Stevens C, Neville HJ (2014) Enhanced peripheral visual processing in congenitally deaf humans is supported by multiple brain regions, including primary auditory cortex. Front Hum Neurosci 8.

Segonne F, Dale AM, Busa E, Glessner M, Salat D, Hahn HK, Fischl B (2004) A hybrid approach to the skull stripping problem in MRI. Neuroimage 22:1060-1075.

Segonne F, Pacheco J, Fischl B (2007) Geometrically accurate topology-correction of cortical surfaces using nonseparating loops. IEEE Transactions on Medical Imaging 26:518-529.

Sereno MI, Dale AM, Reppas JB, Kwong KK, Belliveau JW, Brady TJ, Rosen BR, Tootell RBH (1995) Borders of Multiple Visual Areas in Humans Revealed by Functional Magnetic Resonance Imaging. Science (Washington D C) 268:889-893.

Sereno MI, Lutti A, Weiskopf N, Dick F (2013) Mapping the human cortical surface by combining quantitative T(1) with retinotopy. Cereb Cortex 23:2261-2268.

Sharma A, Campbell J (2011) A sensitive period for cochlear implantation in deaf children. J Matern Fetal Neonatal Med 1:151-153.

Sharma A, Dorman MF (2006) Central auditory development in children with cochlear implants: clinical implications. Adv Otorhinolaryngol 64:66-88.

Sharma A, Martin K, Roland P, Bauer P, Sweeney MH, Gilley P, Dorman M (2005) P1 latency as a biomarker for central auditory development in children with hearing impairment. J Am Acad Audiol 16:564-573.

Shaw P, Kabani NJ, Lerch JP, Eckstrand K, Lenroot R, Gogtay N, Greenstein D, Clasen L, Evans A, Rapoport JL, Giedd JN, Wise SP (2008) Neurodevelopmental trajectories of the human cerebral cortex. J Neurosci 28:3586-3594.

Shen L, Alexander GE (1997) Neural correlates of a spatial sensory-to-motor transformation in primary motor cortex. J Neurophysiol 77:1171-1194.

Sherman SM (2007) The thalamus is more than just a relay. Curr Opin Neurobiol 17:417-422.

Shibata K, Watanabe T, Sasaki Y, Kawato M (2011) Perceptual learning incepted by decoded fMRI neurofeedback without stimulus presentation. Science 334:1413-1415.

Shipp S (2004) The brain circuitry of attention. Trends Cogn Sci 8:223-230.

Shuler MG, Bear MF (2006) Reward timing in the primary visual cortex. Science 311:1606-1609.

Silver MA, Ress D, Heeger DJ (2007) Neural correlates of sustained spatial attention in human early visual cortex. J Neurophysiol 97:229-237.

Smith FW, Goodale MA (2013) Decoding visual object categories in early somatosensory cortex. Cerebral Cortex 25(4): 1020-1031.

Snyder LH (2000) Coordinate transformations for eye and arm movements in the brain. Curr Opin Neurobiol 10:747-754.

Stanton SG, Harrison RV (2000) Projections from the medial geniculate body to primary auditory cortex in neonatally deafened cats. J Comp Neurol 426:117-129.

Stefan K, Kunesch E, Cohen LG, Benecke R, Classen J (2000) Induction of plasticity in the human motor cortex by paired associative stimulation. Brain 3:572-584.

Stein BE, Wallace MW, Stanford TR, Jiang W (2002) Cortex governs multisensory integration in the midbrain. Neuroscientist 8:306-314.

Sterzer P, Haynes JD, Rees G (2006) Primary visual cortex activation on the path of apparent motion is mediated by feedback from hMT+/V5. Neuroimage 32:1308-1316.

Striem-Amit E, Amedi A (2014) Visual cortex extrastriate body-selective area activation in congenitally blind people "seeing" by using sounds. Curr Biol 24:687-692.

Striem-Amit E, Cohen L, Dehaene S, Amedi A (2012) Reading with sounds: sensory substitution selectively activates the visual word form area in the blind. Neuron 76:640-652.

Sugita K, Ando M, Makino M, Takanashi J, Fujimoto N, Niimi H (1991) Magnetic resonance imaging of the brain in congenital rubella virus and cytomegalovirus infections. Neuroradiology 33:239-242.

Sur M, Pallas SL, Roe AW (1990) Cross-modal plasticity in cortical development: differentiation and specification of sensory neocortex. Trends Neurosci 13:227-233.

Tallal P, Poizner H (1985) Temporal processing in deaf signers. Journal of Clinical and Experimental Neuropsychology 7:634.

Telgen S, Parvin D, Diedrichsen J (2014) Mirror Reversal and Visual Rotation Are Learned and Consolidated via Separate Mechanisms: Recalibrating or Learning De Novo? J Neurosci 34:13768-13779.

Thompson KG, Bichot NP (2005) A visual salience map in the primate frontal eye field. Prog Brain Res 147:251-262.

Toni I, Krams M, Turner R, Passingham RE (1998) The time course of changes during motor sequence learning: a whole-brain fMRI study. Neuroimage 8:50-61.

Tyler CW, Likova LT, Chen CC, Kontsevich LL, Schira MM, Wade AR (2005) Extended concepts of occipital retinotopy. Current Medical Imaging Reviews 1:319-329.

Ungerleider LG, Doyon J, Karni A (2002) Imaging brain plasticity during motor skill learning. Neurobiol Learn Mem 78:553-564.

Van Essen DC, Newsome WT, Maunsell JH (1984) The visual field representation in striate cortex of the macaque monkey: asymmetries, anisotropies, and individual variability. Vision Res 24:429-448.

Van Horn SC, Sherman SM (2004) Differences in projection patterns between large and small corticothalamic terminals. J Comp Neurol 475:406-415.

Vetter P, Smith FW, Muckli L (2014) Decoding sound and imagery content in early visual cortex. Curr Biol 24:1256-1262.

Viswanathan A, Freeman RD (2007) Neurometabolic coupling in cerebral cortex reflects synaptic more than spiking activity. Nat Neurosci 10:1308-1312.

Voss P, Gougoux F, Zatorre RJ, Lassonde M, Lepore F (2008) Differential occipital responses in early- and late-blind individuals during a sound-source discrimination task. Neuroimage 40:746-758.

Wallace MT, Carriere BN, Perrault TJ, Jr., Vaughan JW, Stein BE (2006) The development of cortical multisensory integration. J Neurosci 26:11844-11849.

Walther A, Nilli, H., Ejaz, N., Alink, A., Kriegeskorte, N., Diedrichsen, J. (in prep) Representational fMRI analysis: a tutorial.

Wang Q, Burkhalter A (2007) Area map of mouse visual cortex. J Comp Neurol 502:339-357.

Watkins KE, Cowey A, Alexander I, Filippini N, Kennedy JM, Smith SM, Ragge N, Bridge H (2012) Language networks in anophthalmia: maintained hierarchy of processing in visual cortex. Brain 135:1566-77.

Weeks R, Horwitz B, Aziz-Sultan A, Tian B, Wessinger CM, Cohen LG, Hallett M, Rauschecker JP (2000) A positron emission tomographic study of auditory localization in the congenitally blind. J Neurosci 20:2664-2672.

Wenderoth N, Debaere F, Sunaert S, Swinnen SP (2005) The role of anterior cingulate cortex and precuneus in the coordination of motor behaviour. Eur J Neurosci 22:235-246.

Wiesel TN, Hubel DH (1963) Single cell responses of striate cortex of kittens deprived of vision in one eye. Journal Neurophysiology 26:1003-1017.

Wiestler T, Diedrichsen J (2013) Skill learning strengthens cortical representations of motor sequences. Elife 9:00801.

Wong C, Chabot N, Kok MA, Lomber SG (2013) Modified Areal Cartography in Auditory Cortex Following Early- and Late-Onset Deafness. Cereb Cortex 14:14.

Yotsumoto Y, Watanabe T, Sasaki Y (2008) Different dynamics of performance and brain activation in the time course of perceptual learning. Neuron 57:827-833.

Zach N, Inbar D, Grinvald Y, Bergman H, Vaadia E (2008) Emergence of novel representations in primary motor cortex and premotor neurons during associative learning. J Neurosci 28:9545-9556.

Ziemann U (2004) TMS induced plasticity in human cortex. Rev Neurosci 15:253-266.

Zuiderbaan W, Harvey BM, Dumoulin SO (2012) Modeling center-surround configurations in population receptive fields using fMRI. J Vis 12:10.